Delft University of Technology
Faculty of Electrical Engineering, Mathematics and Computer Science
Delft Institute of Applied Mathematics

Probabilistic Inversion Technique for Seismic Data

A thesis submitted to the
Delft Institute of Applied Mathematics
in partial fulfillment of the requirements

for the degree

MASTER OF SCIENCE
in
APPLIED MATHEMATICS

by

Xuan Cui

Delft, the Netherlands
July 2008

Delft University of Technology

MSc THESIS APPLIED MATHEMATICS

"Probabilistic Inversion Technique for Seismic Data"

Xuan Cui

Delft University of Technology

Daily supervisor

Dr. Remus G. Hanea

Responsible professor

Prof. Dr. Ir. Arnold W. Heemink

Other thesis committee members

Prof. Dr. Ir. Rob Arts
Dr. Dorota Kurowicka
Ir. Rabin E. J. Neslo

July, 2008

Delft, the Netherlands

Abstract

In the reservoir engineering, researchers focus on estimating reservoir properties using seismic attributes. However, inverting the model is usually very difficult and computationally expensive. It requires sophisticated methods. We advocate the application of probabilistic inversion technique which is based on sample re-weighting to predict different reservoir properties. This is the first time to apply probabilistic inversion technique to the reservoir engineering.

CONTENTS

List of Tables

List of Figures

1. Introduction

There is no doubt that the Earth is a quite important planet in the solar system even in the whole universe, because it is the home of millions of species including human beings. Up until now, it is the only place where life is known to exist. It is vital to protect the environment in the interests of sustainable development. Many researchers dedicate themselves to performing much different scientific research in order to find out more about the earth and explore resources rationally and reasonably. (Figure 1.1)

Earth science is an all-embracing term concerning the sciences related to the planet Earth. It can be divided into a large number of parts such as the atmosphere, the biosphere, the hydrosphere, the lithosphere, etc. Under each part, there are several disciplines and sub-disciplines. (Figure 1.2) For instance, one of the largest aspects is that of the lithosphere, includes geology, geochemistry, geophysics and petrology. In addition, the majority of those disciplines rely on certain basic disciplines such as mathematics, physics, chemistry or biology to create a quantitative model to achieve their research.

Figure 1.1 the Earth

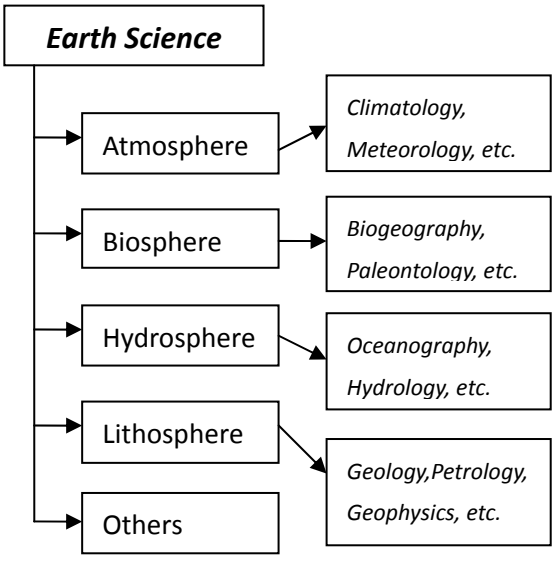

Figure 1.2 the Earth Science

Nowadays, along with the rapid development of technology, petrol plays a vital role all over the world, especially in developed countries. Thus, petroleum engineering is becoming more important than ever before. Because many big firms want to find different advanced ways of detecting and exploiting gas and oil in a reservoir, they

focus on the interactions between the earth science disciplines under the petroleum engineering. (Figure 1.3)

Reservoir engineering is a branch of petroleum engineering that relates to the subsurface engineering activities concerning the production of crude oil or gas. The main target of reservoir engineering is to extract the maximum amount of hydrocarbons in a field at minimal expense. Engineers perform certain research on reservoirs using reservoir simulations which belong to reservoir engineering. Computational models are used to predict the flow of fluids such as water, oil and gas in the given reservoir, and to provide an estimation of the hydrocarbon volume and a large number of properties of the reservoir.

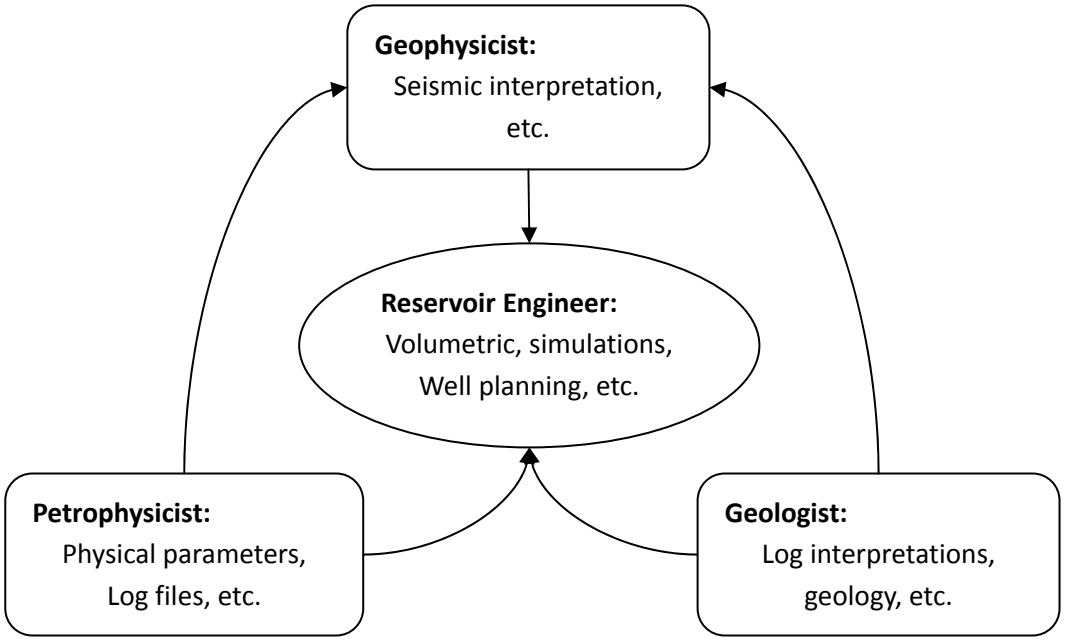

Figure 1.3 the interaction between the earth science disciplines that fall under petroleum engineering

Engineers would like to find out different reservoir properties in order to help them to decide an optimal well position and to determine a suitable drainage pattern. One of the advantages is to reduce the blow-out risks and to prevent damage to production equipment. Moreover, during the exploiting phase, they also want to know about the changes of reservoir properties. In recent years, researchers have applied seismic methods to petroleum engineering to measure and estimate reservoir properties. A brief seismic methods introduction will be presented in the following part.

Seismic method is based on seismology which is scientific research related to wave

propagation through the earth. The principle of any seismic method is that emitted energy, in the form of elastic waves, is transmitted on the ground using some devices and will be reflected at different subsurface layer boundaries. This enables engineers to record the reflected energy at or near the surface. Moreover, they can also image the subsurface geology using seismic data to find out the structure under the ground. As for reservoirs, this reflected phenomenon can also be happened. The transmitted waves are reflected from both the top boundary of the reservoir and the bottom. In accordance with different reservoir properties at each position, the arrival waves that engineer record will be changed to some corresponding properties such as velocities, amplitude, two-way travel time and acoustic impedances. The following step is to interpret the seismic data in order to estimate the properties of reservoir. However, the final results will be different depending on the background, knowledge and abilities of the seismic interpreter or the methods chosen.

In this project, we will perform some research on predicting the reservoir properties using a statistical approach – probabilistic inversion technique. This is the first to apply probabilistic inversion approach to the seismic method. After obtained all the estimations of the reservoir properties by using the seismic data, we will discuss and analyze those final results. Moreover, we will evaluate the performance of this brand new application and try to find different ways to improve the method in order to obtain good predictions of the reservoir properties based on the information of the seismic attributes that we known or measured.

This thesis can be divided into three main parts. The first part consists of the following two chapters. It contains some introduction and mathematical knowledge concerning both the reservoir engineering and probabilistic inversion approach. The second part, chapter 4, is to build a scheme of an experiment and to perform some main experiments such that we can obtain the final results and comparisons from different aspects. Furthermore, in this part, we will discuss and analyze all of the results that we gained and develop sensitivity analysis. Last but not least, chapter 5 is the last part. We would like to draw several conclusions based on those tests and experiments and give some recommendations related to the future works.

2. Reservoir Engineering

Reservoir simulation is an area of reservoir engineering, in which engineers use computer models or simulation software to predict the flow of oil, water and gas. The field of reservoir simulation is quite large, and much knowledge has to be applied to perform the simulation. In this chapter, we just present some brief introduction concerning reservoir engineering which contains reservoir properties, seismic method and seismic data and the rock physics model.

2.1 Reservoir Properties

A reservoir can be presented as a grid structure, and each grid point has its own properties such things as water or oil saturation, pore pressure, porosity and permeability. The definitions and notations of these reservoir properties are shown below, and we use the same symbols in the whole thesis.

a. SAT – saturation, a percentage of a certain liquid within a volume. Actually, there are two different saturations such as water saturation – S_w and oil saturation – S_o, and the relationship between these two saturations are shown in the following equation.

$$S_o + S_w = 1$$

   In this project, we just use SAT to represent water saturation for convenient.

b. PRF – pore pressure, P, the internal pressure of the reservoir.

c. POR – porosity, ϕ, is a measure of the void spaces in a material, and is measured as a fraction between 0 and 1. The porosity of a rock is an important consideration when attempting to evaluate the potential volume of water or hydrocarbons.

d. PER – permeability, k, is a measure of the ability of a material to transmit fluids in the earth sciences. It is a great importance in determining the flow characteristics of hydrocarbons in oil and gas reservoirs.

In this project, however, we just focus on the first three reservoir properties – SAT, PRF and POR, because the part of rock physics model that we will use do not need the last reservoir property – permeability.

Here are some brief introductions of reservoir properties, and the next section contains seismic method and the rock physics model. More information related to these is introduced by [5], while the theoretical part concerning the rock physics model is presented by [4].

2.2 Seismic Method

Seismic method is typically applied in exploration seismology which is the scientific study of earthquakes and the propagation of elastic waves, alternatively known as sound waves through the earth. It is considered an active geophysical method. The principle of this method is to use emitted energy in the form of elastic waves and reflect it at the subsurface layer boundaries. Finally, the reflected waves are recorded near or on the surface. The objective of seismic exploration is to obtain structural information on the subsurface from seismic data.

In reservoir engineering, seismic images are used to estimate the properties of a reservoir. The steps can be simply stated in the following paragraph.

Firstly, seismic sources can be used to transmit elastic wave in different positions. Secondly, the waves pass through the earth's interior and reflection and refraction taking place in both the top and bottom layers of a reservoir. In accordance with the differing saturation, pressure or other properties under the ground, the properties of sound waves such as velocity, amplitude, acoustic impedance are definitely changed. Finally, engineers use recorders to receive those reflected waves with changed properties at the surface. The data obtained from the recorders is called seismic data.

Seismic data can be used to image the subsurface geology in time, while seismic interpretation is a description of the translation process. Seismic interpretation connects with many other earth science disciplines such as the oil industry, geology, petrology as well as reservoir engineering. It plays a vital role in seismic methods, because the final results whether good or bad depend on the background and abilities of the seismic interpreters. Furthermore, there are a lot of different classes of seismic data which can be obtained and used for analysis. In this project, we concentrate on three seismic attributes – velocity of P-waves, velocity of S-waves and the density. Some details of those seismic attributes will be given in the following part.

As mentioned above, in seismic method, the energy is emitted as an elastic wave, which can be used by the seismic sources and receivers. Waves that propagate through the earth as elastic waves are referred to as seismic waves. There are two

categories of seismic waves – body waves and surface waves. A seismic body wave is an elastic wave which propagates through the earth's interior, and it can also be divided into two kinds of waves – P-waves and S-waves. In reservoir engineering, engineers make most use of the properties of these two classes of waves to create reservoir characterization.

The name P-waves stands for primary waves, because it propagates through the medium faster than any other types of waves like S-waves and surface waves. It can also be called longitudinal waves, because the particles move in the same direction as the wave motion. P-waves can travel gas, liquid and solids. This is one of the most frequently recorded seismic waves in reservoir engineering.

By contrast, S-waves, sometimes called secondary waves or shear waves, propagate as transverse waves. The motion of particles is perpendicular to the direction of the wave propagation. Moreover, S-waves are usually subdivided into two perpendiculars which are horizontal and vertical directions, namely, SH-waves and SV-waves. A simple explanation of the propagation of P-waves and S-waves is given below. (Figure 2.1)

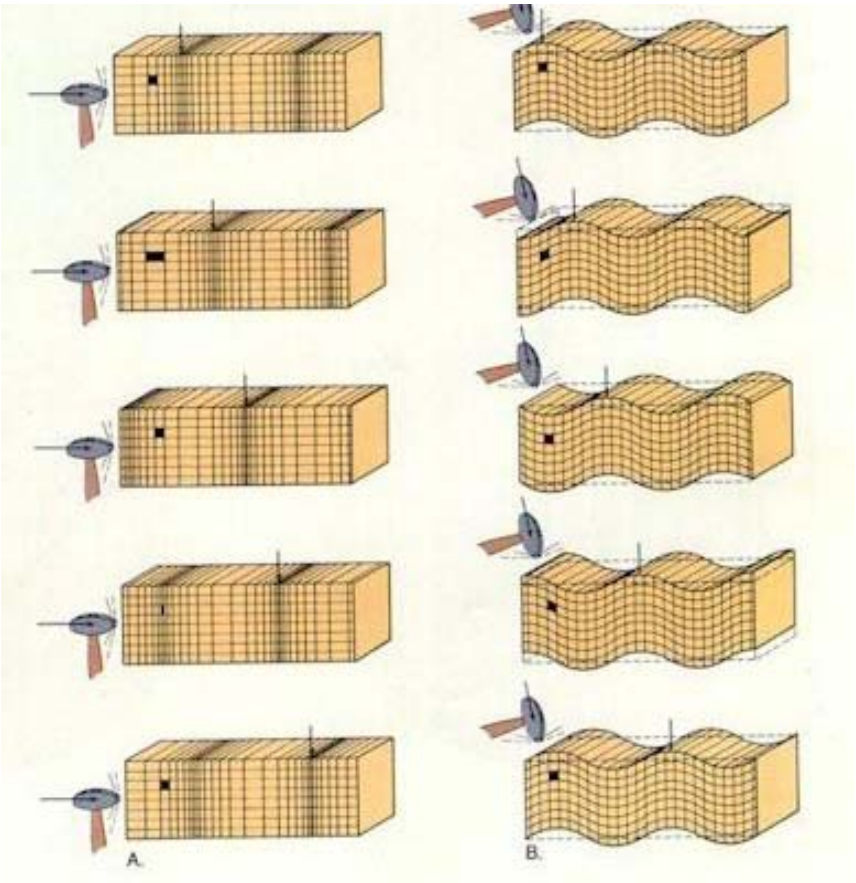

Figure 2.1 the propagation of P-waves (left) and S-waves (Right)

Here several advantages of using P-waves and S-waves are shown below,

a. Distinction between lithology and fluid effects (S-waves show a response on lithological interfaces, but not on fluid interfaces).

b. Use of a limited S-waves survey, calibrated to a larger P-waves survey, to image below gas. Gas can severely attenuate the P-waves signal, but S-waves are insensitive to the pore fill.

c. Prediction of rock parameters such as porosity or lithology by using additional information in the form of the ratio of P-waves velocity versus S-waves velocity.

d. S-waves play an important role in fracture detection and characterization.

It is also quite important for the purposes of seismic interpretation to know the properties of different seismic waves such as velocity and amplitude. For instance, the velocity of P-waves will increase when they propagate in a deeper layer of the earth, because the rigidity of the soil will be greater than the value in an upper layer. Furthermore, depending on how the propagating is done, S-waves cannot propagate through fluids. Thus, only P-waves exist in fluids, while both types could exist in solids and the velocity of P-waves are always faster than S-waves.

In this project, there are three seismic attributes which we should use, and they are given below,

Vp – the velocity of P-waves,
Vs – the velocity of S-waves,
Rho – the bulk-rock-density.

The reason that why we put Rho in the seismic attributes group is that it is one of the outputs of the rock physics model. The rock physics model is a bridge between the reservoir properties and the seismic attributes, and we will introduce it in the following section.

2.3 Rock Physics Model

In this project, the rock physics model plays an important role. As we mentioned at the end of last section, this is a bridge to connect the reservoir properties with the seismic attributes. The main goal of this project is to estimate different reservoir

properties based on application of probabilistic inversion technique using the seismic attributes that engineers could obtain or measure.

We will present the details concerning the rock physics model, especially the main part – Gassmann equation, which is one of the most important parts of that model. A brief scheme of the rock physics model is given below. (Figure 2.2)

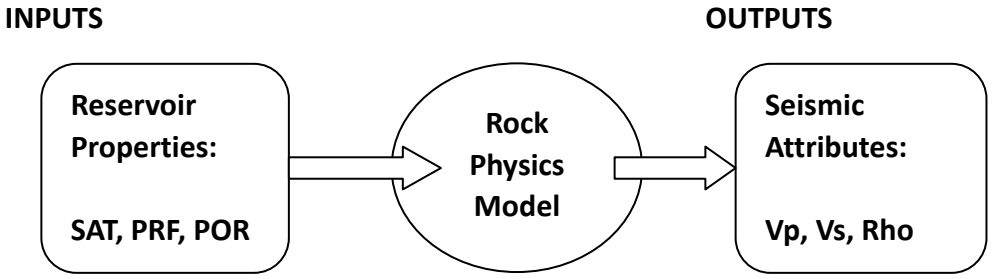

Figure 2.2 A brief scheme of the rock physics model

Details of the rock physics model are shown step by step as follow,

Model input: the reservoir properties – SAT, PRF, POR,

SAT = water saturation which could also be represented by S_w
PRF = pore pressure P_{pore}
POR = porosity ϕ,

Then, we could obtain that

$$P_{eff} = P_{over} - P_{pore}$$

$$C = 9.5 - (\phi - \phi_0) \times 28$$

where
P_{eff} = effective pressure
C = the average number of contact per grain
P_{over}= overburden pressure which is constant in this project
ϕ_0 = a starting porosity which is also constant and equals 0.36

Furthermore, the next step is to calculate the effective bulk K_{HM} and shear G_{HM} by applying Hertz-Mindlin theory below. (Details see the reference [4])

$$K_{HM} = \left[\frac{C^2(1-\phi_0)^2 G^2}{18\pi^2(1-\nu)^2} \times P_{eff}\right]^{\frac{1}{3}}$$

$$G_{HM} = \frac{5-4\nu}{5(2-\nu)}\left[\frac{3C^2(1-\phi_0)^2 G^2}{2\pi^2(1-\nu)^2} \times P_{eff}\right]^{\frac{1}{3}}$$

where
ν = the grain Poisson's ratio which is constant and equals 0.06 in this project
G = the grain shear modulus which is constant and equals 45 [GPa] in this project

To find the effective moduli (K_{eff} and G_{eff}) at different porosity ϕ, a heuristic modified Hashin-Strikman lower bound is used as follows.

$$K_{eff} = \left[\frac{\frac{\phi}{\phi_0}}{K_{HM} + \frac{4}{3}G_{HM}} + \frac{1-\frac{\phi}{\phi_0}}{K_{HM} + \frac{4}{3}G_{HM}}\right]^{-1} - \frac{4}{3}G_{HM}$$

$$G_{eff} = \left[\frac{\frac{\phi}{\phi_0}}{G_{HM} + \frac{1}{6}G_{HM}\left(\frac{9K_{HM}+8G_{HM}}{K_{HM}+2G_{HM}}\right)} + \frac{1-\frac{\phi}{\phi_0}}{G + \frac{1}{6}G_{HM}\left(\frac{9K_{HM}+8G_{HM}}{K_{HM}+2G_{HM}}\right)}\right]^{-1} - \frac{1}{6}G_{HM}\left(\frac{9K_{HM}+8G_{HM}}{K_{HM}+2G_{HM}}\right)$$

where
K = the grain bulk modulus which is constant and equals 36.6 [GPa] in this project

By far the most widely used and successful method for determining the effects of production-induced fluid change is the Gassmann substitution method (Gassmann, 1951), or called Gassmann equation. That model considers the rock to be composed of an assembly of rock grains with a frame modulus and a pore-volume fluid. The bulk modulus is given by the equation below.

$$S_o + S_w = 1$$

$$K_{fl} = \left(\frac{S_w}{2.715} + \frac{S_o}{0.5}\right)^{-1}$$

$$\rho_{fl} = S_w + \frac{4S_o}{5}$$

$$K_{sat} = K_{eff} + \frac{\left(1 - \frac{K_{eff}}{K}\right)^2}{\frac{\phi}{K_{fl}} + \frac{1-\phi}{K} - \frac{K_{eff}}{K^2}}$$

where
K_{eff} = effective bulk modulus of dry rock
K_{sat} = effective bulk modulus of the rock with pore fluid
K = bulk modulus of mineral material making up rock
K_{fl} = effective bulk modulus of pore fluid
ϕ = porosity

Other forms of the Gassmann equation are shown below,

$$\frac{K_{sat}}{K - K_{sat}} = \frac{K_{eff}}{K - K_{eff}} + \frac{K_{fl}}{\phi\left(K - K_{fl}\right)}, \quad \mu_{sat} = \mu_{dry}$$

where
μ_{dry} = effective shear modulus of dry rock
μ_{sat} = effective shear modulus of rock with pore fluid

$$K_{sat} = \frac{\phi\left(\frac{1}{K} - \frac{1}{K_{fl}}\right) + \frac{1}{K} - \frac{1}{K_{eff}}}{\frac{\phi}{K_{eff}}\left(\frac{1}{K} - \frac{1}{K_{fl}}\right) + \frac{1}{K}\left(\frac{1}{K} - \frac{1}{K_{eff}}\right)}$$

$$\frac{1}{K_{sat}} = \frac{1}{K} + \frac{\phi}{K_{eff} + \frac{KK_{fl}}{K - K_{fl}}}$$

$$K_{eff} = \frac{K_{sat}\left(\frac{\phi K}{K_{fl}} + 1 - \phi\right) - K}{\frac{\phi K}{K_{fl}} + \frac{K_{sat}}{K} - 1 - \phi}$$

Finally, in order to compute the seismic attributes Vp, Vs, Rho, we need additional expressions below.

$$\rho = \frac{\phi}{\rho_{fl}} + (1 - \phi) \times \rho_{grain}$$

$$V_p = \sqrt{\frac{K_{sat} + \frac{4}{3}\mu}{\rho}}$$

$$V_s = \sqrt{\frac{\mu}{\rho}}$$

where
ρ_{grain} is constant in this project and equals 2.65 [g/cm3]
μ = the shear modulus and does not depend on fluid, which equals the previous G_{eff}.

Until now, following these steps above, we can obtain those three seismic attributes Vp, Vs and Rho by using the reservoir properties SAT, PRF and POR. In the real world, engineers want to estimate the reservoir properties through the seismic attributes that they already have. An inverse problem that we can be defined is to solve those unknown input parameters by using the output observations. There are several previous approaches such as using stochastic inversion of seismic data to estimate the reservoir properties or other model inversion to predict them.

In this project, we would like to introduce another statistical inversion approach – probabilistic inversion for combining the rock physics to predict the reservoir properties. The advantage of this method is only to apply the forward model and develop a statistical inversion rather than model inversion, because it is often difficult to achieve a model inversion in the real world. In the next chapter, the basic ideas of probabilistic inversion and a simple example will be presented to illustrate how it works, and then we will build an experiment for applying this new mathematical inversion technique to the seismic data.

3. Probabilistic Inversion

The goal of this chapter is to introduce the probabilistic inversion technique developed in [1] and apply it to the seismic attributes in order to predict the reservoir properties. Firstly we present a mathematical formulation of the probabilistic inversion problem and the method of sample re-weighting that is going to be used later on in this thesis. We explain here relevant concepts using simple examples to give the reader an intuitive understanding of the method that is going to be applied. We conclude this chapter the application of probabilistic inversion to the seismic attribute data for estimating the reservoir properties is introduced.

3.1 Brief Introduction

Let us consider random vectors Y and X taking values in $\mathbb{R}^M$ and $\mathbb{R}^N$ respectively, and measurable function as follows,

$$F: \mathbb{R}^N \rightarrow \mathbb{R}^M$$

such that $Y = F(X)$. X is called the input of the model F, while Y is the output.

Probabilistic inversion problem is defined mathematically as follows,
Find a distribution of a random vector X such that $F(X) \sim Y$ which means that $F(X)$ and Y have the same distribution. There may be many solutions if the problem is feasible, then we need to find the best one. However, if the problem is infeasible, we have to search a distribution of X such that the distribution of $F(X)$ is as close as possible to the distribution of Y. We call X the probabilistic inverse of Y through the function F.

Inverting the model is usually very difficult. It requires sophisticated methods that need extra information about the problem as well as some intelligent steering. They are usually computationally expensive. We advocate here the use of the probabilistic inversion technique which is based on sample re-weighting. This is a very promising technique as it does not need any extra knowledge about the model. It avoids difficulty of inverting the model. However, it requires specific information about the output. Namely only few quantiles of Y (usually 5%, 50% and 95%) can be specified. This technique has been successfully applied in other inversion problems and we will test it here to the seismic attributes in order to predict the reservoir properties.

3.2 Detailed Introduction

As mentioned above, the main idea of probabilistic inversion is based on sample re-weighting. The strategy of sample re-weighting can be presented in an intuitive way below. The mathematical aspects and more details we refer the reader to [1, 2].

We start the sampling re-weighting method for probabilistic inversion by choosing a suitable initial distribution for the input. Large number of Monte Carlo samples for vector X is generated and propagated through the model. Obviously, the choice of this starting is important and influences the results. However, it has been noticed [1] that the results are usually not that sensitive to this choice. The starting distribution should contain all information that is available about inputs and can be obtain from experts, literature, etc. In general a wide distribution over possible ranges of input variable is chosen.

Information about quantiles of outputs is usually available from measurements. If we choose some 5%, 50% and 95% outputs then the initial samples can be prune by removing samples yielding values for outputs that are very 'far' from the measured ones (hence are much small than 5% or much bigger than 95% values). This is called conditional sampling. We will investigate the influence of initial distribution as well as an impact of conditional sampling later on this thesis.

Once the initial samples have been obtained and propagated through the model we can see if distributions of outputs have specified quantile information. If they do no extra procedure is necessary. This is however rarely the case. The sampling re-weighting procedure proposes to find weights for these samples such that after re-weighting outputs satisfy required quantile information.

The procedure is shown graphically in the following scheme (Figure 3.1)

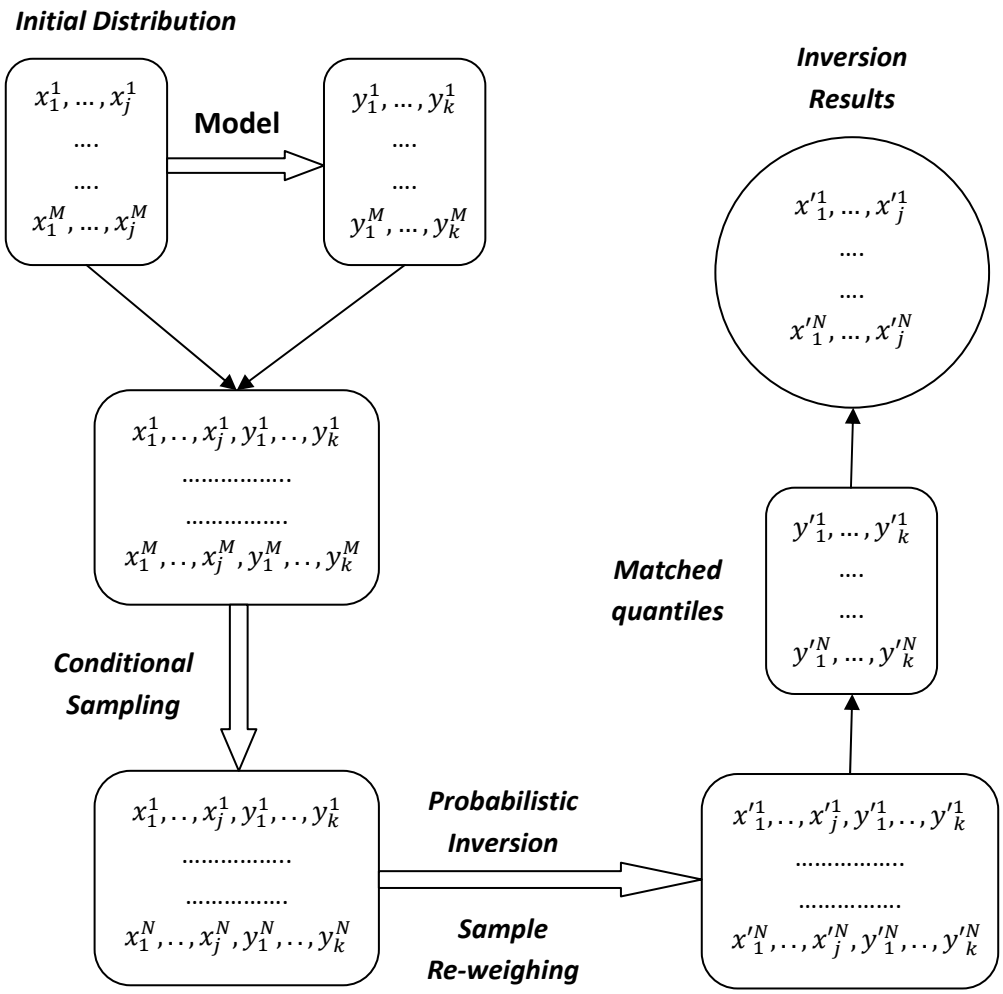

Figure 3.1 Probabilistic inversion scheme

The most challenging part of the sampling re-weighting procedure is to find the weight. We explain it on a simple intuitive example. Let us consider only one output Y which range is the interval [0, 1]. Moreover from measures or experts, we have acquired values of 5th, 50th, and 95th quantile of distribution of Y. In Figure 3.2 these values are indicated as 5%, 50% and 95%. The interquantile mass that is the mass between e.g. 5th and 95th quantile values is also shown in Figure 3.2 and is equal to 0.45.

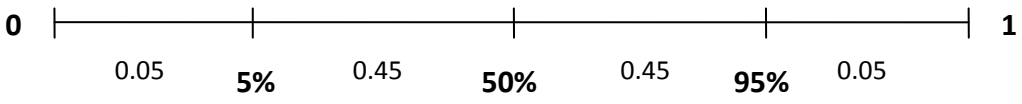

Figure 3.2 Quantiles example

We assume that there are 10 initial samples for Y. They all have the same weight initially. The initial sampling distribution of Y is shown in Figure 3.3

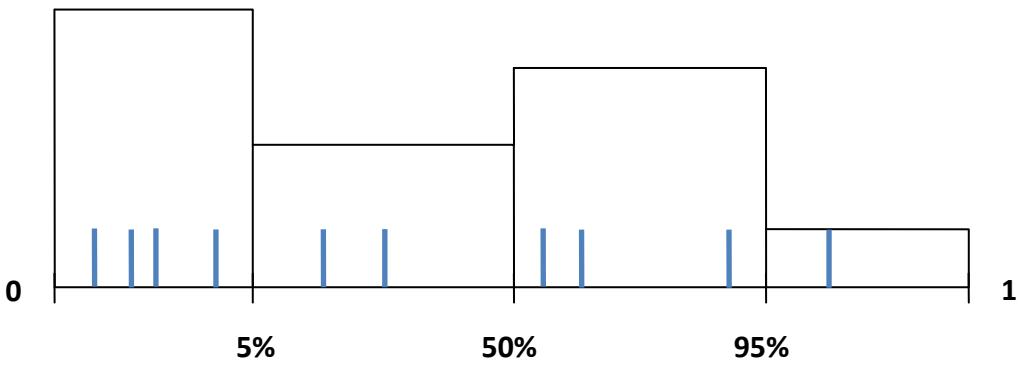

Figure 3.3 Before sample re-weighting

The mass in the first interquantile interval does not add to 0.05. It is equal to 0.4. Other interquantile intervals do not have the correct mass. The initial distribution is (0.4, 0.2, 0.3, 0.1). We need to re-weight these 10 samples in the first interquantiles will have to get much smaller weight than 1/10. It is easy in this case to see that the samples in the first interquantile interval will get weight equal to 0.05/0.4. Similarly for other interquantile intervals.

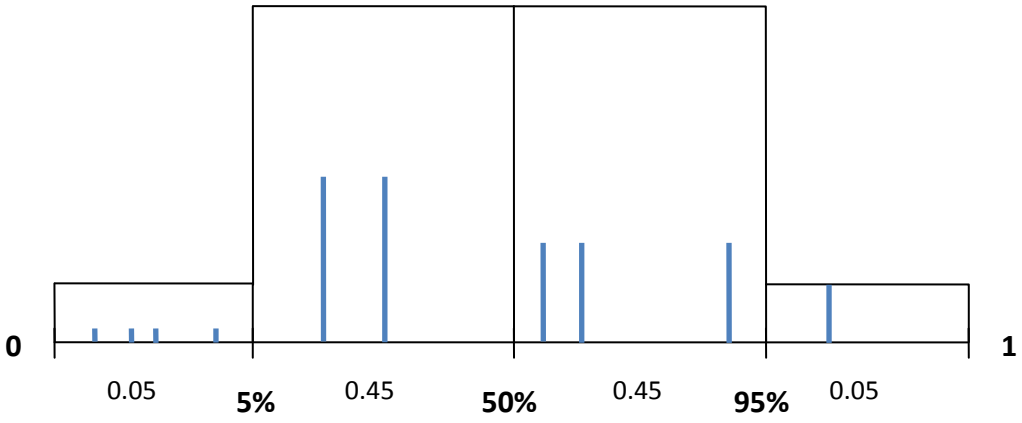

Figure 3.4 After sample re-weighting

After sample re-weighting, it looks like the above figure. (Figure 3.4) The mass of each interquantile equals 0.05, 0.45, 0.45, 0.05, respectivity.

For only one output it is easy to see how samples should be re-weighted. For multidimensional output we require methods to be able to find appropriate weight.

There are various ways for calculating the weights. We could find them using optimization methods. In [1] they are not advised as the number of samples for probabilistic inversion can be very large. We briefly present two iterative algorithms that can be used in finding weights:

IPF – Iterative Proportional Fitting
PARFUM – PARameter Fitting for Uncertain Models

Those two iterative methods adjust the starting weights in order to satisfy the quantiles constrains. We explain them on a simple example. For more details see [1, 2].

Let us consider two outputs Y_1 and Y_2. We measure 3 quantiles 5%, 50% and 95% of their distributions. As in one dimensional case we get 4 interquantile intervals for each output. Combined together they form a 4×4 matrix shown below. (Figure 3.5)

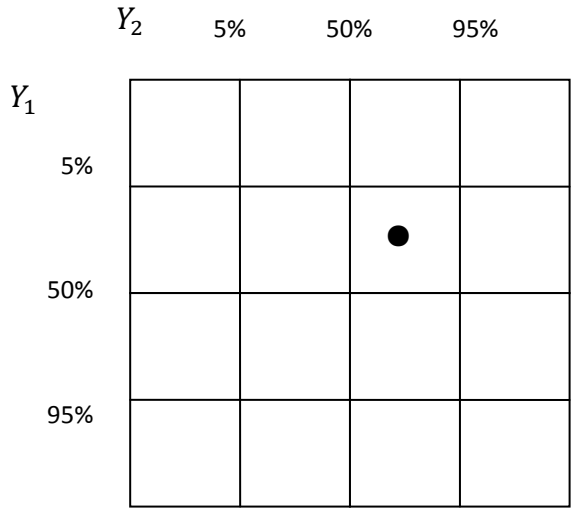

Figure 3.5 Interquantile cells

Each sample for Y_1 and Y_2 must fall into one cell of this matrix. If a sample falls into cell (2,3), then Y_1 is between 5% and 50% quantiles of its distribution and Y_2 between 50% and 95% quantiles (see the dot in Figure 3.5). Let us assume that we have 100 initial sample for the outputs Y_1 and Y_2. They are shown in Table 3.1.

5	7	8	4
5	11	3	6
6	4	9	1
2	8	13	8

Table 3.1 Number of samples in each cell

Hence the initial joint distribution of the output is obtained by dividing numbers in each cell by total number of samples and is shown in Table 3.2. Notice that marginal distributions for Y_1 and Y_2 are not (0.05, 0.45, 0.45, 0.05) as we would want. The margins are shown in Table 3.3.

0.05	0.07	0.08	0.04
0.05	0.11	0.03	0.06
0.06	0.04	0.09	0.01
0.02	0.08	0.13	0.08

Table 3.2 Probability in each cell

0.05	0.07	0.08	0.04		**0.24**
0.05	0.11	0.03	0.06		**0.25**
0.06	0.04	0.09	0.01		**0.20**
0.02	0.08	0.13	0.08		**0.31**
0.18	**0.30**	**0.33**	**0.19**		

Table 3.3 Initial and marginal distributions over interquantile cells

The idea is to iteratively change this distribution to get required margins. This is don with the following algorithms.

IPF – Iterative Proportional Fitting

The IPF algorithm was introduced in [1]. Intuitively in order to fit both margins IPF changes the distribution to fit first margin that alters this result to fit the second margin. This procedure is applied in turns to each margin as long as both margins are like required. The results of IPF for first two iterations are shown in Table 3.4 and 3.5

0.0104	0.0146	0.0167	0.0083		**0.05**
0.0900	0.1980	0.0540	0.1080		**0.45**
0.1350	0.0900	0.2025	0.0225		**0.45**
0.0032	0.0129	0.0210	0.0129		**0.05**
0.2386	**0.3155**	**0.2942**	**0.1517**		

Table 3.4 IPF row sums fit

0.0022	0.0208	0.0255	0.0027		**0.0512**
0.0189	0.2824	0.0826	0.0356		**0.4195**
0.0283	0.1284	0.3097	0.0074		**0.4738**
0.0007	0.0184	0.0321	0.0043		**0.0555**
0.0501	**0.4500**	**0.4499**	**0.0500**		

Table 3.5 IPF column sums fit

Notice that after these two steps our both margins are close to specified one. This is not always the case that the convergence is so fast but it is proved that IPF procedure converges if problem is feasible. If problem is infeasible (there is no distribution that has specified margins and the same support as the initial one) than IPF will not converge.

Results after some iterations are shown below. (Figure 3.6)

0.0021	0.0196	0.0258	0.0025		**0.05**
0.0207	0.2984	0.0937	0.0372		**0.45**
0.0266	0.1161	0.3007	0.0066		**0.45**
0.0006	0.0159	0.0297	0.0038		**0.05**
0.05	**0.45**	**0.45**	**0.05**		

Figure 3.6 IPF results

Iterative PARFUM – Iterative PARameter Fitting for Uncertain Models

The PARFUM algorithm was also introduced in [1]. The difference between IPF and PARFUM is that IPF adjusts rows and columns in turn while PARFUM develops fit row and fits column simultaneously, and takes averages of obtained distributions. Application of PARFUM algorithm to the example above yields distributions with row and column fits shown below.

0.0104	0.0146	0.0167	0.0083		**0.05**
0.0900	0.1980	0.0540	0.1080		**0.45**
0.1350	0.0900	0.2025	0.0225		**0.45**
0.0032	0.0129	0.0210	0.0129		**0.05**
0.2386	**0.3155**	**0.2942**	**0.1517**		

Table 3.7 PARFUM row sums fit

0.0139	0.1050	0.1091	0.0105		**0.2385**
0.0139	0.1650	0.0409	0.0158		**0.2356**
0.0167	0.0600	0.1227	0.0026		**0.2020**
0.0056	0.1200	0.1773	0.0211		**0.3240**
0.05	**0.45**	**0.45**	**0.05**		

Table 3.8 PARFUM column sums fit

The average of the above distributions can be then found and is shown in Table 3.9. Notice that after this first iteration margins are very far from what we have required.

0.0122	0.0598	0.0629	0.0094		**0.1443**
0.0519	0.1815	0.0474	0.0619		**0.3427**
0.0758	0.0750	0.1626	0.0125		**0.3259**
0.0044	0.0664	0.0992	0.0170		**0.1870**
0.1443	**0.3827**	**0.3721**	**0.1008**		

Table 3.9 PARFUM first iteration result

However, after several iterations we get the following result. (Table 3.10)

0.0006	0.0210	0.0275	0.0009		**0.05**
0.0206	0.2966	0.0924	0.0403		**0.45**
0.0286	0.1154	0.2984	0.0077		**0.45**
0.0002	0.0171	0.0317	0.0011		**0.05**
0.05	**0.45**	**0.45**	**0.05**		

Table 3.10 PARFUM result

In general PARFUM converges slower than IPF but it is proven that it converges even in the problem is infeasible.Notice that results obtained with IPF and PARFUM are not the same. We will investigate in this thesis whether the choice of the algorithm to find the weights has a big impact on the results.

3.2 PI Application on this Project

In this project, we aim to apply probabilistic inversion technique to the seismic data in order to predict the reservoir properties. The application of probabilistic inversion can be presented as following steps.

Let us assume that a reservoir contains n grid points. At each grid point we would want to know three reservoir properties such as SAT, PRF and POR. We denote these as SAT_i , PRF_i , and POR_i , where $i = 1, \dots, n$.

We choose suitable initial distributions SAT_i , PRF_i , and POR_i. It is know that SAT is in (0, 1), and PRF is around 5600 psi to 6100 psi, and POR is between 0 and 0.3. We could consider the simplest uninformative distribution over these ranges or acquire extra information if available. We generate M samples from the joint distribution of SAT_i , PRF_i , and POR_i. M should be quite large, as we are trying to approximate a very highly dimensional initial distribution.

$$(SAT_1, \dots, SAT_n, PRF_1, \dots, PRF_n, POR_1, \dots, POR_n)^j \qquad \text{where } j = 1, \dots, M$$

These samples of the reservoir properties are taken into the rock physics model in order to obtain the seismic attributes such as Vp, Vs and Rho at each grid point. These samples are denoted as follows,

$$(Vp_1, \dots, Vp_n, Vs_1, \dots, Vs_n, Rho_1, \dots, Rho_n)^j \qquad \text{where } j = 1, \dots, M$$

We have M samples, and each of them contains both reservoir properties and seismic attributes.

$$(SAT_1, \dots, SAT_n, PRF_1, \dots, PRF_n, POR_1, \dots, POR_n, Vp_1, \dots, Vp_n, Vs_1, \dots, Vs_n, Rho_1, \dots, Rho_n)^j$$
$$\text{where } j = 1, \dots, M$$

At this point we could check if all seismic attributes obtained from the initial samples are physically possible and cover the range of their realistic values. If not we should remove those unrealistic or unreasonable samples. After this conditional sampling, we have N samples containing both reservoir properties and seismic attributes.

$$(SAT_1, \dots, SAT_n, PRF_1, \dots, PRF_n, POR_1, \dots, POR_n, Vp_1, \dots, Vp_n, Vs_1, \dots, Vs_n, Rho_1, \dots, Rho_n)^j$$
$$\text{where } j = 1, \dots, N$$

It would be a miracle if all Vp, Vs, Rho have specified quantile information, hence at this point the probabilistic inversion via sample re-weighting is performed. We use iterative algorithms (IPF or PARFUM) to re-weight those N samples to specify measurement information.

Finally, after re-sampling we obtain the sampling distribution of the model input vectors SAT, PRF and POR. The scheme of probabilistic inversion technique application for this project is shown below:

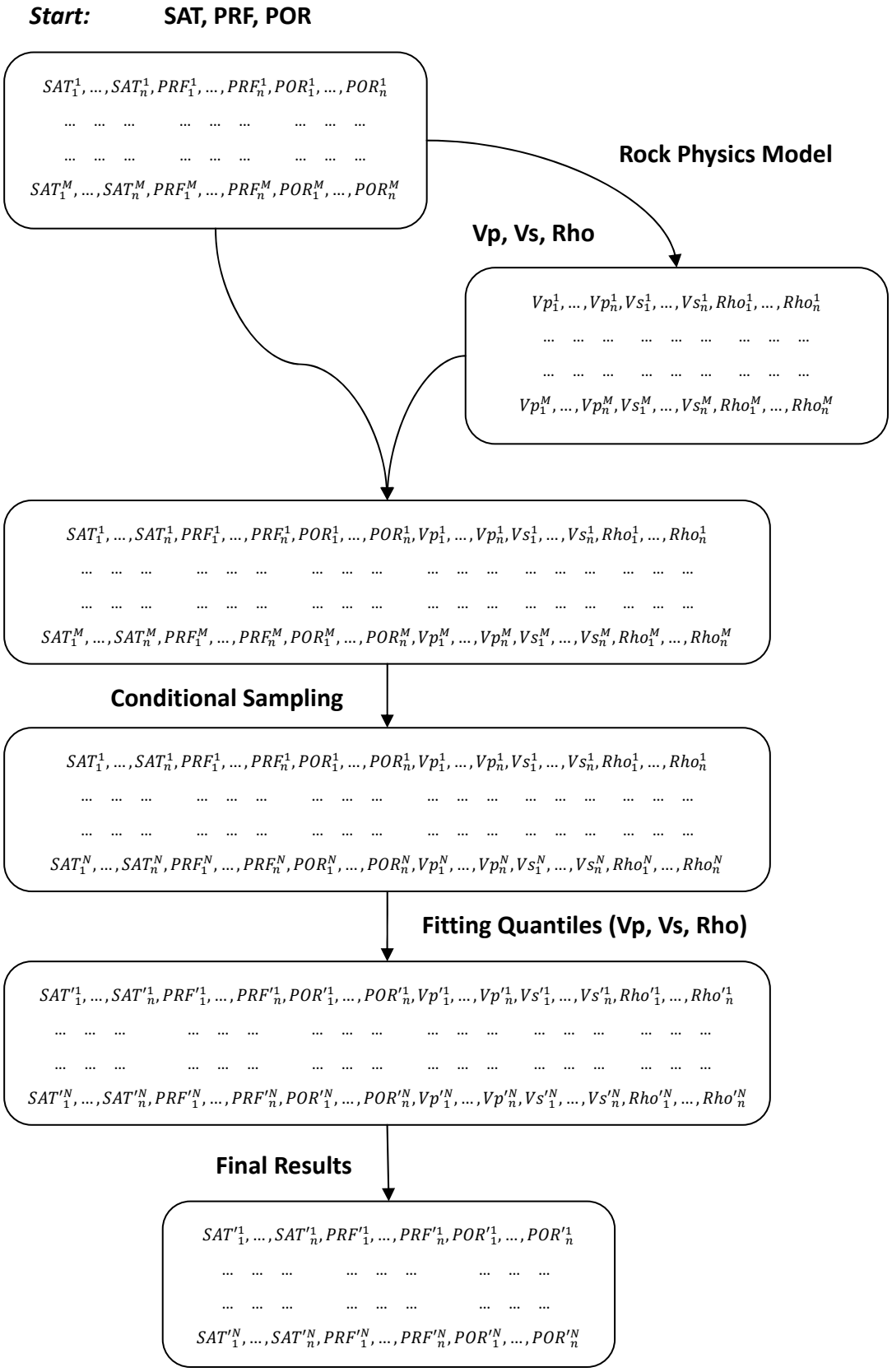

Figure 3.6 Scheme of probabilistic inversion technique application for this project

4. Experiments and Results

In the previous chapters, we presented the introduction of reservoir engineering and probabilistic inversion technique. Furthermore, the application of probabilistic inversion for this project was introduced. In this chapter, we will perform a series of experiments for applying probabilistic inversion to the seismic data where following the scheme mentioned in the last section of chapter 3.

In the first section of this chapter, we will setup an experimental scheme in order to make sure how to develop different experiments. Secondly, conditional sampling for this project will be introduced. After that, we will illustrate a large number of experiments from different aspects, most of the results and comparisons. Besides, a series of discussions related to probabilistic inversion will be presented so as to analyze the influence of different probabilistic inversion setting options on the final results. Last but not least, we will develop sensitivity analysis based on the results that we obtained.

4.1 Setup an Experimental Scheme

A reservoir can be represented as a grid structure, while each grid point or each position has its own reservoir properties such as water and oil saturation, pore pressure, porosity, permeability, etc. and seismic attributes such as velocity of P-waves, velocity of S-waves and density.

In this project, there are 4125 grid points to represent the given reservoir, and the grid structure of reservoir is 15×25×11, where 15 points are in the x-coordinate, 25 points are in the y-coordinate and 11 points are indicated the depth of reservoir, namely, the vertical direction, z-coordinate. However, in the real world, engineers apply seismic method to obtain different seismic attributes. They could not gain seismic data such as Vp, Vs and Rho from each grid point, and they just analyze the changes of the elastic waves' properties to estimate seismic attributes at different positions in the same layer. Thus, we do our experiments for each layer or all vertical grid points which equals 15×25=375 grid points. Figures are shown below. (Figure 4.1 and 4.2)

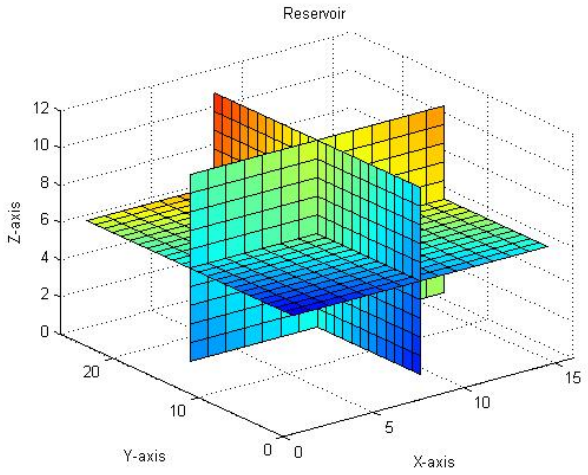

Figure 4.1 Reservoir grid structure

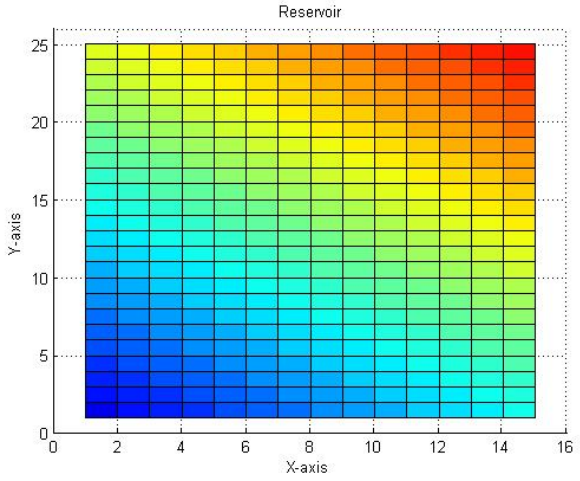

Figure 4.2 Horizontal plane (15×25 grid points)

For probabilistic inversion technique, the number of variables is equal to 375×3=1125, because there are 375 grid points to represent this reservoir and each point contains 3 different seismic attributes – Vp, Vs and Rho, which are the observable variables. Following the scheme in the previous chapter, if we apply 3 quantiles or called 4 interquantiles for each variable, there are 4^{1125} interquantile cells for all of them. Moreover, we need to generate a quite large number of samples in order to satisfy that some of them fall into each cell. This is not a problem for probabilistic inversion technique, but it is difficult for the software and computer that we used now. Therefore, we decide to build a small experiment to apply probabilistic inversion to the seismic data firstly so as to analyze and evaluate the application of this new technique. We will develop other experiments with more variables if the level of computer and software are improved. Here, we discuss the reservoir which could be

divided into 5×5=25 grid points in the horizontal direction. It means that we combine 15 grid points together as 1 grid point, namely, 3 from x-axis and 5 from y-axis. In the vertical direction, the technique is similar as the previous one, which means we perform the experiment for each layer or the mean value of all layers. The number of grid points equals 25, while the observable variable is 25×3=75. Following the notation in the application of probabilistic inversion, the letter n is equal to 25. Two new grid structures of the reservoir that we used are shown as follows. (Figure 4.3 and 4.4) Furthermore, we order all grid points from 1 to 25 in the following table. (Table 4.1)

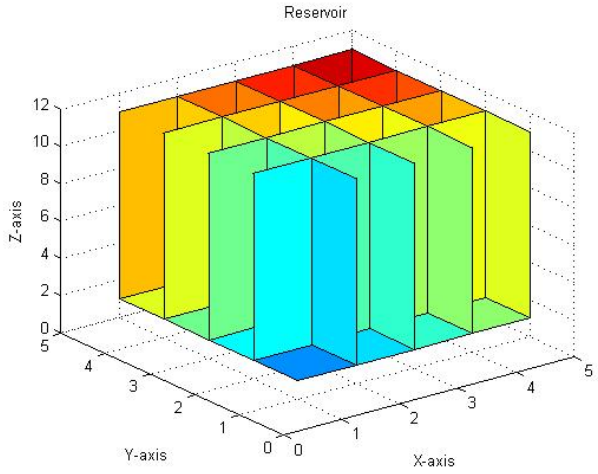

Figure 4.3 A reservoir 5×5 grid structure

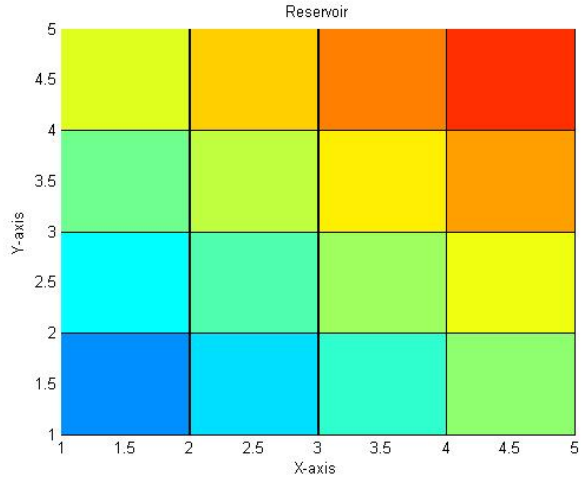

Figure 4.4 A reservoir grid structure in 2D

5	10	15	20	25
4	9	14	19	24
3	8	13	18	23
2	7	12	17	22
1	6	11	16	21

Table 4.1 the order of all 25 grid points

Next step is to determine the scheme of combining probabilistic inversion technique with the seismic data. Experimental details can be presented as follows,

a. From the reservoir simulation program, we could obtain samples of each reservoir property at each grid point, or the distribution for each property. We assume those as a truth for this reservoir. Actually, engineers do not know these kinds of data before using a particular seismic inversion or measure these directly.

b. The data of those reservoir properties are taken into the Rock Physics Model, and we could obtain the values of seismic attributes at each point. We suppose these seismic data we measured in the real world. The use of all seismic data is to calculate different quantiles for each attribute at one grid point. As for a particular real reservoir, engineers can measure these seismic attributes using advanced seismic instrument for computing the quantiles.

c. From now on, we assume that we do not know the data of reservoir properties anymore until evaluate the application of probabilistic inversion. Now, we are beginning to use probabilistic inversion technique to estimate reservoir properties. Firstly, we create a large number of samples with different initial distributions for each property based on the information concerning the reservoir that we know about. We then put these samples into the rock physics model in order to obtain the corresponding samples for the seismic attributes. Secondly, we apply probabilistic inversion technique to these seismic attributes samples following the scheme of probabilistic inversion with the quantile constraints that we gained in the previous step or in a real measurement. The details of how probabilistic inversion works has been presented in chapter 3. Last but not least, we can compare the final results concerning the reservoir properties estimated from probabilistic inversion with the truth values that we assumed above.

d. Evaluated the new inversion method on the seismic data can be performed, as well as analyzed the influences on these data. Moreover, we can try to find better ways to predict reservoir properties and to decrease uncertainties in this project.

The scheme of these steps are shown below,

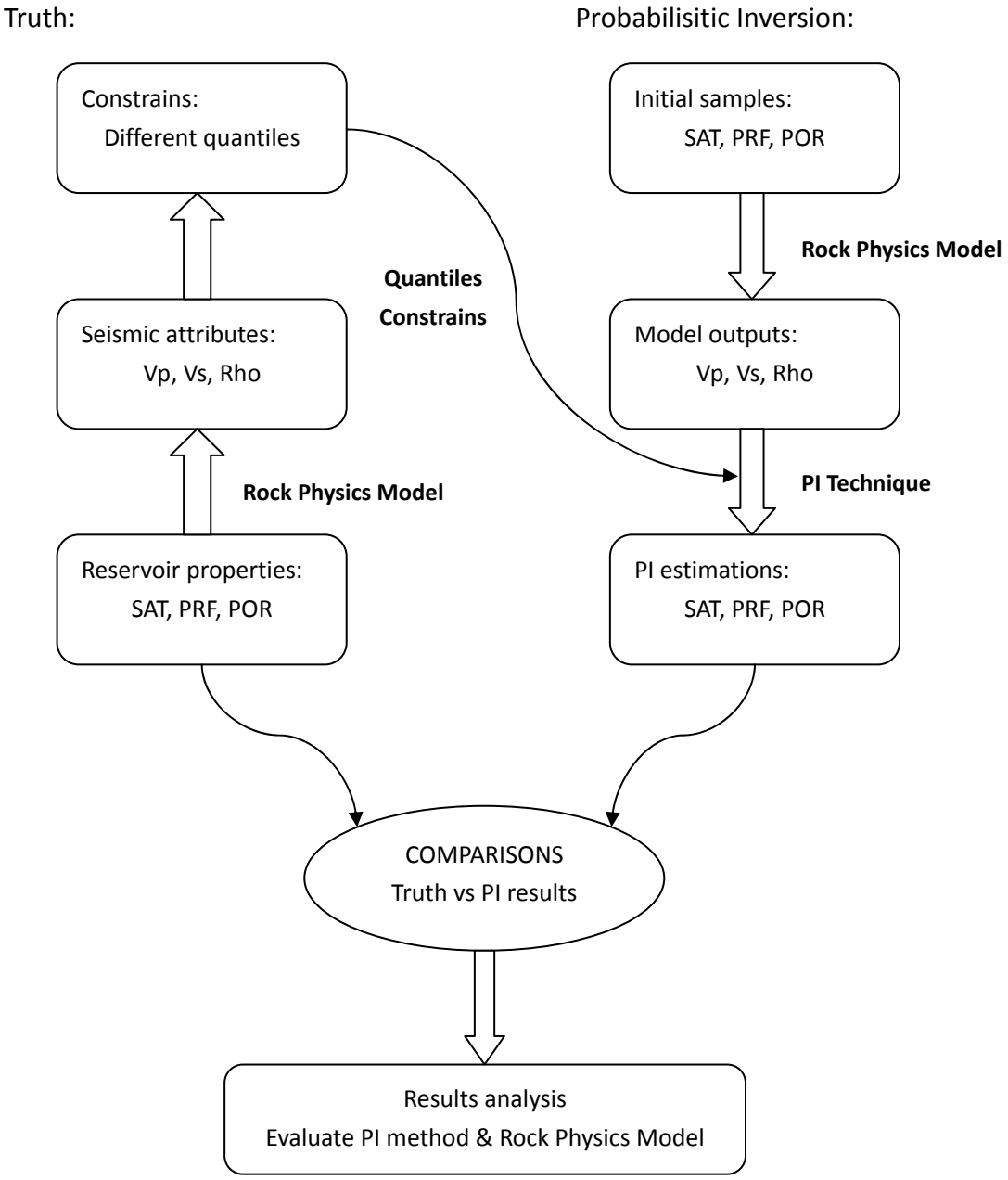

Figure 4.5 Experimental scheme

In the next section, we will perform a series of experiments from different aspects for applying probabilistic inversion method to the seismic data. After that, we will discuss other influence concerning the final results such as comparing different probabilistic inversion methods – IPF and PARFUM, analyzing the results after changing the number of quantiles, iteration steps and the number of input samples. The most important part is to try to find effects of the starting distribution for

generating samples for each variable such that the predictions of probabilistic inversion technique will be as close as the truth that we assumed. Thus, engineers could apply this new inversion method to the seismic data for estimating the reservoir properties in the real world in future.

4.2 Conditional Sampling

Conditional sampling is to add some certain conditions on the samples of the observable variables of probabilistic inversion. In the introduction of probabilistic inversion part, we presented the reason that why we perform conditional sampling before applying sample re-weighting, and we will apply this to the project. Following the experimental scheme (Figure 4.5) of probabilistic inversion part, we generate a large number of samples related to the initial distribution of every reservoir property in its range based on the information that engineers have already known. After we put these samples into the rock physics model to obtain the samples of seismic attributes for probabilistic inversion, we could add some particular conditions on those samples in order to improve the approach and to gain better final results. Although the samples of reservoir properties that we generated are in their domains, it is possible that some samples of seismic attributes from the rock physics model are already out of their realistic intervals. Thus, we could remove those unreasonable samples which may affect on the final results.

In this project, we could obtain 5% quantile and 95% quantile from outputs of the rock physics model or in a real measure procedure. Moreover, we choose 2% quantile and 98% quantile as the conditions of the samples of observable variables, where can make sure each interquantile contains some samples. Those samples that we obtained from the initial distributions after the rock physics model but out of this interval should be removed. Thus, different variables at each grid point have different conditions. There is an example in the following table concerning sample conditions of seismic attributes – Vp, Vs and Rho. (Table 4.2)

In the real world, researchers or engineers know about ranges of different seismic attributes or obtain from many times measures. They can put conditions on the outputs of the rock physics model before applying probabilistic inversion. It could improve the calculation of probabilistic inversion.

	Truth quantiles		Sample conditions	
	5%	95%	2%	98%
Vp1	3445.5890	5726.3162	3335.2387	5986.6067
Vp2	3712.0514	5646.0314	3404.1102	5816.6149
Vp3	3441.8614	5673.1387	3253.3386	5859.9169

Vp4	3011.5835	5626.8290	2762.4084	5875.1647
……	……	……	……	……
Vp22	3574.4854	5846.5378	3368.7049	6017.2374
Vp23	3402.5206	5582.4046	3032.4258	5757.2376
Vp24	3339.1848	5856.8075	2943.4048	6017.8228
Vp25	3429.7307	5846.8440	2450.8352	5966.2491
Vs1	1929.5785	3843.6809	1804.8294	4076.3084
Vs2	2062.8284	3771.6121	1940.9911	3927.5070
Vs3	1909.4684	3797.5281	1778.4263	3962.0021
Vs4	1584.1419	3754.0138	1373.6756	3979.3633
……	……	……	……	……
Vs22	2052.8107	3945.8880	1902.2855	4101.6562
Vs23	1863.7406	3722.3608	1632.7440	3865.7011
Vs24	1753.8006	3958.3329	1508.2085	4103.3939
Vs25	1952.7483	3951.7455	1134.6026	4057.6292
Rho1	2.1897	2.6191	2.1468	2.6452
Rho2	2.2528	2.6105	2.1866	2.6286
Rho3	2.1852	2.6134	2.1365	2.6329
Rho4	2.0488	2.6080	1.9550	2.6344
……	……	……	……	……
Rho22	2.2324	2.6316	2.1725	2.6481
Rho23	2.1770	2.6034	2.0606	2.6224
Rho24	2.1499	2.6326	2.0149	2.6482
Rho25	2.1921	2.6316	1.8223	2.6433

Table 4.2 Sample conditions of the seismic attributes

From the above table, we could find the conditions for each variable. The number of removed samples depends on how to choose the conditional interval and the initial distribution for creating samples. For the influence on the final estimations of conditional sampling, we will compare and discuss in the latter section.

4.3 Main Experiments

In this section, we will perform several main experiments to estimate reservoir properties in order to evaluate the applications of probabilistic inversion on seismic data. As mentioned in previous chapters, the starting distributions of reservoir properties play vital roles in the probabilistic inversion scheme. We should create samples related to the starting distributions based on information of the reservoir properties that engineers have already know or could obtain. If the initial distributions are not quite far from the truth, it is easy for probabilistic inversion to

give good estimations of reservoir properties. On the other hand, it is quite hard to fit the measurable quantiles if the starting distributions are far away from the realistic ones.

Following the steps presented in chapter 3 in the next experiments, we will generate samples based on different starting distributions for the reservoir properties – SAT (saturation), PRF (pressure) and POR (porosity) such as uniform distribution, gamma distribution, normal distribution, lognormal distributions and beta distribution with different parameter coefficients. Those distributions should be based on the information of reservoir that engineers have known such as the mean or range of each property. Taking those samples into the rock physics model, we could obtain samples of the seismic attributes. The matrix which contains both reservoir properties and seismic attributes should be put into the probabilistic inversion technique. After that, the seismic attributes are imposed on some quantiles constrains which we get from the truth part or from the measures in the real world. Applying the idea of sample re-weighting, each sample could get its own weight and probabilistic inversion provides the estimations of reservoir properties. Finally, we could compare and analyze those results with the truth that we assumed.

In this section, the setting options of probabilistic inversion technique are shown in the following table. (Table 4.3) We will explain how to decide these setting options in the following discussion section. The questions might be like as follows.

1. Why do we generate 60,000 samples? Can we use more samples or less?
2. What is the influence on the final estimations of conditional sampling?
3. Why do we perform all experiments using IPF method? Is it possible to use another iterative method – PARFUM.
4. Why do we use 3 quantiles such as 5%, 50% and 95%? Could we take more quantiles, and what is the influence?
5. Why do we take 100 iteration steps? Can we take more iteration or less?

We will present the explanations for all of the above questions in the following discussion.

# Samples	60,000
Starting distributions	Depend on each experiment
Conditional sampling	Yes
Method	IPF
Probability quantiles	3 (5%, 50%, 95%)
# Iteration steps	100

Table 4.3 Setting options of all main experiments

Actually, in this project, we performed hundreds of experiments based on different starting distributions or a particular distribution with different parameter coefficients. It is easy for probabilistic inversion approach to match the measurable quantiles if the distribution is not quite far away from the real one. Otherwise, it is also difficult for this iteration method to close the truth. Hence, the main target is to try to find out proper initial distributions for each variable based on the information of reservoir properties that engineers could know or measure them in the real world.

Here, we just discuss a few experiments that we performed, and show that which property that probabilistic inversion could estimate well and which is not. Besides, we try to find out the reasons of those phenomena in order to improve the application of probabilistic inversion to obtain better results.

4.3.1 Experiment I

In the first experiment, the starting distributions of reservoir properties for generating samples are presented in the table below. (Table 4.4) We know about the range of each reservoir property. Uniform and normal distributions are simple. Thus, we generate normal distribution for pore pressure (PRF) and uniform distributions for water saturation (SAT) and porosity (POR) as the following three starting distributions.

For instance, the values of saturation should be between 0 and 1, and the range of pressure is from 5600 psi (pound per square inch) to 6100 psi where we choose the median and generate normal distribution for cover the range, and the interval of porosity that we choose is from 0 to 0.3.

Reservoir property	Starting distribution
SAT (saturation)	Uniform (0,1)
PRF (pressure)	Normal (5850,50)
POR (porosity)	Uniform (0,1) × 0.3

Table 4.4 Initial distributions of the 1st experiment

Result IPF

	Q1	Q2	Q3
Vp1	0.04988	0.49904	0.94949
Vp2	0.04996	0.49954	0.94952
Vp3	0.04997	0.49970	0.94995
Vp4	0	0.47370	0.94741
Vp5	0.05000	0.49978	0.94946
Vp6	0.04993	0.49962	0.94981
Vp7	0.05008	0.50060	0.95060
Rho19	0.05001	0.50005	0.94996
Rho20	0.05000	0.49998	0.95001
Rho21	0.05002	0.50005	0.95002
Rho22	0.04998	0.49994	0.94999
Rho23	0.05035	0.50018	0.95002
Rho24	0.04997	0.49980	0.95002
Rho25	0.05000	0.50000	0.95000

	Errors
1	9.85245856146855E-05
2	4.08243712220688E-05
3	3.16010376768178E-05
4	2.7991207779767E-05
5	2.59003416045715E-05
6	2.42733698637406E-05
7	2.29401760429178E-05
94	6.45161148172216E-06
95	6.43233323407734E-06
96	6.41399980564848E-06
97	6.3960567006163E-06
98	6.37895967098238E-06
99	6.3627158631251E-06
100	6.34669835430485E-06

	Weights
1	2.3517729759726E-08
2	2.20084973938649E-05
3	0.000778243027829275
4	0.000584120166715135
5	0.000269693585023167
6	1.276749494981 68E-08
7	3.491131748976 93E-05
61207	1.487647812002 97E-07
61208	1.173924420795 29E-09
61209	1.166680996151 25E-06
61210	5.671858977738 24E-07
61211	1.492464282757 82E-05
61212	1.212084096901 59E-11
61213	1.051977979085 95E-07

Figure 4.6 Result, errors and weights of the 1st experiment

In Figure 4.6, as for the result of IPF, there is a variable that Q1 equals 0. It means there is no sample in the interquantile interval 0 to 0.05 after conditional sampling, while other quantiles do not fit quite well. The way to solve this problem is to take more samples in future experiment. In the middle part, errors are decreasing step by step. There are more than 60,000 input samples in this experiment, and each of them gains its own weight.

	Truth	Before PI	After PI
POR	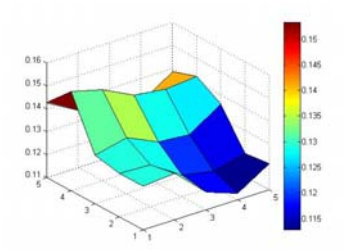	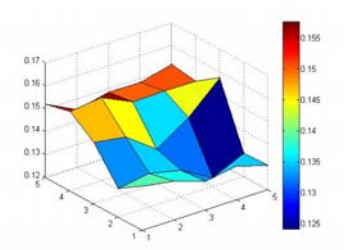	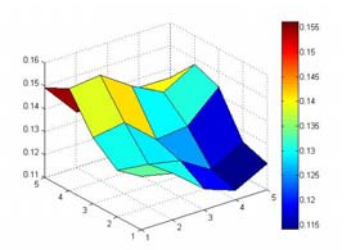
SAT	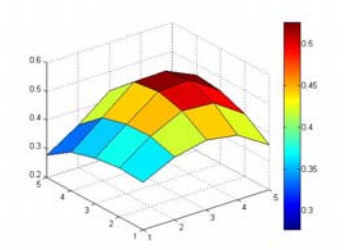	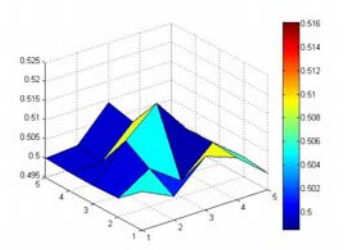	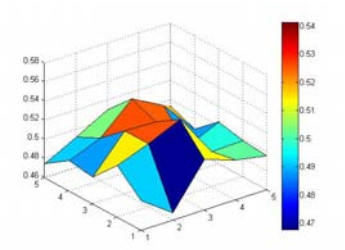

PRF

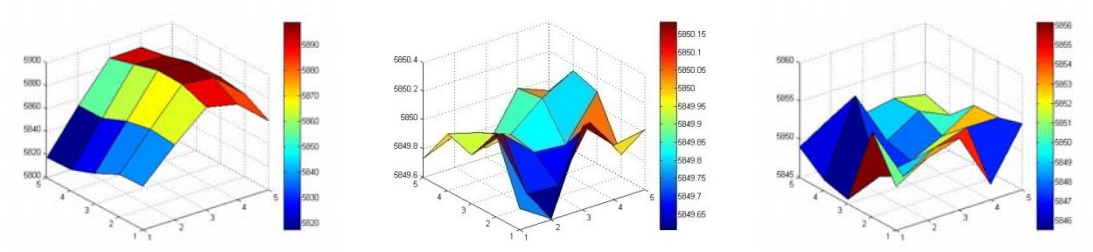

Vp

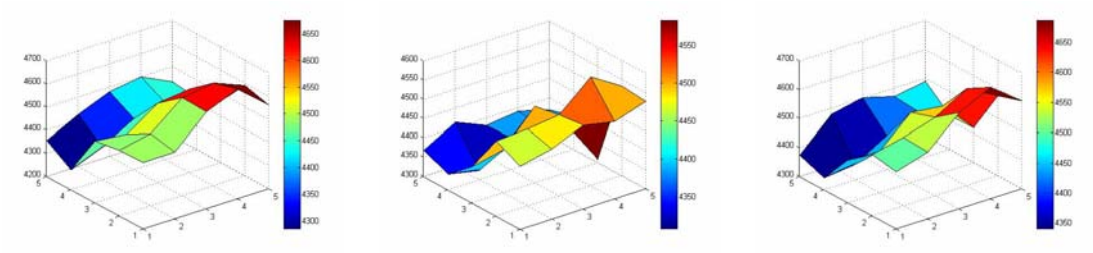

Vs

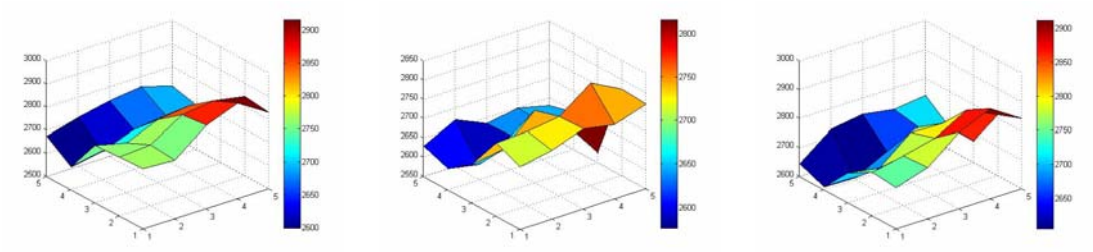

Rho

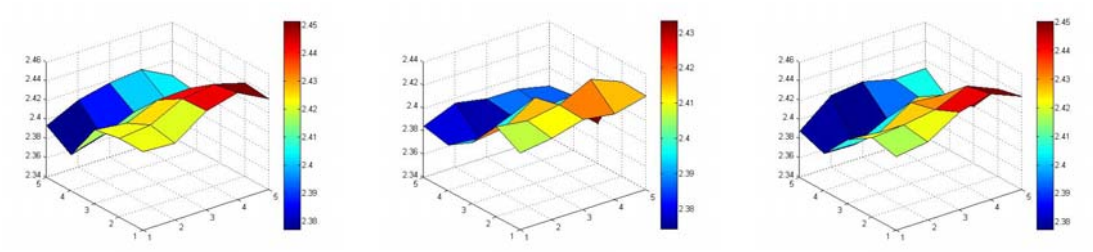

Figure 4.7 Comparison between truth, before PI and after PI in experiment I

After conditional sampling, one of the reservoir properties – POR and all seismic attributes are already closed to the truth. By contrast, the other two reservoir properties – SAT and PRF is far away from the real ones. We performed IPF method with uniform starting distribution and normal distribution using 3 quantiles in the first experiment. Three seismic attributes are all matched measurement quantiles, and we could conclude that those are similar as the truth, but we can still easily find out the differences between them. Probabilistic inversion can give a good estimation of POR, but for SAT and PRF, those are not the same or similar as the truth that we

assumed.

In this experiment, we just generated the starting distributions based on the domain information of each reservoir property. We tend to try to change the initial distributions for finding better estimations of the reservoir properties.

4.3.2 Experiment II

Starting from the second experiment, we will apply another class of important distribution as the reservoir properties starting distribution which is the beta distribution. The curves of probability density function of the beta distribution are shown in the following figure. (Figure 4.8)

There are several advantages of the beta distribution. In probability theory and statistics, the beta distribution is a family of continuous probability distribution which defined on the interval from 0 to 1 and parameterized by two positive shape parameters using α and β.

We will present some properties of the beta distribution firstly, and then show the results of application of probabilistic inversion.

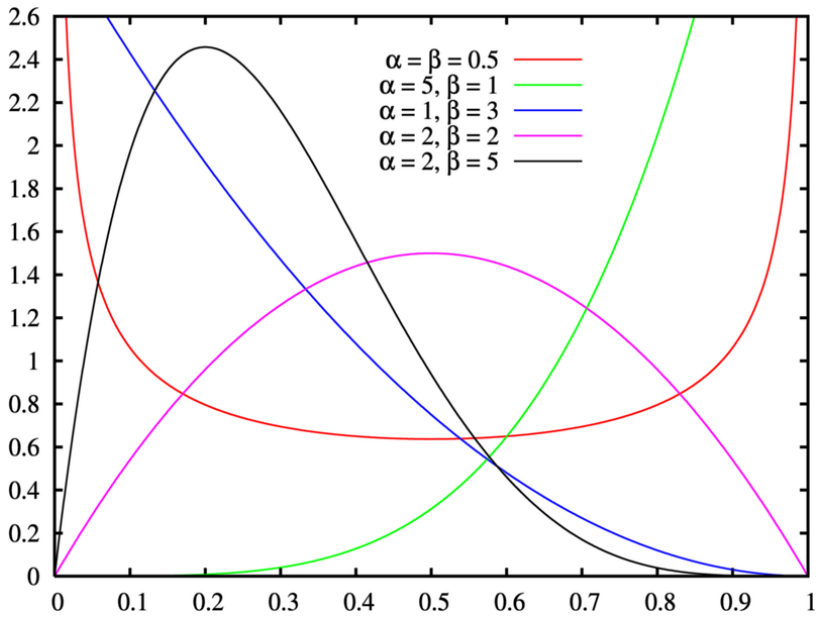

Figure 4.8 Curves of PDF of beta distribution with different coefficients

Generally speaking, the probability density function of beta distribution with two

parameters α and β is given by,

$$f(x;\ \alpha,\beta) = \frac{x^{\alpha-1}(1-x)^{\beta-1}}{\int_0^1 u^{\alpha-1}(1-u)^{\beta-1}du}$$
$$= \frac{\Gamma(\alpha+\beta)}{\Gamma(\alpha)\Gamma(\beta)} x^{\alpha-1}(1-x)^{\beta-1}$$
$$= \frac{1}{\mathrm{B}(\alpha,\beta)} x^{\alpha-1}(1-x)^{\beta-1}$$

where Γ is the gamma function. The beta function B, appears as a normalization constant to ensure that the total probability integrates to unity.

As mentioned before, the domain of beta distribution is between 0 and 1. Moreover, the mean is equal to the value of $\frac{\alpha}{\alpha+\beta}$, while the variance is $\frac{\alpha\beta}{(\alpha+\beta)^2(\alpha+\beta+1)}$.

In this experiment, we generate the starting distributions of saturation at each grid point using the beta distribution, but we choose different parameter coefficients for each reservoir property. The settings of starting distributions are shown in the following table. (Table 4.5)

Reservoir property	Starting distribution
SAT (saturation)	Beta (2,2)
PRF (pressure)	Beta (3,2) × 500+5600
POR (porosity)	Beta (2,4) × 0.5

Table 4.5 Starting distributions of the 2nd experiment

SAT can be applied a starting distribution with coefficients $\alpha = 2$ and $\beta = 2$ which satisfies all of sample values in the domain of saturation, and the mean is equal to $\frac{\alpha}{(\alpha+\beta)} = 0.5$ which is the median of the domain. As for POR, we create its distribution using the beta distribution with coefficients $\alpha = 2$ and $\beta = 4$. Furthermore, all of porosity distributions multiply by a coefficient 0.5, because most values of porosity should be smaller than 0.3 for this given reservoir, and the mean of this beta distribution is equal to $0.5 \times \frac{\alpha}{(\alpha+\beta)} = 0.15$ which is around the half of the interval. We generate another beta distribution with parameter coefficients $\alpha = 3$ and $\beta = 2$ for PRF, while all the values should be in the interval between 5600 psi and 6100 psi.

Result IPF

	Q1	Q2	Q3
Vp1	0.04992	0.49947	0.94975
Vp2	0.04999	0.49983	0.94985
Vp3	0.05008	0.50006	0.94985
Vp4	0.05000	0.50006	0.94998
Vp5	0.04979	0.49938	0.94949
Vp6	0.05000	0.49993	0.94989
Vp7	0.05001	0.49985	0.94975
...	...	...	...
Rho19	0.05000	0.50009	0.95001
Rho20	0.04999	0.49994	0.94998
Rho21	0.05000	0.50000	0.95001
Rho22	0.05000	0.49994	0.94997
Rho23	0.04998	0.49993	0.95000
Rho24	0.04999	0.50001	0.94999
Rho25	0.05000	0.50000	0.95000

	Errors
1	9.30348530354487E-05
2	3.48292926346521E-05
3	2.77562984240451E-05
4	2.40231343864515E-05
5	2.16649054943663E-05
6	1.99034053230449E-05
7	1.85079979440841E-05
...	...
94	8.09208277527836E-07
95	7.94003357923871E-07
96	7.79141742049795E-07
97	7.6471751208835E-07
98	7.50640853634688E-07
99	7.36885843952232E-07
100	7.23444115893745E-07

	Weights
1	1.88409727408756E-06
2	2.05684791526368E-06
3	3.89346662712915E-07
4	5.24792164014 63E-07
5	9.58078708513522E-09
6	2.15930907059463E-06
7	2.55662291572589E-06
...	...
63915	2.09507844186604E-06
63916	3.72038997169049E-06
63917	2.69930037983274E-07
63918	1.57829090572946E-06
63919	9.95533904030997E-07
63920	7.54017395702508E-07
63921	3.82433523979789E-06

Figure 4.9 Result, errors and weights of the 2nd experiment

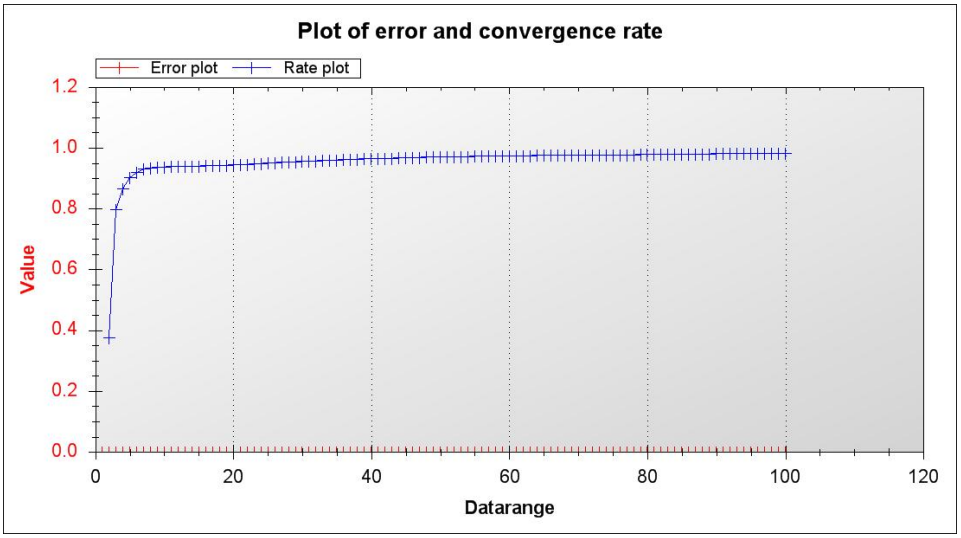

Figure 4.10 Error and convergence rate of IPF in the 2nd experiment

After running probabilistic inversion software, results are shown in the two above figures. (Figure 4.9, Figure 4.10) For each variable, its probability quantiles are almost the same as the quantiles that we chosen. Error is decreasing step by step, and each sample gains its weight after 100 iteration steps. Outputs of re-samples are shown as below.

Truth Before PI After PI

POR

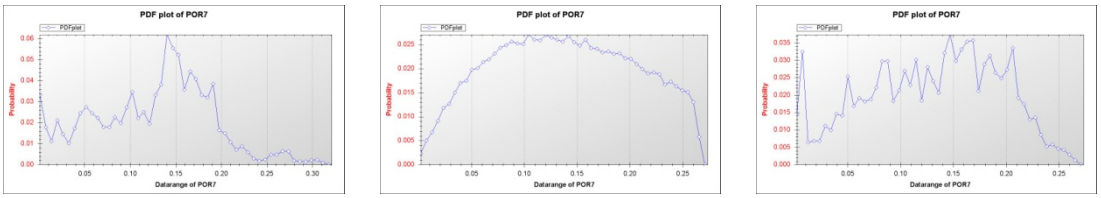

SAT

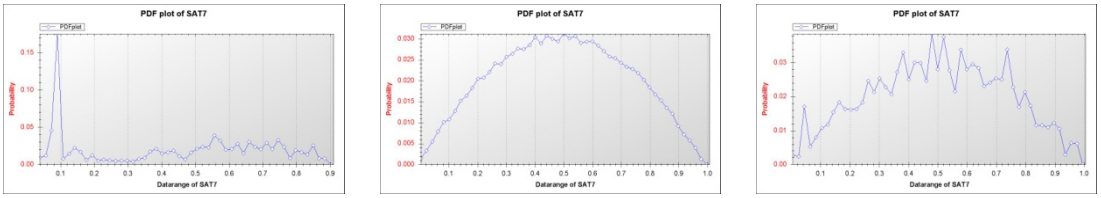

PRF

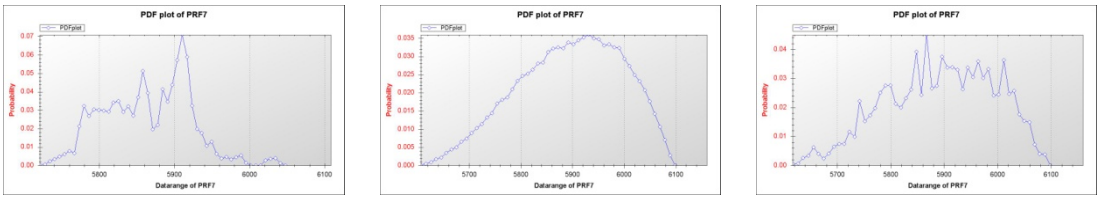

Vp

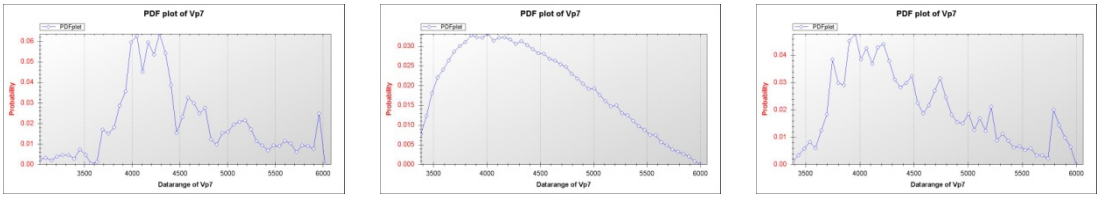

Vs

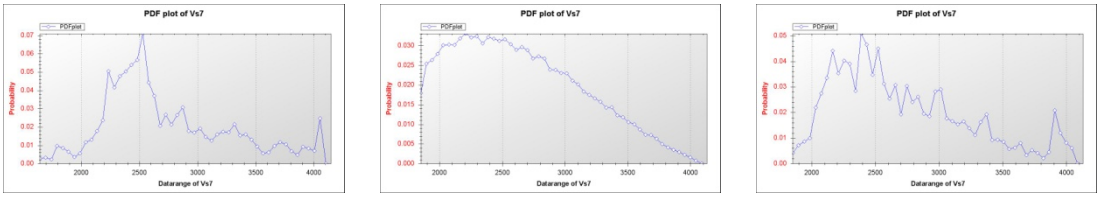

Rho

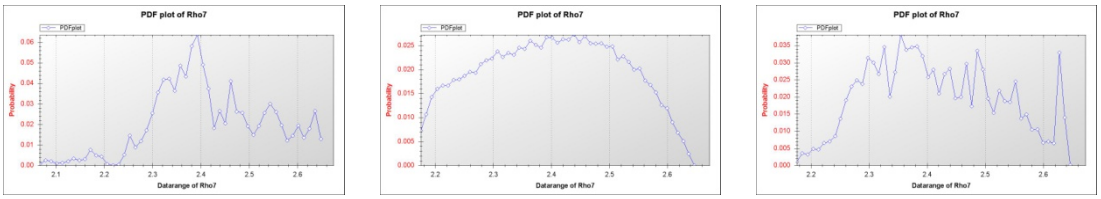

Figure 4.11 Comparisons at the 7th grid point

	Truth	Before PI	After PI
POR	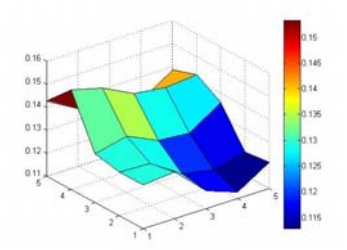	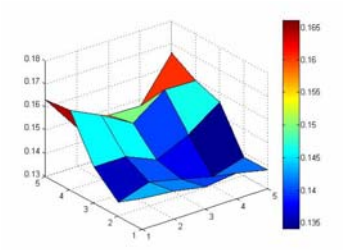	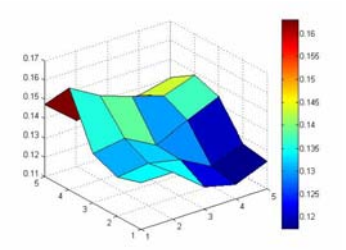
SAT	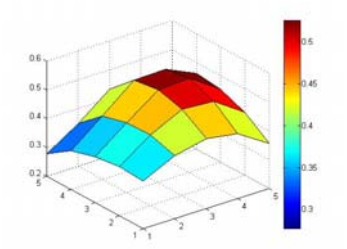	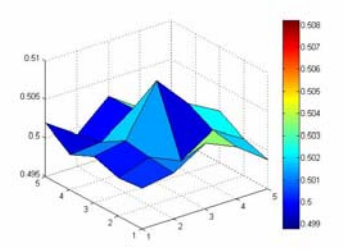	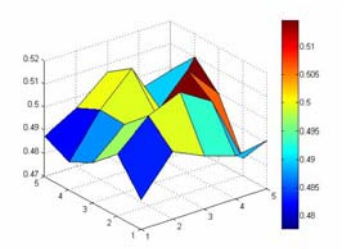
PRF	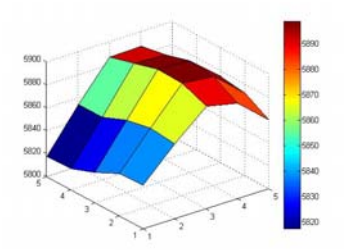	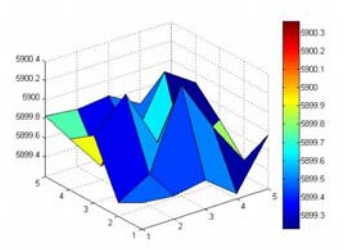	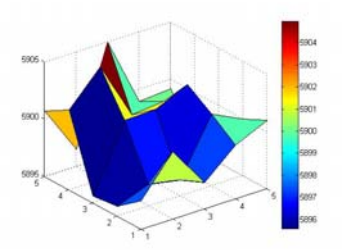
Vp	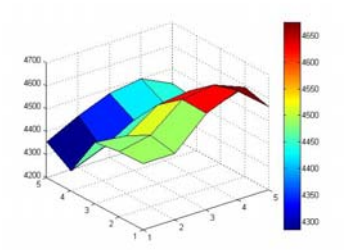	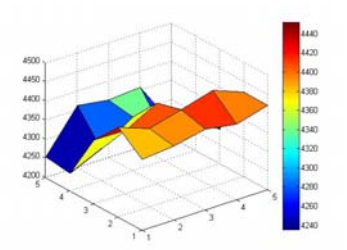	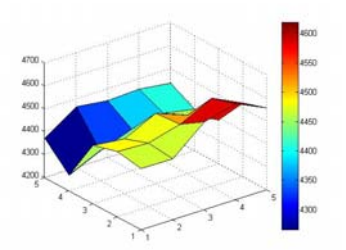
Vs	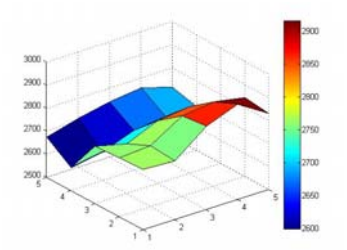	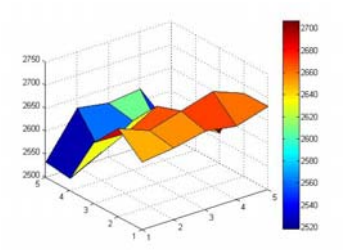	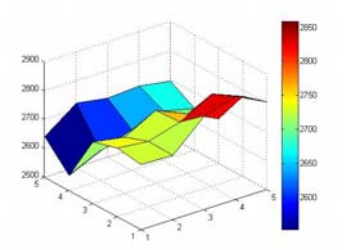

Rho

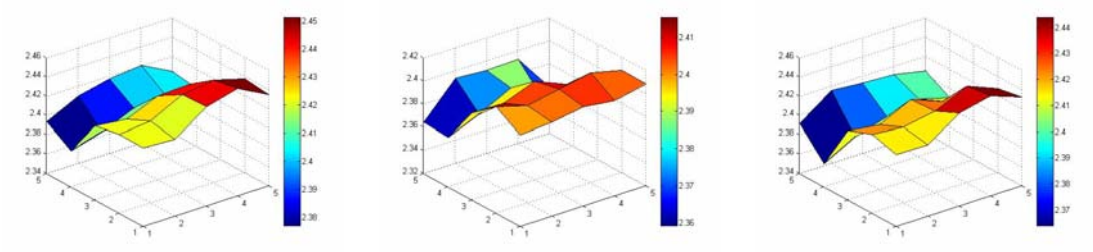

Figure 4.12 Comparison between truth, before PI and after PI in experiment II

Figure 4.11 shows the comparison of distributions at one certain grid point – the 7th one. Samples of the seismic attributes can be changed through obtained different weights, and the right column presents distributions of re-sample for the reservoir properties and the seismic attributes.

In this experiment, probabilistic inversion could also obtain a good estimation of porosity, but it still cannot predict other two properties – saturation and pressure. (Figure 4.12) The measurable variables such as Vp, Vs and Rho could be adjusted the number of quantiles in order to improve the results.

Porosity

Truth					PI Estimation				
0.1291	**0.1304**	**0.1178**	**0.1129**	**0.1215**	0.1342	0.1345	0.1216	0.1175	0.1242
0.1290	**0.1283**	**0.1194**	**0.1169**	**0.1203**	0.1304	0.1324	0.1290	0.1201	0.1266
0.1313	**0.1346**	**0.1282**	**0.1271**	**0.1361**	0.1357	0.1386	0.1296	0.1372	0.1443
0.1533	**0.1496**	**0.1428**	**0.1412**	**0.1424**	0.1630	0.1535	0.1478	0.1431	0.1484
0.1427	**0.1351**	**0.1323**	**0.1300**	**0.1387**	0.1473	0.1336	0.1358	0.1364	0.1402

Table 4.6 PI POR results for all 25 grid point in the 2nd experiment
(Left – truth, right – PI estimation)

Absolute Errors					Relative Errors				
0.0051	**0.0041**	**0.0038**	**0.0046**	**0.0027**	3.95%	3.14%	3.23%	4.07%	2.22%
0.0014	**0.0041**	**0.0096**	**0.0032**	**0.0063**	1.09%	3.20%	8.04%	2.74%	5.24%
0.0044	**0.0040**	**0.0014**	**0.0101**	**0.0082**	3.35%	2.97%	1.09%	7.95%	6.02%
0.0097	**0.0039**	**0.0050**	**0.0019**	**0.0060**	6.33%	2.61%	3.50%	1.35%	4.21%
0.0046	**0.0015**	**0.0035**	**0.0064**	**0.0015**	3.22%	1.11%	2.65%	4.92%	1.08%

Table 4.7 POR errors between PI estimations and the truth in the 2nd experiment

From Table 4.6 and 4.7, we could compare the probabilistic inversion estimation of porosity with the truth. For all grid points, the maximal relative error is equal to 8.04%, while the minimal is 1.09%.

Now, we could draw several conclusions after we finished two main experiments, but we present steps briefly in the first three parts.

1. After generated samples based on the reservoir properties initial distributions, we put them into the rock physics model and obtained the samples of the seismic attributes for all variables. Here, we choose the seventh grid point as an example to analyze. Applying conditional sampling is to remove unreasonable samples, and then we gained the matrix for probabilistic inversion.

2. We took the starting matrix into probabilistic inversion approach and imposed some probability quantiles to the observable vectors such as Vp, Vs and Rho. After several certain iteration steps, probabilistic inversion approach provided different weights to every sample in order to fit the distributions of seismic attributes with the real measures.

3. Re-samples procedure is to obtain the distributions of both reservoir properties and seismic attributes after probabilistic inversion technique.

4. We could find out that the last three groups of figures shows the comparisons of the measurable vectors, and those fit the truth probability quantiles well. If the problem is infeasible, those vectors could not fit the quantiles. Actually, the reservoir properties have already changed closely to the truth after conditional sampling.

5. As for the reservoir properties, probabilistic inversion offered an excellent estimation of porosity, even if we do not have other information of those vectors. However, saturation and pressure are not fit the truth well. The estimation of saturation is still far away from the truth that we supposed, while the pressure estimation at each grid point changed a little which is also similar as its starting distribution.

6. Since we use beta distributions with two coefficients $\alpha = 2$ and $\beta = 2$ for the saturation starting distributions and $\alpha = 2$ and $\beta = 4$ for the porosity ones, we will try to test whether different coefficients affect the estimations of probabilistic inversion. In this experiment, we assume the saturation starting distribution as beta (2, 2) because the mean of this distribution is equal to 0.5 and the domain is 0 to 1. In the following experiment, a new plan is to change the saturation starting distribution to beta (2, 13), because we could know the information that the values of saturation of a large number of grid points are almost equal to 0.1. We would like to check whether this distribution could

match the truth after probabilistic inversion. On the other hand, we also revise the porosity distribution with different coefficients as beta (2, 6) in order to compare the effects of the distribution coefficients on the final estimations.

4.3.3 Experiment III

In this experiment, the starting distributions for creating samples show in the following table. (Table 4.8) As we mentioned above, we change the starting distributions of saturation and porosity based on those certain information.

Reservoir property	Starting distribution
SAT (saturation)	Beta (2,13)
PRF (pressure)	Beta (3,2) × 500+5600
POR (porosity)	Beta (2,6) × 0.5

Table 4.8 Starting distributions of the 3rd experiment

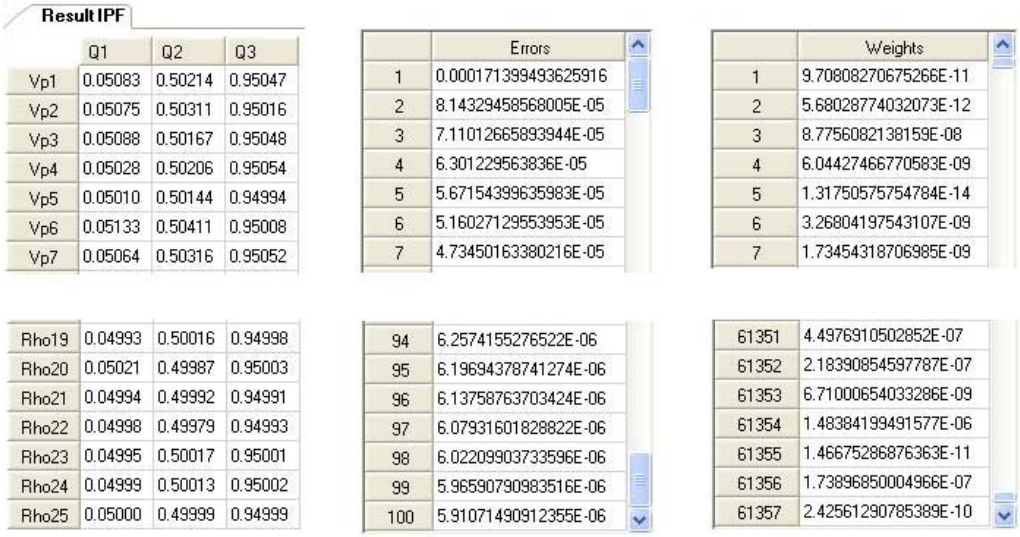

Figure 4.13 Result, errors and weights of the 3rd experiment

From the above figure (Figure 4.13), we notice that the probabilities do not fit as well as previous one, while errors are a little larger than those in all steps. Comparisons between the truth and PI estimations are also presented in the following part, but we just compare the predictions of reservoir properties with the truth. (Figure 4.14)

Estimations of the reservoir properties

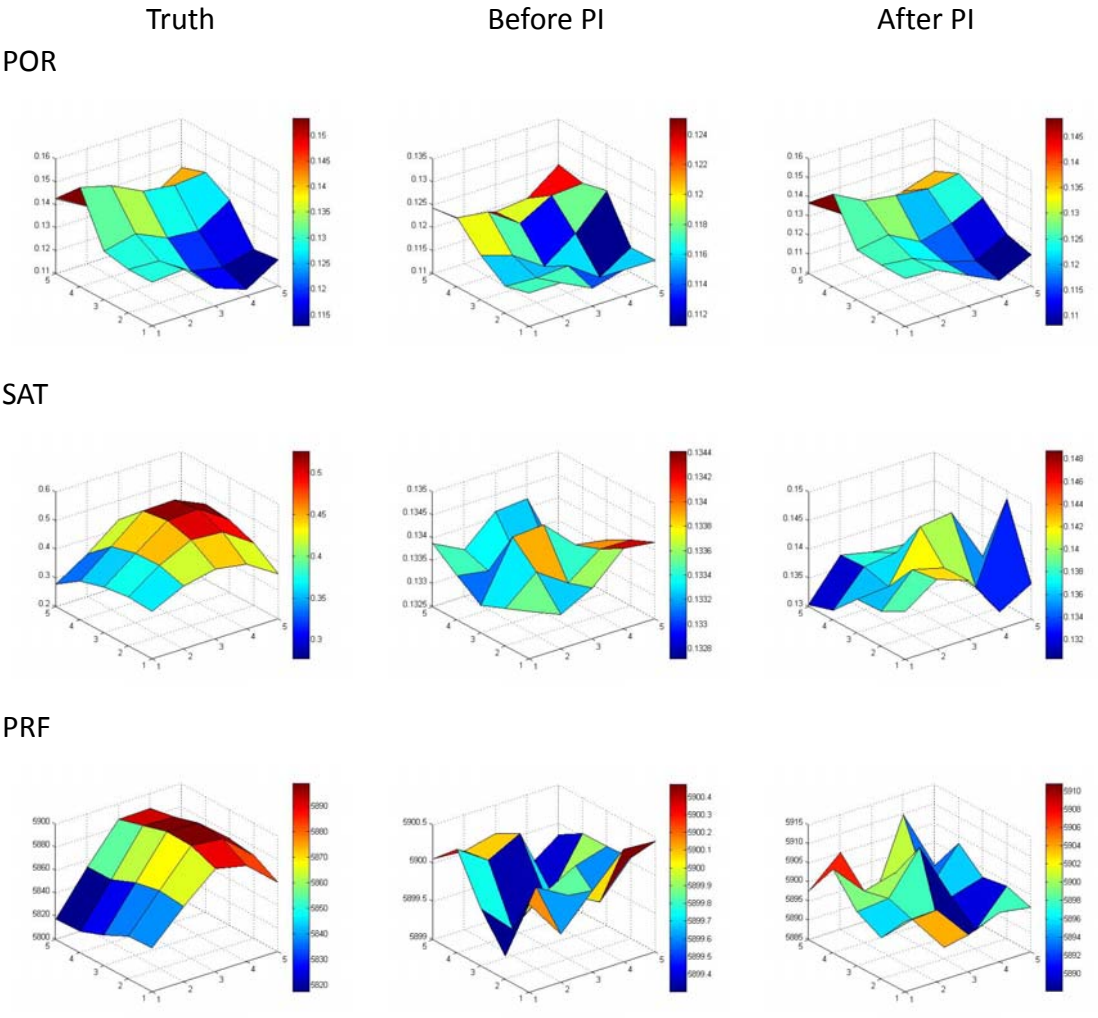

Figure 4.14 Comparison between truth, before PI and after PI in experiment III

POROSITY, SATURATION, PRESSURE (respectively)

Truth					PI Estimations				
0.1291	**0.1304**	**0.1178**	**0.1129**	**0.1215**	0.1343	0.1342	0.1221	0.1172	0.1239
0.1290	**0.1283**	**0.1194**	**0.1169**	**0.1203**	0.1302	0.1322	0.1288	0.1200	0.1270
0.1313	**0.1346**	**0.1282**	**0.1271**	**0.1361**	0.1354	0.1389	0.1301	0.1368	0.1437
0.1533	**0.1496**	**0.1428**	**0.1412**	**0.1424**	0.1625	0.1536	0.1470	0.1431	0.1487
0.1427	**0.1351**	**0.1323**	**0.1300**	**0.1387**	0.1475	0.1341	0.1357	0.1359	0.1404

0.3651	**0.4188**	**0.4440**	**0.4248**	**0.3570**	0.1384	0.1421	0.1402	0.1330	0.1361
0.3715	**0.4460**	**0.4990**	**0.4928**	**0.4190**	0.1360	0.1416	0.1401	0.1350	0.1487
0.3588	**0.4425**	**0.5210**	**0.5258**	**0.4545**	0.1359	0.1363	0.1451	0.1457	0.1363
0.3351	**0.4199**	**0.5087**	**0.5125**	**0.4636**	0.1316	0.1376	0.1382	0.1342	0.1361
0.2774	**0.3495**	**0.4323**	**0.4299**	**0.3972**	0.1303	0.1373	0.1360	0.1355	0.1322
5838.4	**5865.6**	**5889.4**	**5883.4**	**5860.0**	5903.5	5903.9	5894.8	5897.9	5896.6
5837.1	**5867.8**	**5898.3**	**5895.3**	**5872.0**	5895.7	5897.8	5888.0	5890.0	5898.6
5826.3	**5863.3**	**5899. 1**	**5897.8**	**5874.8**	5899.1	5900.1	5910.7	5895.3	5897.6
5818.3	**5854.7**	**5892. 7**	**5891.2**	**5871.7**	5906.8	5898.4	5900.8	5893.3	5903.1
5817.5	**5854.0**	**5886.8**	**5887.5**	**5863.7**	5897.7	5905.1	5888.4	5909.7	5893.8

Table 4.9 Truth and PI outputs for POR, SAT, PRF at all grid point in the 3rd experiment

Porosity									
Absolute Errors					**Relative Errors**				
0.0052	**0.0038**	**0.0043**	**0.0043**	**0.0024**	4.03%	2.91%	3.65%	3.81%	1.98%
0.0012	**0.0039**	**0.0094**	**0.0031**	**0.0067**	0.93%	3.04%	7.87%	2.65%	5.57%
0.0041	**0.0043**	**0.0019**	**0.0097**	**0.0076**	3.12%	3.19%	1.48%	7.63%	5.58%
0.0092	**0.0040**	**0.0042**	**0.0019**	**0.0063**	6.00%	2.67%	2.94%	1.35%	4.42%
0.0048	**0.0010**	**0.0034**	**0.0059**	**0.0017**	3.36%	0.74%	2.57%	4.54%	1.23%

Table 4.10 POR errors between PI estimations and the truth in the 3rd experiment

From the above tables, (Table 4.9 and 4.10) we notice that it is not so difficult for probabilistic inversion approach to obtain an excellent estimation of POR, even if the starting distribution is not quite close to the real one. Furthermore, in this experiment, the relative error for POR is between 0.74% and 7.87%, which are both smaller than former experiment. However, as for SAT and PRF, we have performed several experiments with different starting distributions or different parameter coefficients, and the estimations are still far away from the truth all the time.

4.3.4 Experiment IV

In this experiment, we apply the gamma distribution as the starting distributions to develop the experiment. The following figure is to show the curves of probability density function of gamma distribution with different coefficients. (Figure 4.15)

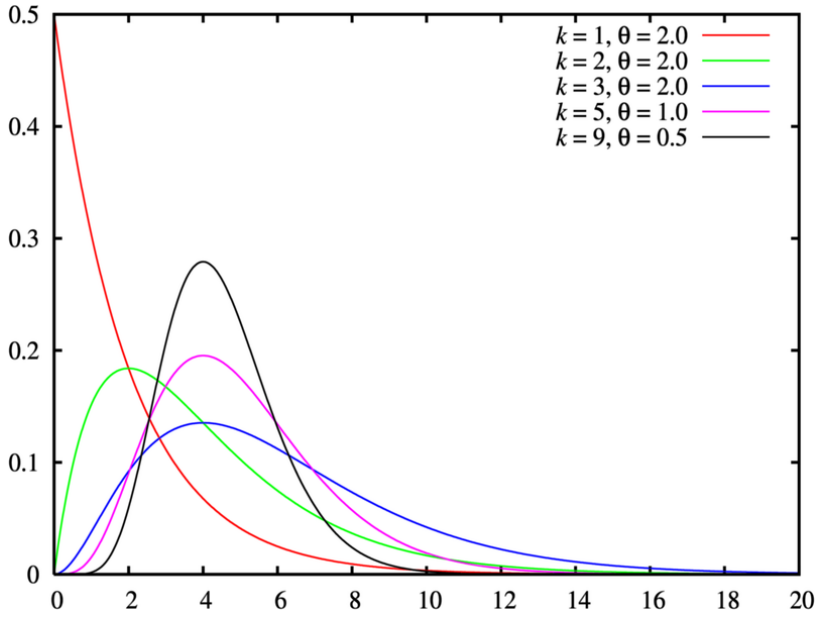

Figure 4.15 Curves of PDF of gamma distribution with different coefficients

In probability theory and statistics, the gamma distribution is a two-parameter family of continuous probability distributions. It has a scale parameter θ and a shape parameter κ. If κ is an integer then the distribution represents the sum of κ exponentially distributed random variables, each of which has a mean of θ.

The probability density function of the gamma distribution can be expressed in terms of the gamma function parameterized in terms of a shape parameter κ and scale parameter θ.

$$f(x;\ \kappa,\theta) = x^{\kappa-1}\frac{e^{-x/\theta}}{\theta^{\kappa}\Gamma(\kappa)}\ ,for\ x > 0\ and\ \kappa,\theta > 0$$

Alternatively, the gamma distribution can be parameterized in terms of a shape parameter $\alpha = \kappa$ and an inverse scale parameter $\beta = 1/\theta$, called a rate parameter.

$$g(x;\ \alpha,\beta) = x^{\alpha-1}\frac{\beta^{\alpha}e^{-\beta x}}{\Gamma(\alpha)}\ ,for\ x > 0$$

The mean of gamma distribution is equal to $\kappa\theta$, while the variance is $\kappa\theta^2$.

In this experiment, we create samples based on the gamma distributions of reservoir properties at each grid point, which are shown in the following table. (Table 4.11)

Reservoir property	Starting distribution
SAT (saturation)	Gamma (8,1/4) × 0.1
PRF (pressure)	Gamma (50,10) + 5300
POR (porosity)	Gamma (3,1/2) × 0.1

Table 4.11 Starting distributions of the 4th experiment

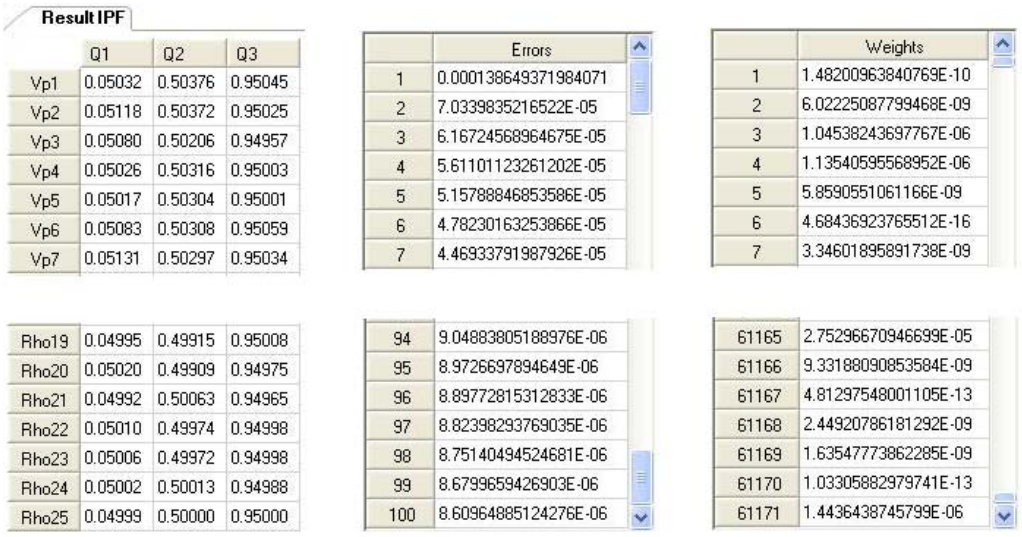

Result IPF

	Q1	Q2	Q3
Vp1	0.05032	0.50376	0.95045
Vp2	0.05118	0.50372	0.95025
Vp3	0.05080	0.50206	0.94957
Vp4	0.05026	0.50316	0.95003
Vp5	0.05017	0.50304	0.95001
Vp6	0.05083	0.50308	0.95059
Vp7	0.05131	0.50297	0.95034
Rho19	0.04995	0.49915	0.95008
Rho20	0.05020	0.49909	0.94975
Rho21	0.04992	0.50063	0.94965
Rho22	0.05010	0.49974	0.94998
Rho23	0.05006	0.49972	0.94998
Rho24	0.05002	0.50013	0.94988
Rho25	0.04999	0.50000	0.95000

	Errors
1	0.00013864937198407 1
2	7.0339835216522E-05
3	6.16724568964675E-05
4	5.61101123261202E-05
5	5.15788846853586E-05
6	4.78230163253866E-05
7	4.46933791987926E-05
94	9.04883805188976E-06
95	8.9726697894649E-06
96	8.89772815312833E-06
97	8.82398293769035E-06
98	8.75140494524681E-06
99	8.6799659426903E-06
100	8.60964885124276E-06

	Weights
1	1.48200963840769E-10
2	6.02225087799468E-09
3	1.04538243697767E-06
4	1.13540595568952E-06
5	5.8590551061166E-09
6	4.68436923765512E-16
7	3.34601895891738E-09
61165	2.75296670946699E-05
61166	9.33188090853584E-09
61167	4.81297548001105E-13
61168	2.44920786181292E-09
61169	1.63547773862285E-09
61170	1.03305882979741E-13
61171	1.4436438745799E-06

Figure 4.16 Result, errors and weights of the 4th experiment

Estimations of the reservoir properties

Truth before PI after PI

POR

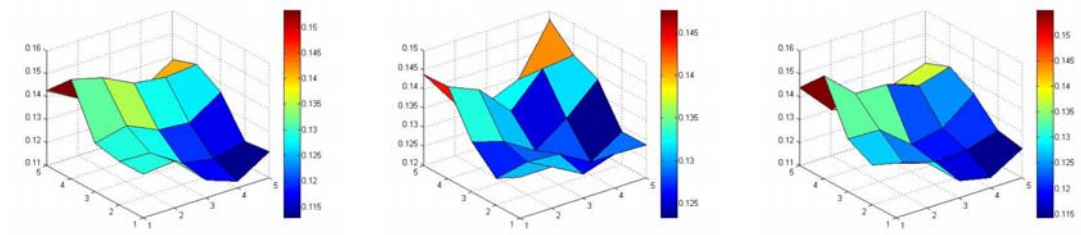

SAT

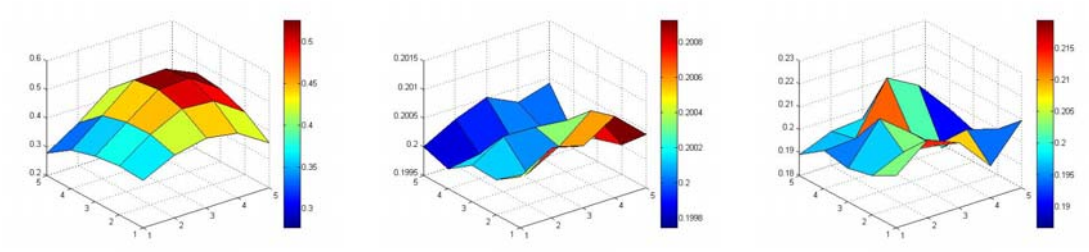

PRF

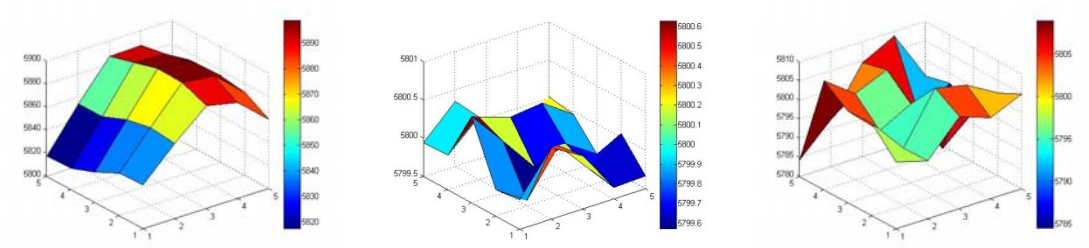

Figure 4.17 Comparison between truth, before PI and after PI in experiment IV

POROSITY

Truth					PI Estimations				
0.1291	**0.1304**	**0.1178**	**0.1129**	**0.1215**	0.1339	0.1296	0.1175	0.1143	0.1228
0.1290	**0.1283**	**0.1194**	**0.1169**	**0.1203**	0.1274	0.1240	0.1199	0.1208	0.1250
0.1313	**0.1346**	**0.1282**	**0.1271**	**0.1361**	0.1332	0.1327	0.1220	0.1247	0.1352
0.1533	**0.1496**	**0.1428**	**0.1412**	**0.1424**	0.1549	0.1428	0.1425	0.1376	0.1411
0.1427	**0.1351**	**0.1323**	**0.1300**	**0.1387**	0.1440	0.1299	0.1261	0.1325	0.1370

Table4.12 Truth and PI estimations for POR at all grid point in the 4th experiment

Porosity

Absolute Errors					Relative Errors				
0.0048	**0.0008**	**0.0003**	**0.0014**	**0.0013**	3.71%	0.61%	0.25%	1.24%	1.07%
0.0016	**0.0043**	**0.0005**	**0.0039**	**0.0047**	1.24%	3.35%	0.42%	3.34%	3.91%
0.0019	**0.0019**	**0.0062**	**0.0024**	**0.0009**	1.45%	1.41%	4.83%	1.89%	0.66%
0.0016	**0.0068**	**0.0003**	**0.0036**	**0.0013**	1.04%	4.55%	0.21%	2.55%	0.91%
0.0013	**0.0052**	**0.0062**	**0.0025**	**0.0017**	0.91%	3.85%	4.69%	1.92%	1.26%

Table 4.13 POR errors between PI estimations and the truth in the 4rd experiment

Starting from gamma distributions can also obtain a very good estimation of the

reservoir property – POR. (Table 4.12) Unfortunately, those two properties – SAT and PRF that we want to predict could not be solved. The relative errors of porosity for all grid points became smaller than former experiments, which are between 0.21% and 4.83%.

4.3.5 Conclusions

We performed several other experiments with different starting distributions of reservoir properties such as normal distribution, lognormal distribution, Weibull distribution etc. and also applied gamma distribution, beta distribution with different parameter coefficients. We cannot put all these tests, figures, tables and comparisons in the thesis, while we may draw the conclusions after those experiments in the following paragraph and in the chapters of conclusions, recommendations and future work.

After performed many experiments, especially experiment I, II,III and IV, we find out that probabilistic inversion approach could offer an excellent result of porosity, even if the starting distribution are not quite similar as the real one. If we choose a proper starting distribution of this to the rock physics model such as beta distribution with different coefficients, probabilistic inversion can obtain a good estimation. It also contains some uncertainties in the final results, but the errors are quite small and the shape of porosity output figure are almost the same as the truth, especially we apply probabilistic inversion with more quantiles or other ways to decrease the error.

By contrast, the estimations of saturation and pressure using probabilistic inversion are not closed to the truth that we assumed, even if we did hundreds of experiments with different starting distributions or the same distribution with different coefficients. We could find that those results still have a lot of noise which make inversion results are far away from the truth.

The reasons that we guess why these classes of phenomena appeared depend on three aspects. Firstly, the measurable variables Vp, Vs and Rho at each grid point are strongly influence by the reservoir property – porosity rather than other two – saturation and pressure. Secondly, as for the assumptions of the starting distributions, we generated distributions of those reservoir properties separately. Actually, it is possible that there are some relationships between two properties – saturation, pressure and another one – porosity. In the following section, we tend to check this reason that we thought about and try to find other ways to improve the method. For instance, we cannot create those distributions separately but adding more physical information concerning reservoir properties, or running with the data we got from other reservoir rather than created randomly, because the data from other reservoir contains those relationships. Last but not least, another reason that we guess is there

are some certain influences between each two neighbor grid point. If we have more information concerning those relations, probabilistic inversion maybe solve this easily and obtain better estimations than before.

In the next section, we will develop small test to explain why we set those options before all experiments. After that, we will test that whether or not there are some effects between porosity and other two properties, while we will analyze the results and try to find out some ways to improve the method.

4.4 Discussion

In this section, we will perform a series of tests to discuss the influence of other setting options on the results. Here are answers of the previous questions such as the choice of IPF not PARFUM, the use of conditional sampling, etc. There are several factors affecting the speed of calculation and the results such that conditional samples, the different number of input samples, the choice of IPF and PARFUM, different quantiles and the number of iteration steps. General speaking, those setting options depends on the performances of computer and software. In the most of these tests, we just take one reservoir property – POR and one seismic attribute – Vp as examples for comparison and analysis.

In these tests, all the starting distributions are following the 2nd experiment by using the beta distributions. For example, when we compare one factor such iteration method – IPF and PARFUM, the other options do not change for a clear comparison.

4.4.1 Conditional Sampling

The advantages of conditional sampling have been introduced in chapter 3 and the previous section. Now, we compare the influence on the results between with conditional sampling and without conditional sampling. Setting options are shown in Table 4.14 below.

After we add conditions on samples, there are a large number of unused samples to remove. For instance, if we generate around 60,000 available samples based on the beta distribution, the number of starting samples of each reservoir property should exceed 1,200,000. The rest of samples are deleted because those are out of realistic interval.

# Samples	60,000
Starting distributions	SAT ~ Beta(2,2), PRF ~ Beta(3,2) × 500+5600, POR ~ Beta(2,4) × 0.5
Method	IPF
Probability quantiles	3 (5%, 50%, 95%)
# Iteration steps	100

Table 4.14 Setting options of the 1st discussion

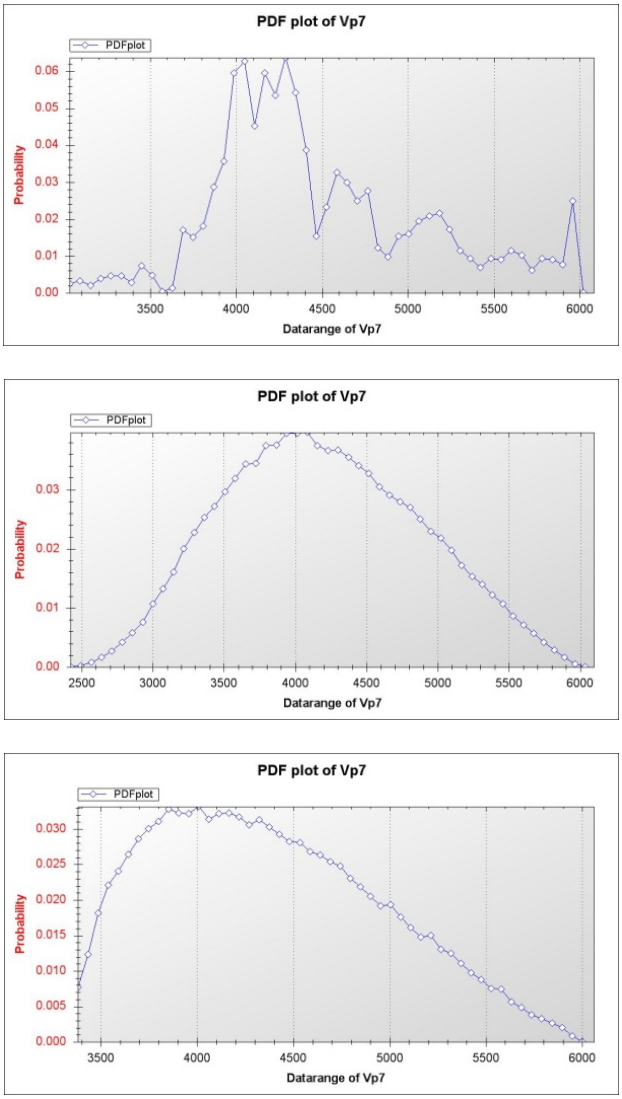

Figure 4.18 Truth and starting distributions for Vp at the 7th grid point (Top – Truth, middle – non-condition, bottom – conditions)

Result IPF | Error and Convergen

	Q1	Q2	Q3
Vp1	0.05010	0.50021	0.95001
Vp2	0.05005	0.50053	0.95032
Vp3	0.04992	0.49995	0.94979
Vp4	0.05015	0.50053	0.95016
Vp5	0.04959	0.49964	0.95003
Vp6	0.05002	0.49994	0.95007
Vp7	0.05010	0.50059	0.95005
Rho19	0.04995	0.49958	0.95002
Rho20	0.05003	0.49987	0.94997
Rho21	0.04998	0.49971	0.94992
Rho22	0.04999	0.49999	0.95001
Rho23	0.05002	0.50005	0.94989
Rho24	0.05003	0.49996	0.95003
Rho25	0.04999	0.49999	0.94999

Result IPF

	Q1	Q2	Q3
Vp1	0.04992	0.49947	0.94975
Vp2	0.04999	0.49983	0.94985
Vp3	0.05008	0.50006	0.94985
Vp4	0.05000	0.50006	0.94998
Vp5	0.04979	0.49938	0.94949
Vp6	0.05000	0.49993	0.94989
Vp7	0.05001	0.49985	0.94975
Rho19	0.05000	0.50009	0.95001
Rho20	0.04999	0.49994	0.94998
Rho21	0.05000	0.50000	0.95001
Rho22	0.05000	0.49994	0.94997
Rho23	0.04998	0.49993	0.95000
Rho24	0.04999	0.50001	0.94999
Rho25	0.05000	0.50000	0.95000

Figure 4.19 Comparison result between non-condition and conditions
(Left – non-condition, right – condition)

	Errors
87	2.58271595154499E-06
88	2.54667415341436E-06
89	2.51124286835763E-06
90	2.47627620804172E-06
91	2.44182714301073E-06
92	2.40790909105224E-06
93	2.37455812427473E-06
94	2.34162027876491E-06
95	2.30909434657356E-06
96	2.27697889344308E-06
97	2.24542223559634E-06
98	2.21452903144197E-06
99	2.18402271101404E-06
100	2.15390175106904E-06

	Errors
87	9.29235540855067E-07
88	9.10465188740603E-07
89	8.92173405363678E-07
90	8.74355235859873E-07
91	8.57379142472904E-07
92	8.40894068435455E-07
93	8.24833591089777E-07
94	8.09208277527836E-07
95	7.94003357923871E-07
96	7.79141742049795E-07
97	7.64717512088 35E-07
98	7.50640853634688E-07
99	7.36885843952232E-07
100	7.23444115893745E-07

Figure 4.20 Comparison errors between non-condition and conditions
(Left – non-condition, right – condition)

From the above Figure 4.18, we could easily find that those samples in the interval 2400 to 3400 are removed by adding some certain conditions. As for probabilistic inversion, it is easy to find sample weights for matching starting distribution with the truth, and the accuracy of results will also increase.

It shows that the conditional sampling result is better than using non-condition, while the errors are also smaller than non-condition in every step. (Figure 4.19 and

4.20) Next, we will compare the results of POR and Vp before and after probabilistic inversion.

Before PI:

Truth Non-condition Conditions

POR

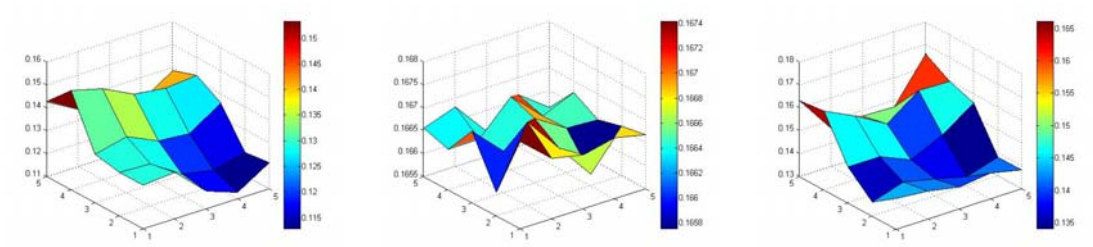

Vp

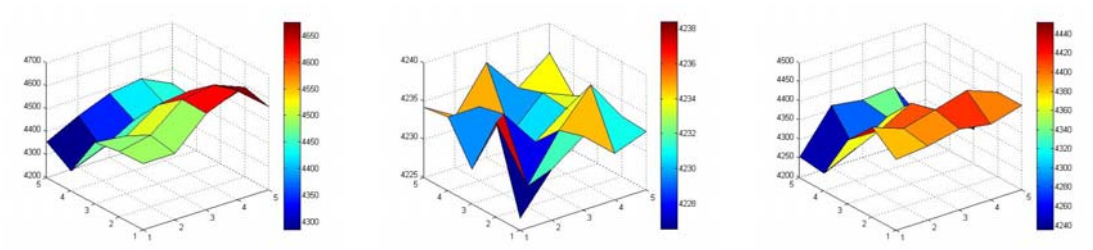

Figure 4.21 Comparison between non-condition and conditions before PI
(Left – truth, middle – non-condition, right – conditions)

After conditional sampling, the samples before re-weighting are already closed to the truth, because it removed a large number of unreasonable samples. (Figure 4.21) This can also help probabilistic inversion to estimate the final results faster and correctly.

After PI:

Truth Non-condition Conditions

POR

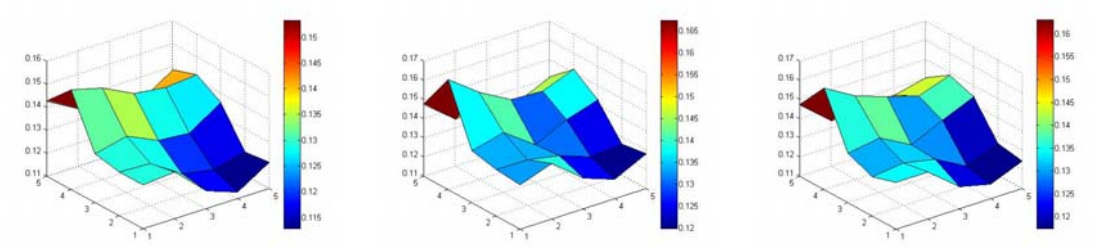

Vp

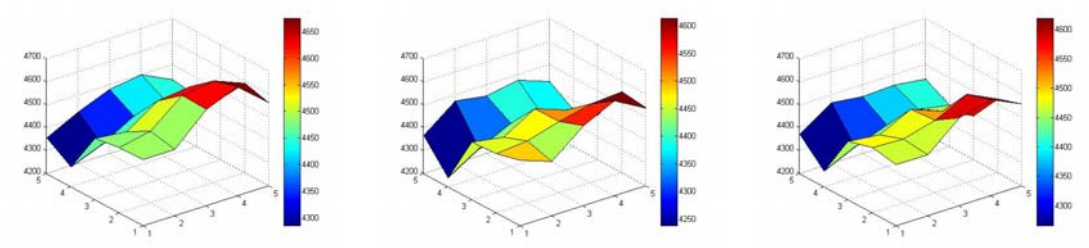

Figure 4.22 Comparison between non-condition and conditions after PI
(Left – truth, middle – non-condition, right – conditions)

The probabilistic inversion estimations of POR after conditions can be better than the outputs without using any conditions for the inputs. (Figure 4.22)

	Truth				
POR	0.1291	0.1304	0.1178	0.1129	0.1215
	0.1290	0.1283	0.1194	0.1169	0.1203
	0.1313	0.1346	0.1282	0.1271	0.1361
	0.1533	0.1496	0.1428	0.1412	0.1424
	0.1427	0.1351	0.1323	0.1300	0.1387
Vp	4489.7	4489.9	4621.5	4675.8	4561.9
	4484.9	4512.8	4623.9	4643.4	4589.3
	4466.4	4453.6	4543.3	4559.6	4463.1
	4285.3	4340.5	4421.6	4443.0	4420.6
	4355.7	4426.4	4478.8	4498.6	4433.9

Non-condition					Conditions				
0.1332	**0.1389**	**0.1259**	**0.1200**	**0.1281**	0.1342	0.1345	0.1216	0.1175	0.1242
0.1339	**0.1338**	**0.1307**	**0.1248**	**0.1264**	0.1304	0.1324	0.1290	0.1201	0.1266
0.1372	**0.1413**	**0.1297**	**0.1374**	**0.1425**	0.1357	0.1386	0.1296	0.1372	0.1443
0.1674	**0.1553**	**0.1462**	**0.1455**	**0.1518**	0.1630	0.1535	0.1478	0.1431	0.1484
0.1476	**0.1347**	**0.1366**	**0.1331**	**0.1406**	0.1473	0.1336	0.1358	0.1364	0.1402
4487.4	**4439.1**	**4550.9**	**4614.2**	**4539.4**	4469.1	4466.4	4583.3	4619.4	4556.3
4458.8	**4471.4**	**4510.8**	**4544.4**	**4552.4**	4485.8	4479. 3	4516.2	4586.1	4522.5
4451.0	**4428.4**	**4510.2**	**4460.3**	**4392.8**	4455.3	4439.8	4506.0	4454.7	4389.5
4238.1	**4322.0**	**4388.3**	**4377.9**	**4358.1**	4266.3	4329.0	4380.2	4405.1	4379.4
4366.5	**4472.1**	**4451.5**	**4475.3**	**4426.2**	4370.6	4466.3	4449.0	4453.2	4436.8

Table 4.15 PI estimations – POR and Vp for each grid point
(Top – truth, bottom left – non-condition, bottom right – conditions)

Relative error of porosity										
Non-condition					Conditional Sampling					
3.18%	6.52%	6.88%	6.29%	5.43%	3.95%	3.14%	3.23%	4.07%	2.22%
3.80%	4.29%	9.46%	6.76%	5.07%	1.09%	3.20%	8.04%	2.74%	5.24%
4.49%	4.98%	1.17%	8.10%	4.70%	3.35%	2.97%	1.09%	7.95%	6.02%
9.20%	3.81%	2.38%	3.05%	6.60%	6.33%	2.61%	3.50%	1.35%	4.21%
3.43%	0.30%	3.25%	2.38%	1.37%	3.22%	1.11%	2.65%	4.92%	1.08%

Table 4.16 Relative error of porosity in the 1st discussion
(Left – Non-condition, Right – conditional sampling)

In the above two tables (Table 4.15 and 4.16), most of values of reservoir properties and seismic attributes at every grid point using conditional sampling are more accurate than without it.

From those figures and tables above, it is easy to find out the differences between using conditional sampling and without using it. We could draw the conclusion that if we put some certain conditions on the probabilistic inversion inputs to remove those unreasonable samples, it will help probabilistic inversion to improve the approach and to obtain better results. Therefore, we perform all experiments with conditional sampling.

4.4.2 Different Number of Input Samples

In this test, we will try to find out the effects of the number of input samples. Two different numbers of input samples will be chosen for the comparison such as 10,000 and 60,000. The setting options of this test will be presented in the following table.

# Samples	10,000 & 60,000
Starting distributions	SAT ~ Beta(2,2), PRF ~ Beta(3,2) × 500+5600, POR ~ Beta(2,4) × 0.5
Conditional sampling	Yes
Method	IPF
Probability quantiles	3 (5%, 50%, 95%)
# Iteration steps	100

Table 4.17 Setting options of the 2nd discussion

Result IPF

	Q1	Q2	Q3
Vp1	0.04954	0.49805	0.94919
Vp2	0.05004	0.50032	0.95010
Vp3	0.04984	0.49967	0.95026
Vp4	0.04973	0.49937	0.94973
Vp5	0.04965	0.49904	0.95011
Vp6	0.04983	0.49865	0.94975
Vp7	0.05045	0.50027	0.95014
Rho19	0.04994	0.50007	0.94989
Rho20	0.05004	0.50003	0.95004
Rho21	0.04999	0.50038	0.95009
Rho22	0.04993	0.49980	0.94987
Rho23	0.04999	0.50003	0.95003
Rho24	0.05001	0.49998	0.94994
Rho25	0.05000	0.49999	0.94999

Result IPF

	Q1	Q2	Q3
Vp1	0.04992	0.49947	0.94975
Vp2	0.04999	0.49983	0.94985
Vp3	0.05008	0.50006	0.94985
Vp4	0.05000	0.50006	0.94998
Vp5	0.04979	0.49938	0.94949
Vp6	0.05000	0.49993	0.94989
Vp7	0.05001	0.49985	0.94975
Rho19	0.05000	0.50009	0.95001
Rho20	0.04999	0.49994	0.94998
Rho21	0.05000	0.50000	0.95001
Rho22	0.05000	0.49994	0.94997
Rho23	0.04998	0.49993	0.95000
Rho24	0.04999	0.50001	0.94999
Rho25	0.05000	0.50000	0.95000

Figure 4.23 Comparison result between 10,000 and 60,000
(Left – 10,000 input samples, right – 60,000 input samples)

	Errors
87	1.79231780401724E-05
88	1.76640626766344E-05
89	1.74088607829888E-05
90	1.71573886103289E-05
91	1.69123568924203E-05
92	1.6676049007422E-05
93	1.6446209864304E-05
94	1.62223861172659E-05
95	1.60066805722767E-05
96	1.57969611372344E-05
97	1.55902297355723E-05
98	1.53864645583573E-05
99	1.51863849979733E-05
100	1.49921336392813E-05

	Errors
87	9.29235540855067E-07
88	9.10465188740603E-07
89	8.92173405363678E-07
90	8.74355235859873E-07
91	8.57379142472904E-07
92	8.40894068435455E-07
93	8.24833591089777E-07
94	8.09208277527836E-07
95	7.94003357923871E-07
96	7.79141742049795E-07
97	7.6471751208835E-07
98	7.50640853634688E-07
99	7.36885843952232E-07
100	7.23444115893745E-07

Figure 4.24 Comparison errors between 10,000 and 60,000
(Left – 10,000 input samples, right – 60,000 input samples)

When using more input samples, we can gain better results and smaller errors. In Figure 4.23, it shows that 60,000 input samples are easy to match the truth quantiles, and the errors of using 10,000 samples are more or less 20 times larger than the other one at each step. Even though we would like to use the number of samples as more as possible to improve the results, on the other hand, we have to think about the computational abilities of computer and software. We must find out a balance

between computer level, calculation time and the results accuracy.

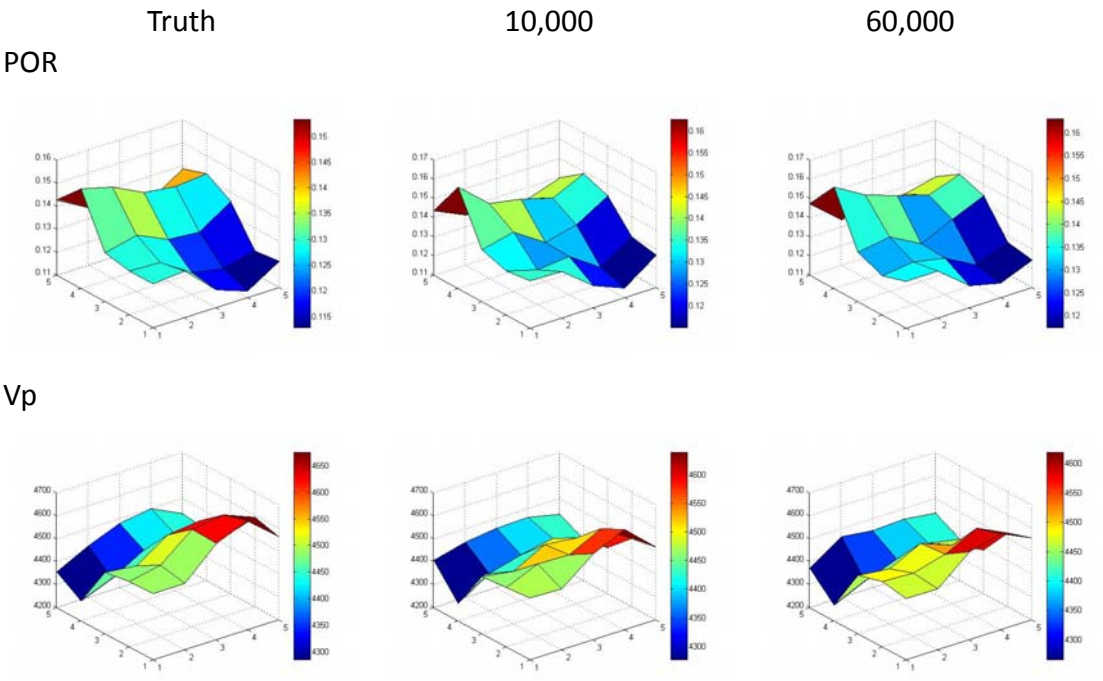

Figure 4.25 Comparison of estimations between 10,000 and 60,000 input sample (Left – truth, middle – 10,000 input samples, right – 60,000 input samples)

Actually, PI estimations will be close to the truth if we used more input samples because it is not difficult to match the quantiles. However, as mentioned before, there are some limitations for using samples as more as we want such as computer level and program computational abilities. Therefore, in this project, since there are 3 seismic attributes and 25 grid points which equals 75 variables totally, the maximal number of input sample that we could use is around 60,000 or less than 70,000. We could take more samples if the program's calculation speed and computer level improve.

4.4.3 IPF & PARFUM

As mentioned in chapter 3, there are two main different methods using probabilistic inversion technique such as iterative proportional fitting (IPF) and parameter fitting for uncertain models (PARFUM). This test is to show the comparison between those two methods. We set the same options except solving methods IPF and PARFUM so as to obtain a clear comparison. The choices are shown in Table 4.18.

# Samples	60,000
Starting distributions	SAT ~ Beta(2,2), PRF ~ Beta(3,2) × 500+5600, POR ~ Beta(2,4) × 0.5
Conditional sampling	Yes
Method	IPF & PARFUM
Probability quantiles	3 (5%, 50%, 95%)
# Iteration steps	100

Table 4.18 Setting options of the 3rd discussion

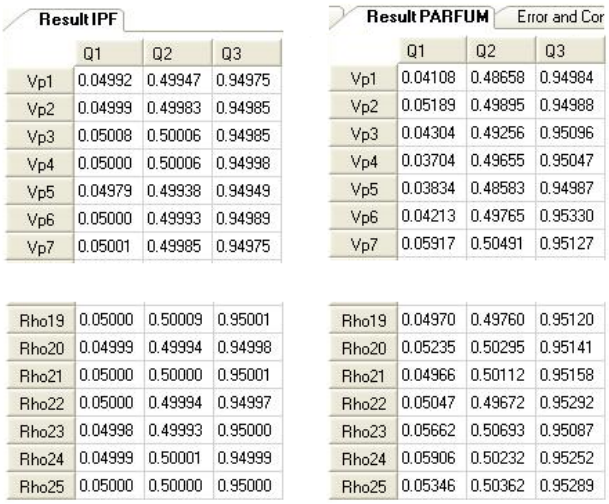

Result IPF

	Q1	Q2	Q3
Vp1	0.04992	0.49947	0.94975
Vp2	0.04999	0.49983	0.94985
Vp3	0.05008	0.50006	0.94985
Vp4	0.05000	0.50006	0.94998
Vp5	0.04979	0.49938	0.94949
Vp6	0.05000	0.49993	0.94989
Vp7	0.05001	0.49985	0.94975
Rho19	0.05000	0.50009	0.95001
Rho20	0.04999	0.49994	0.94998
Rho21	0.05000	0.50000	0.95001
Rho22	0.05000	0.49994	0.94997
Rho23	0.04998	0.49993	0.95000
Rho24	0.04999	0.50001	0.94999
Rho25	0.05000	0.50000	0.95000

Result PARFUM | Error and Cor

	Q1	Q2	Q3
Vp1	0.04108	0.48658	0.94984
Vp2	0.05189	0.49895	0.94988
Vp3	0.04304	0.49256	0.95096
Vp4	0.03704	0.49655	0.95047
Vp5	0.03834	0.48583	0.94987
Vp6	0.04213	0.49765	0.95330
Vp7	0.05917	0.50491	0.95127
Rho19	0.04970	0.49760	0.95120
Rho20	0.05235	0.50295	0.95141
Rho21	0.04966	0.50112	0.95158
Rho22	0.05047	0.49672	0.95292
Rho23	0.05662	0.50693	0.95087
Rho24	0.05906	0.50232	0.95252
Rho25	0.05346	0.50362	0.95289

Figure 4.26 Comparison result between IPF (left) and PARFUM (right)

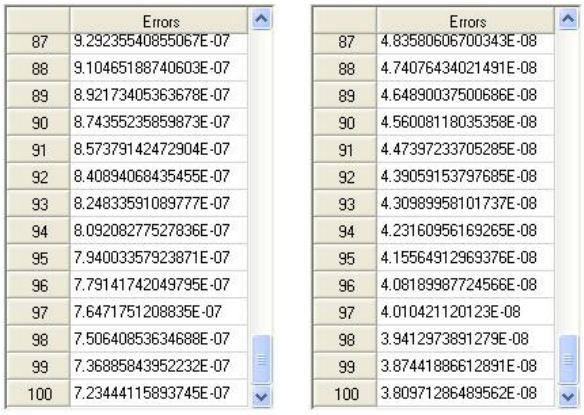

	Errors
87	9.29235540855067E-07
88	9.10465188740603E-07
89	8.92173405363678E-07
90	8.74355235859873E-07
91	8.57379142472904E-07
92	8.40894068435455E-07
93	8.24833591089777E-07
94	8.09208277527836E-07
95	7.94003357923871E-07
96	7.79141742049795E-07
97	7.6471751208835E-07
98	7.50640853634688E-07
99	7.36885843952232E-07
100	7.23444115893745E-07

	Errors
87	4.83580606700343E-08
88	4.74076434021491E-08
89	4.64890037500686E-08
90	4.56008118035358E-08
91	4.47397233705285E-08
92	4.39059153797685E-08
93	4.30989958101737E-08
94	4.23160956169265E-08
95	4.15564912969376E-08
96	4.08189987724566E-08
97	4.010421120123E-08
98	3.9412973891279E-08
99	3.87441886612891E-08
100	3.80971286489562E-08

Figure 4.27 Comparison errors between IPF (left) and PARFUM (right)

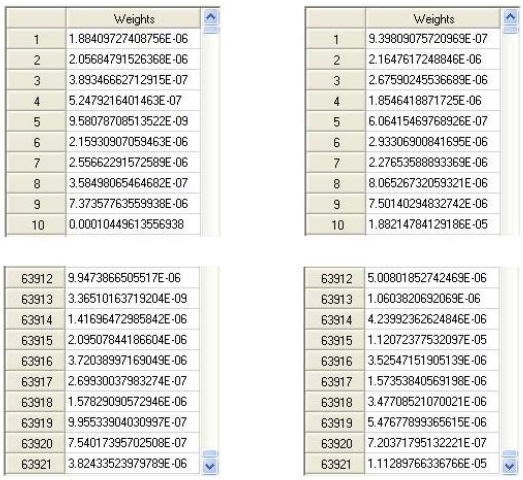

	Weights
1	1.884097274087 56E-06
2	2.056847915263 68E-06
3	3.893466627129 15E-07
4	5.247921640146 3E-07
5	9.580787085135 22E-09
6	2.159309070594 63E-06
7	2.556622915725 89E-06
8	3.584980654646 82E-07
9	7.373577635593 38E-06
10	0.000104496135 56938
63912	9.947386650551 7E-06
63913	3.365101637192 04E-09
63914	1.416964729858 42E-06
63915	2.095078441866 04E-06
63916	3.720389971690 49E-06
63917	2.699300379832 74E-07
63918	1.578290905729 46E-06
63919	9.955339040309 97E-07
63920	7.540173957025 08E-07
63921	3.824335239797 89E-06

	Weights
1	9.398090757209 69E-07
2	2.164761724884 6E-06
3	2.675902455366 89E-06
4	1.854641887172 5E-06
5	6.064154697689 26E-07
6	2.933069008416 95E-06
7	2.276535888933 69E-06
8	8.065267320593 21E-06
9	7.501402948327 42E-06
10	1.882147841291 86E-05
63912	5.008018527424 69E-06
63913	1.060382069206 9E-06
63914	4.239923626248 46E-06
63915	1.120723775320 97E-05
63916	3.525471519051 39E-06
63917	1.573538405691 98E-06
63918	3.477085210700 21E-06
63919	5.476778993656 15E-06
63920	7.203717951322 21E-07
63921	1.112897663367 66E-05

Figure 4.28 Comparison the weights between IPF (left) and PARFUM (right)

From the Figure 4.26, we could easily notice that the probability results of IPF are much closer to the truth quantiles than PARFUM's. However, it shows the PARFUM's error is a little smaller than IPF's at each step in Figure 4.27. Those two methods give different weight for each sample. (Figure 4.28) Thus, it leads to provide different sample re-weighting in the following comparisons.

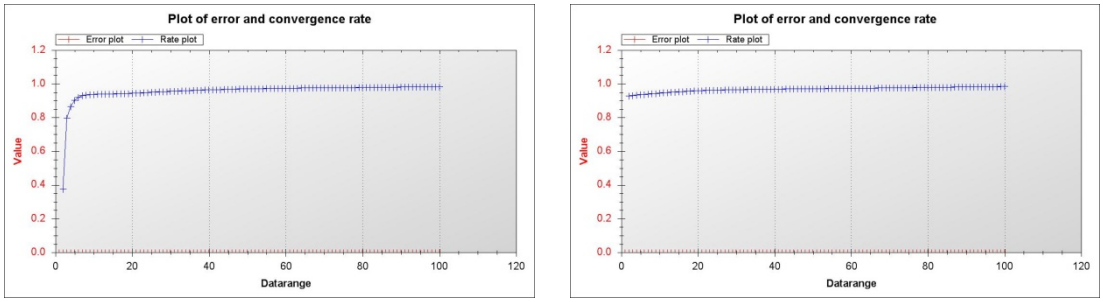

Figure 4.29 Error & Convergence rate (IPF – left, PARFUM – right)

The convergence of IPF is faster to 1 than PARFUM. The advantage of PARFUM is that it always converges even if problem is not feasible, and it converges to a solution for feasible problems, but IPF does not converge it oscillates in some cases. The important thing is if the problem is feasible, we should choose IPF because of the faster convergence.

Truth IPF PARFUM

POR

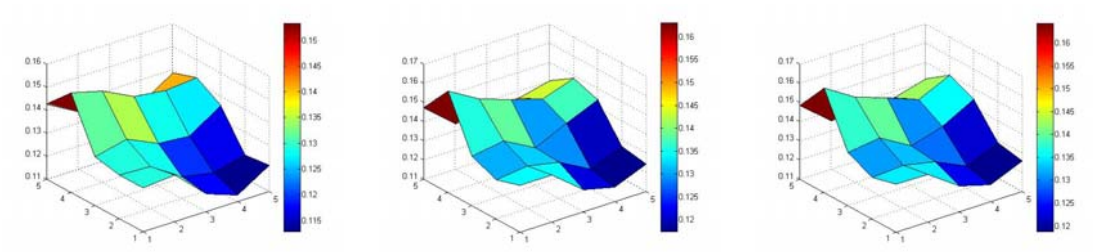

Vp

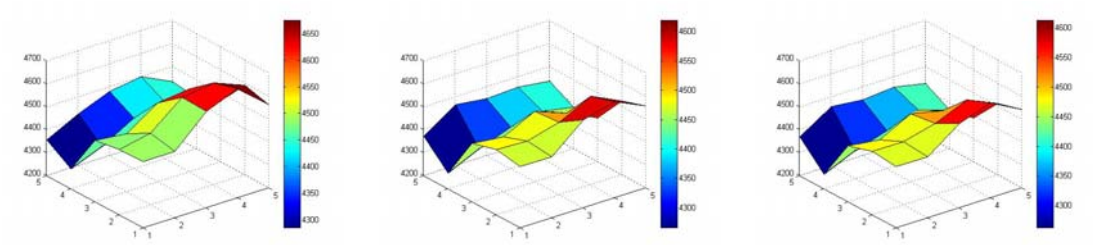

Figure 4.30 Comparison of PI estimations between IPF and PARFUM
(Left – truth, middle – IPF, right – PARFUM)

	Truth				
POR	0.1291	0.1304	0.1178	0.1129	0.1215
	0.1290	0.1283	0.1194	0.1169	0.1203
	0.1313	0.1346	0.1282	0.1271	0.1361
	0.1533	0.1496	0.1428	0.1412	0.1424
	0.1427	0.1351	0.1323	0.1300	0.1387

IPF					PARFUM				
0.1342	**0.1345**	**0.1216**	**0.1175**	**0.1242**	0.1348	0.1347	0.1234	0.1188	0.1260
0.1304	**0.1324**	**0.1290**	**0.1201**	**0.1266**	0.1314	0.1325	0.1292	0.1218	0.1286
0.1357	**0.1386**	**0.1296**	**0.1372**	**0.1443**	0.1376	0.1399	0.1307	0.1355	0.1445
0.1630	**0.1535**	**0.1478**	**0.1431**	**0.1484**	0.1644	0.1545	0.1489	0.1427	0.1500
0.1473	**0.1336**	**0.1358**	**0.1364**	**0.1402**	0.1483	0.1351	0.1365	0.1367	0.1414

Table 4.19 PI estimation of POR for each grid point between IPF and PARFUM
(Top – truth, bottom left – IPF, bottom right – PARFUM)

Relative error of porosity										
IPF						PARFUM				
3.95%	**3.14%**	**3.23%**	**4.07%**	**2.22%**	4.42%	3.30%	4.75%	5.23%	3.70%
1.09%	**3.20%**	**8.04%**	**2.74%**	**5.24%**	1.86%	3.27%	8.21%	4.19%	6.90%
3.35%	**2.97%**	**1.09%**	**7.95%**	**6.02%**	4.80%	3.94%	1.95%	6.61%	6.17%
6.33%	**2.61%**	**3.50%**	**1.35%**	**4.21%**	7.24%	3.28%	4.27%	1.06%	5.34%
3.22%	**1.11%**	**2.65%**	**4.92%**	**1.08%**	3.92%	0.00%	3.17%	5.15%	1.95%

Table 4.20 Relative error of porosity in the 3rd discussion
(Left – Non-condition, Right – conditional sampling)

Those results from either IPF or PARFUM are all close to the truth. (Table 4.19, Table 4.20) In this project, there is only a few different between IPF and PARFUM, even though the probability results of PARFUM are no better than IPF's. PARFUM always converges even if the problem is infeasible.

However, if we check the results carefully, it is not hard to find out that almost all of results of IPF are more accurate to the truth than PARFUM. That is why we use IPF method because the convergence rate is faster than PARFUM's when the problem is feasible.

4.4.4 Different Quantiles

In this test, we will present the effects related to different quantiles that we choose in probabilistic inversion. Obviously, variables will match the measurable distributions quite well if we use a large number of quantiles, however, the calculation is also increasing because of adding quantiles. Therefore, we should find a balance between choosing the number of quantiles and improving the final results. We will show the results using 3 quantiles (5%, 50%, 95%) and 5 quantiles (5%, 25%, 50%, 75%, 95%) in the following comparison. Other setting options do not change. (Table 4.17)

# Samples	**60,000**
Starting distributions	SAT ~ Beta(2,2), PRF ~ Beta(3,2) × 500+5600, POR ~ Beta(2,4) × 0.5
Conditional sampling	Yes
Method	IPF
Probability quantiles	3 (5%, 50%, 95%)

	5 (5%, 25%, 50%, 75%, 95%)
# Iteration steps	100

Table 4.21 Setting options of the 4th discussion

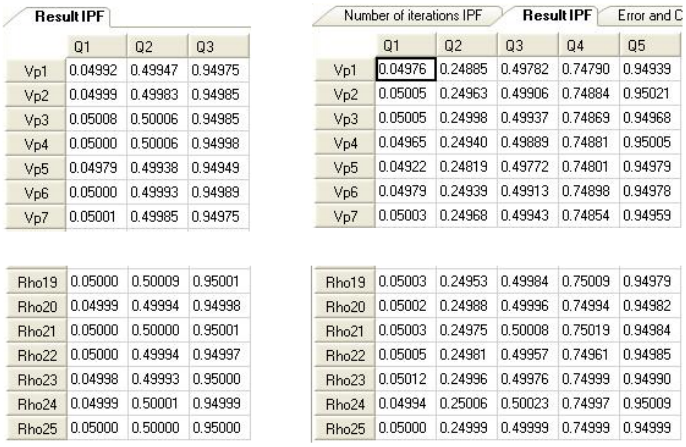

Result IPF

	Q1	Q2	Q3
Vp1	0.04992	0.49947	0.94975
Vp2	0.04999	0.49983	0.94985
Vp3	0.05008	0.50006	0.94985
Vp4	0.05000	0.50006	0.94998
Vp5	0.04979	0.49938	0.94949
Vp6	0.05000	0.49993	0.94989
Vp7	0.05001	0.49985	0.94975
Rho19	0.05000	0.50009	0.95001
Rho20	0.04999	0.49994	0.94998
Rho21	0.05000	0.50000	0.95001
Rho22	0.05000	0.49994	0.94997
Rho23	0.04998	0.49993	0.95000
Rho24	0.04999	0.50001	0.94999
Rho25	0.05000	0.50000	0.95000

Number of iterations IPF | Result IPF | Error and C

	Q1	Q2	Q3	Q4	Q5
Vp1	0.04976	0.24885	0.49782	0.74790	0.94939
Vp2	0.05005	0.24963	0.49906	0.74884	0.95021
Vp3	0.05005	0.24998	0.49937	0.74869	0.94968
Vp4	0.04965	0.24940	0.49889	0.74881	0.95005
Vp5	0.04922	0.24819	0.49772	0.74801	0.94979
Vp6	0.04979	0.24939	0.49913	0.74898	0.94978
Vp7	0.05003	0.24968	0.49943	0.74854	0.94959
Rho19	0.05003	0.24953	0.49984	0.75009	0.94979
Rho20	0.05002	0.24988	0.49996	0.74994	0.94982
Rho21	0.05003	0.24975	0.50008	0.75019	0.94984
Rho22	0.05005	0.24981	0.49957	0.74961	0.94985
Rho23	0.05012	0.24996	0.49976	0.74999	0.94990
Rho24	0.04994	0.25006	0.50023	0.74997	0.95009
Rho25	0.05000	0.24999	0.49999	0.74999	0.94999

Figure 4.31 Results between using 3-quantile and 5-quantile (Left – 3, right – 5)

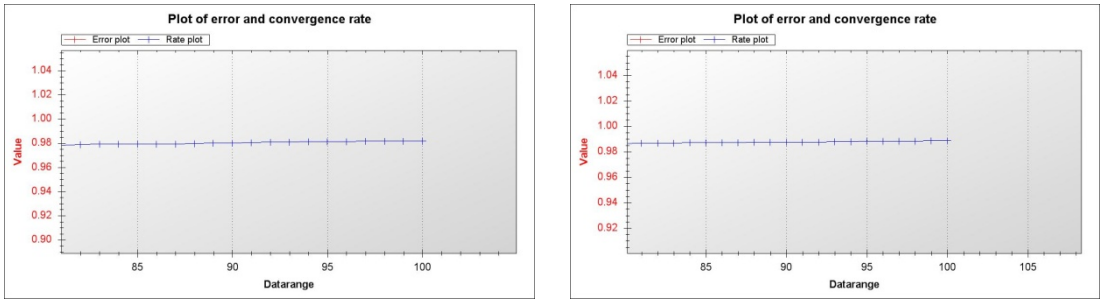

Figure 4.32 Zoom in the convergence rate (Left – 3 quantiles, right – 5 quantiles)

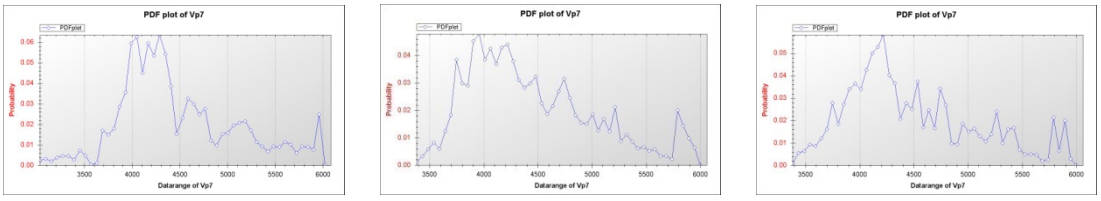

Figure 4.33 Output distribution of Vp for the 7th grid point
(Left – truth, middle – 3 quantiles, right – 5 quantiles)

The results using 3-quantile and 5-quantile show in Figure 5.11. The problem is feasible, while all variables' probabilities match the truth quantiles. The following figure (Figure 4.32) indicates the difference of convergence rate between 3-quantile and 5-quantile. The result of 5-quantile is greater than 0.98, while it is smaller than this value using 3-quantile. We conclude that more quantiles give faster convergence. The last figure above (Figure 4.33) is to choose the 7^{th} grid point of variable Vp to compare two different quantiles. The right one using 5-quantile is a little more similar to the left one. The output distribution will be more closed to the truth one if we use more quantiles.

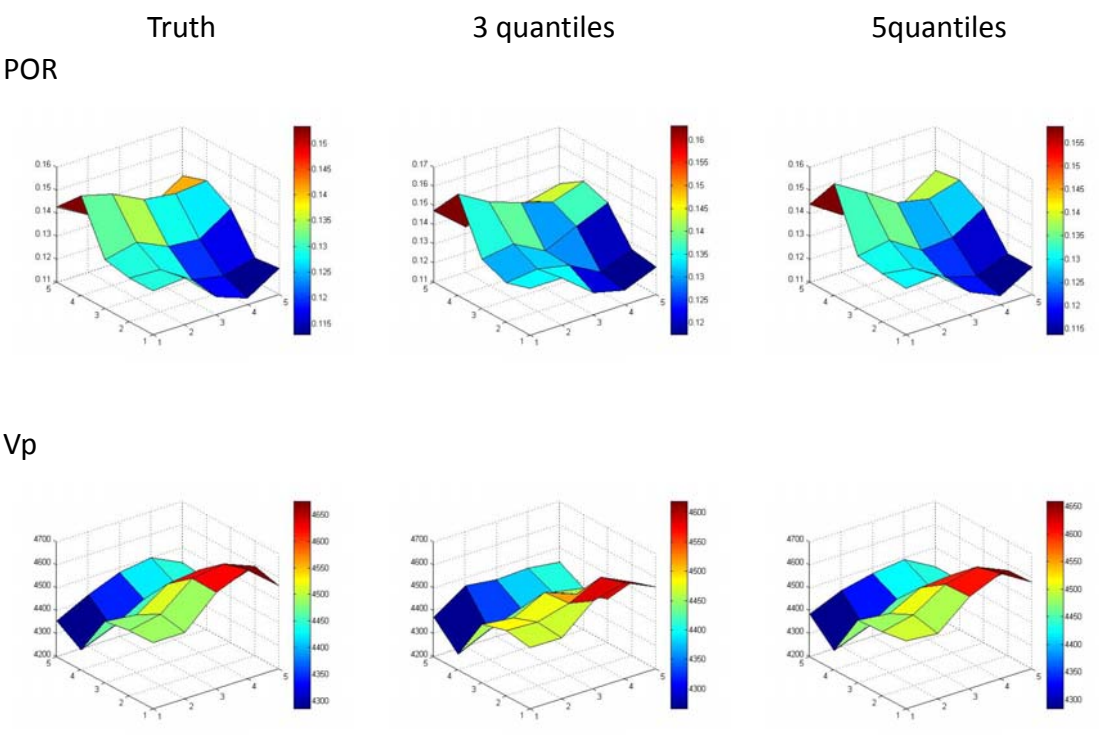

Figure 4.34 Outputs comparison between 3 quantiles and 5 quantiles
(Left – truth, middle – 3 quantiles, right – 5 quantiles)

	Truth				
POR	0.1291	0.1304	0.1178	0.1129	0.1215
	0.1290	0.1283	0.1194	0.1169	0.1203
	0.1313	0.1346	0.1282	0.1271	0.1361
	0.1533	0.1496	0.1428	0.1412	0.1424
	0.1427	0.1351	0.1323	0.1300	0.1387

3-quantile					5-quantile				
0.1342	**0.1345**	**0.1216**	**0.1175**	**0.1242**	0.1301	0.1314	0.1198	0.1138	0.1218
0.1304	**0.1324**	**0.1290**	**0.1201**	**0.1266**	0.1308	0.1289	0.1208	0.1166	0.1219
0.1357	**0.1386**	**0.1296**	**0.1372**	**0.1443**	0.1328	0.1352	0.1268	0.1278	0.1363
0.1630	**0.1535**	**0.1478**	**0.1431**	**0.1484**	0.1585	0.1506	0.1415	0.1389	0.1427
0.1473	**0.1336**	**0.1358**	**0.1364**	**0.1402**	0.1438	0.1349	0.1327	0.1316	0.1410

Table 4.22 PI estimation of POR results for each grid point
(Top – truth, bottom left – 3 quantiles, bottom right – 5 quantiles)

Relative error of porosity

3 quantiles					5 quantiles				
3.95%	**3.14%**	**3.23%**	**4.07%**	**2.22%**	0.77%	0.77%	1.70%	0.80%	0.25%
1.09%	**3.20%**	**8.04%**	**2.74%**	**5.24%**	1.40%	0.47%	1.17%	0.26%	1.33%
3.35%	**2.97%**	**1.09%**	**7.95%**	**6.02%**	1.14%	0.45%	1.09%	0.55%	0.15%
6.33%	**2.61%**	**3.50%**	**1.35%**	**4.21%**	3.40%	0.67%	0.91%	1.63%	0.21%
3.22%	**1.11%**	**2.65%**	**4.92%**	**1.08%**	0.77%	0.15%	0.30%	1.23%	1.66%

Table 4.23 Relative error of porosity in the 4th discussion
(Left – 3 quantiles, right – 5 quantiles)

We could easily find out from the above figure (Figure 4.34) that probabilistic inversion using 5-quantile provide better results than 3-quantile. In Table 4.22, most of values applying 5-quantile are closer than the other one. As for the relative errors in Table 4.23, the interval for 3 quantiles is from 1.09% to 8.04%, while the interval is between 0.15% and 3.40% using 5 quantiles, which are much smaller than the previous one.

However, although it could provide more accurate estimations with more quantiles, we decide to use 3-quantile for the calculation, because the current computer and software abilities cannot use too many quantiles with 75 variables in this project.

4.4.5 Number of Iteration Steps

In the last discussion, we will apply probabilistic inversion approach with different number of iteration steps in order to find out the influence of the iteration step on the final results. The options are set as follows. (Table 4.24)

# Samples	60,000
Starting distributions	SAT ~ Beta(2,2), PRF ~ Beta(3,2) × 500+5600, POR ~ Beta(2,4) × 0.5
Conditional sampling	Yes
Method	IPF
Probability quantiles	3 (5%, 50%, 95%)
# Iteration steps	50, 100, 200

Table 4.24 Setting options of the 5th discussion

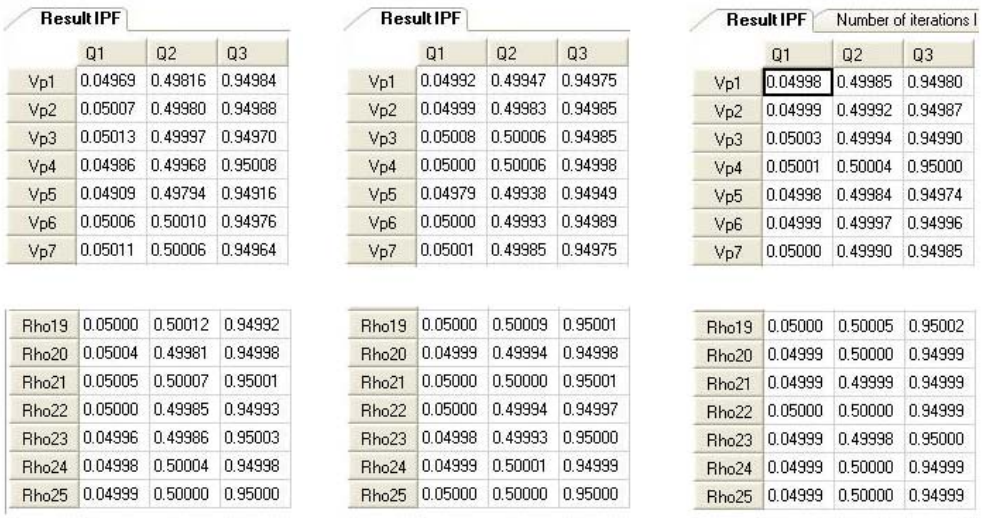

Result IPF

	Q1	Q2	Q3
Vp1	0.04969	0.49816	0.94984
Vp2	0.05007	0.49980	0.94988
Vp3	0.05013	0.49997	0.94970
Vp4	0.04986	0.49968	0.95008
Vp5	0.04909	0.49794	0.94916
Vp6	0.05006	0.50010	0.94976
Vp7	0.05011	0.50006	0.94964
Rho19	0.05000	0.50012	0.94992
Rho20	0.05004	0.49981	0.94998
Rho21	0.05005	0.50007	0.95001
Rho22	0.05000	0.49985	0.94993
Rho23	0.04996	0.49986	0.95003
Rho24	0.04998	0.50004	0.94998
Rho25	0.04999	0.50000	0.95000

Result IPF

	Q1	Q2	Q3
Vp1	0.04992	0.49947	0.94975
Vp2	0.04999	0.49983	0.94985
Vp3	0.05008	0.50006	0.94985
Vp4	0.05000	0.50006	0.94998
Vp5	0.04979	0.49938	0.94949
Vp6	0.05000	0.49993	0.94989
Vp7	0.05001	0.49985	0.94975
Rho19	0.05000	0.50009	0.95001
Rho20	0.04999	0.49994	0.94998
Rho21	0.05000	0.50000	0.95001
Rho22	0.05000	0.49994	0.94997
Rho23	0.04998	0.49993	0.95000
Rho24	0.04999	0.50001	0.94999
Rho25	0.05000	0.50000	0.95000

Result IPF | Number of iterations I

	Q1	Q2	Q3
Vp1	0.04998	0.49985	0.94980
Vp2	0.04999	0.49992	0.94987
Vp3	0.05003	0.49994	0.94990
Vp4	0.05001	0.50004	0.95000
Vp5	0.04998	0.49984	0.94974
Vp6	0.04999	0.49997	0.94996
Vp7	0.05000	0.49990	0.94985
Rho19	0.05000	0.50005	0.95002
Rho20	0.04999	0.50000	0.94999
Rho21	0.04999	0.49999	0.94999
Rho22	0.05000	0.50000	0.94999
Rho23	0.04999	0.49998	0.95000
Rho24	0.04999	0.50000	0.94999
Rho25	0.04999	0.50000	0.94999

Figure 4.35 Result using different iteration steps (Left – 50, middle – 100, right – 200)

POROSITY

Truth					50				
0.1291	**0.1304**	**0.1178**	**0.1129**	**0.1215**	0.1343	0.1342	0.1221	0.1172	0.1239
0.1290	**0.1283**	**0.1194**	**0.1169**	**0.1203**	0.1302	0.1322	0.1288	0.1200	0.1270
0.1313	**0.1346**	**0.1282**	**0.1271**	**0.1361**	0.1354	0.1389	0.1301	0.1368	0.1437
0.1533	**0.1496**	**0.1428**	**0.1412**	**0.1424**	0.1625	0.1536	0.1470	0.1431	0.1487
0.1427	**0.1351**	**0.1323**	**0.1300**	**0.1387**	0.1475	0.1341	0.1357	0.1359	0.1404

100					200				
0.1342	**0.1345**	**0.1216**	**0.1175**	**0.1242**	0.1334	0.1343	0.1221	0.1166	0.1240
0.1304	**0.1324**	**0.1290**	**0.1201**	**0.1266**	0.1303	0.1323	0.1296	0.1197	0.1270
0.1357	**0.1386**	**0.1296**	**0.1372**	**0.1443**	0.1353	0.1387	0.1299	0.1371	0.1444
0.1630	**0.1535**	**0.1478**	**0.1431**	**0.1484**	0.1620	0.1538	0.1469	0.1432	0.1486
0.1473	**0.1336**	**0.1358**	**0.1364**	**0.1402**	0.1477	0.1341	0.1363	0.1368	0.1407

Table 4.25 PI estimation of POR using different iteration steps
(Top left – truth, top right – 50, bottom left – 100, bottom right – 200)

Relative error of porosity

50				
4.03%	**2.91%**	**3.65%**	**3.81%**	**1.98%**
0.93%	**3.04%**	**7.87%**	**2.65%**	**5.57%**
3.12%	**3.19%**	**1.48%**	**7.63%**	**5.58%**
6.00%	**2.67%**	**2.94%**	**1.35%**	**4.42%**
3.36%	**0.74%**	**2.57%**	**4.54%**	**1.23%**

100					200				
3.95%	**3.14%**	**3.23%**	**4.07%**	**2.22%**	3.33%	2.99%	3.65%	3.28%	2.06%
1.09%	**3.20%**	**8.04%**	**2.74%**	**5.24%**	1.01%	3.12%	8.54%	2.40%	5.57%
3.35%	**2.97%**	**1.09%**	**7.95%**	**6.02%**	3.05%	3.05%	1.33%	7.87%	6.10%
6.33%	**2.61%**	**3.50%**	**1.35%**	**4.21%**	5.68%	2.81%	2.87%	1.42%	4.35%
3.22%	**1.11%**	**2.65%**	**4.92%**	**1.08%**	3.50%	0.74%	3.02%	5.23%	1.44%

Table 4.26 Relative error of porosity in the 5th discussion
(Top left – truth, top right – 50, bottom left – 100, bottom right – 200)

As increasing of iteration steps, the result tends to be closer to the truth quantiles. (Figure 4.35) However, the number of iteration steps does not have much influence on the final results. We could draw this conclusion from Table 4.25 and 4.26. Some outputs using 50 steps are closed to the truth; some are better using 100 steps; others with 200 steps. This kind of situation does not look like previous discussions such as using different quantiles. For instance, the results accuracy will be improved as we increase the number of quantiles. We use 100 iteration steps in the all experiments, because we can already obtain good results and it does not cost too much time for the computation. Based on all results that we obtained, we will develop a sensitivity analysis in order to find out why probabilistic inversion cannot offer good estimations to the reservoir properties such as SAT and PRF.

4.5 Sensitivity Analysis

In the first part of this section, there are three small tests in order to check the dependence between reservoir properties. In test I, we use the truth distributions of saturation and pressure as the starting distributions. In test II, only saturation uses truth data and pressure will change to normal distribution like we created it before. In test III, the situations of saturation and pressure starting distributions will be changed, namely, using beta distribution for saturation and the truth data for pressure. In all tests, we still apply beta distribution with parameters $\alpha = 2$ and $\beta = 4$ for the starting distribution of porosity, because probabilistic inversion could obtain an excellent estimation.

After that, a research on correlation between the reservoir properties and the seismic attributes at one grid point or two neighbor points will be performed. We try to find the reason why probabilistic inversion cannot predict SAT and PRF well.

4.5.1 Test I

As mentioned above, the starting distributions are setting in the following table for the first test in this section. (Table 4.27)

Reservoir property	Starting distribution
SAT (saturation)	Truth distribution
PRF (pressure)	Truth distribution
POR (porosity)	Beta (2,4) × 0.5

Table 4.27 Setting options of the starting distributions in the 1st test

Result IPF

	Q1	Q2	Q3
Vp1	0.04999	0.49992	0.95005
Vp2	0.04999	0.49997	0.94990
Vp3	0.05000	0.50000	0.94999
Vp4	0.04999	0.49998	0.94995
Vp5	0.04990	0.49965	0.94973
Vp6	0.04998	0.49991	0.94966
Vp7	0.05000	0.49997	0.94997
Rho19	0.04998	0.50004	0.94998
Rho20	0.05004	0.50003	0.94998
Rho21	0.05000	0.50000	0.94997
Rho22	0.04998	0.49997	0.95000
Rho23	0.05000	0.50004	0.95000
Rho24	0.05000	0.49993	0.94999
Rho25	0.05000	0.49999	0.95000

	Errors
1	9.69643844825475E-05
2	2.76729729194339E-05
3	2.01667746492404E-05
4	1.68091002126971E-05
5	1.45749249556776E-05
6	1.28378529476845E-05
7	1.14713218594111E-05
94	4.69274392617063E-07
95	4.61508158856888E-07
96	4.5399293553159E-07
97	4.46713691147303E-07
98	4.39677944699729E-07
99	4.3285307701884E-07
100	4.26244173124158E-07

	Weights
1	8.60531540292881E-06
2	1.13592173342278E-06
3	1.59291204922472E-05
4	1.24843204976469E-06
5	8.66196937547756E-06
6	2.04724661469948E-06
7	2.07929688908707E-06
63334	9.91798283787E-06
63335	1.53918333328805E-06
63336	1.84184799593847E-06
63337	1.09407138228611E-06
63338	3.61888514550826E-06
63339	1.04922972901243E-06
63340	4.19934178319792E-05

Figure 4.36 Result, errors and weights of the 1st test

Truth Before PI After PI

POR

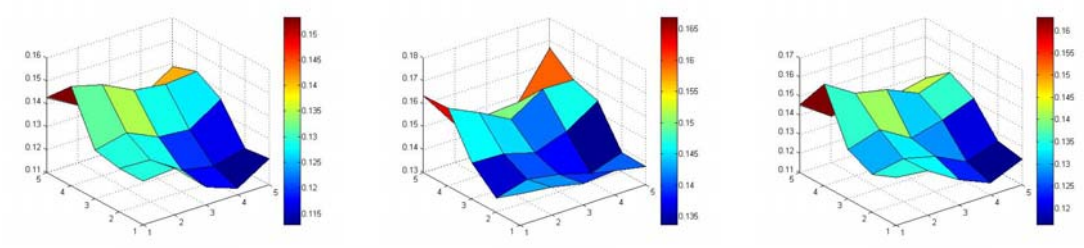

SAT

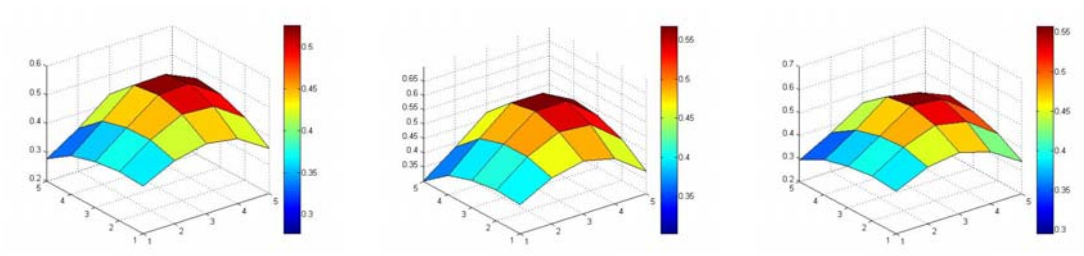

PRF

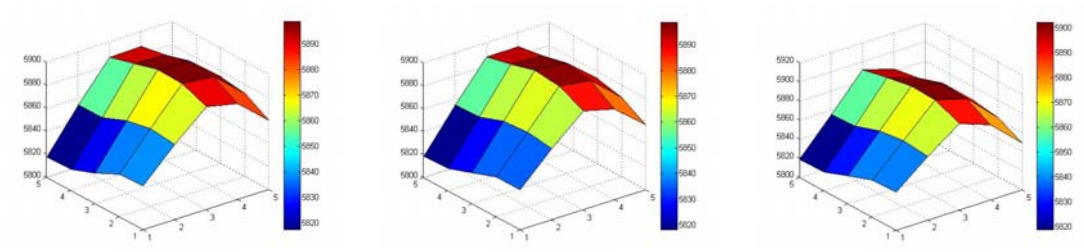

Vp

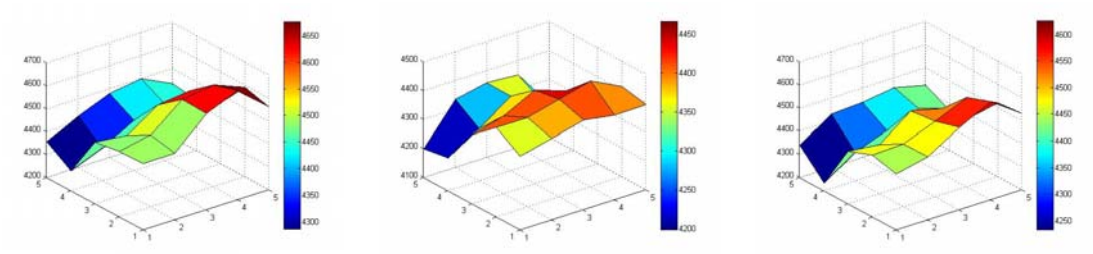

Vs

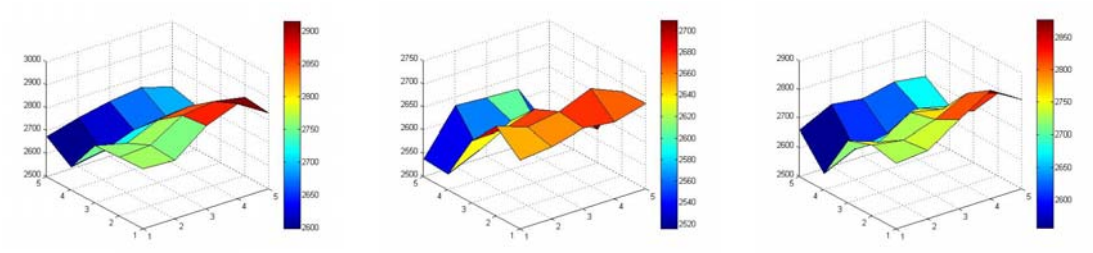

Rho

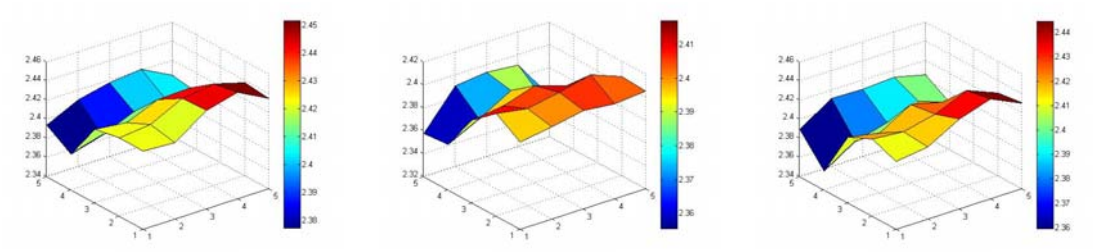

Figure 4.37 Comparison between truth, before PI and after PI in the 1st test

In this dependence test, we put saturation and pressure with the truth distribution and porosity with beta distribution into the rock physics model to obtain distributions of Vp, Vs and Rho. Those are closed to the truth by using conditional sampling. After probabilistic inversion, those seismic attributes are fit as the truth quantiles, and saturation and pressure did not change so much after probabilistic inversion. One of the figures of porosity is also closed to the truth as we expected. We can conclude that there is no influence between porosity and the other two properties. Those are independence. In the following two tests, we will check that saturation and pressure are independent or dependent.

4.5.2 Test II

In dependence test II, the starting distributions are setting as in the following table. We would like to check whether or not there are some relationships between

saturation and pressure, because we have concluded that there is no influence on saturation and pressure distributions, even though we generated the porosity starting distribution randomly just based on some information. In this test, we still use truth distribution as the saturation starting distribution, while we take beta distribution for pressure. (Table 4.28) By contrast, we will switch those two situations to perform another test in the next one.

Reservoir property	Starting distribution
SAT (saturation)	Truth distribution
PRF (pressure)	Beta (3,2) × 500+5600
POR (porosity)	Beta (2,4) × 0.5

Table 4.28 Setting options of the starting distributions in the 2nd test

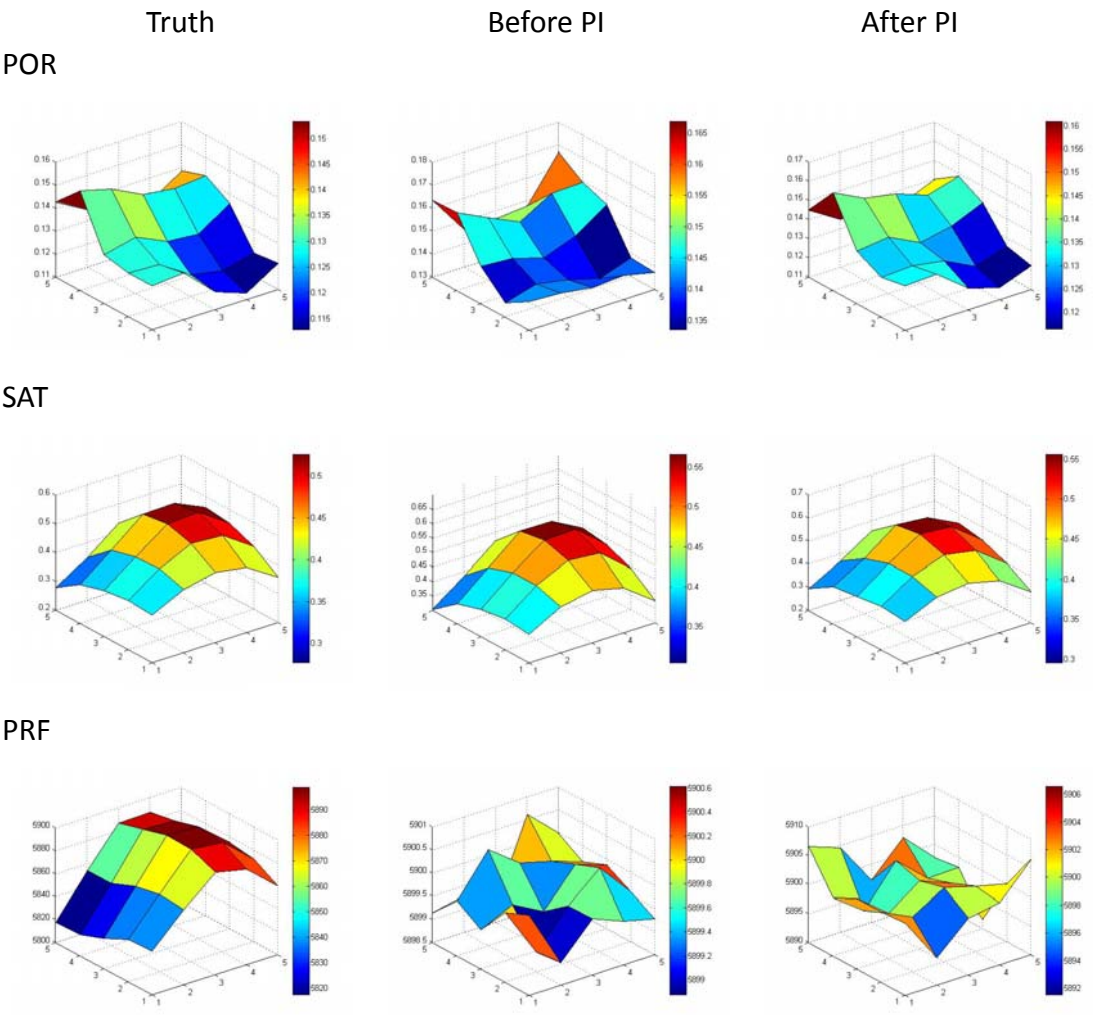

Vp

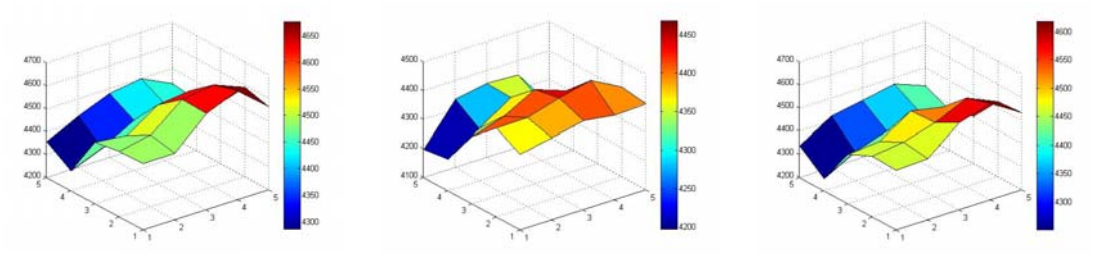

Vs

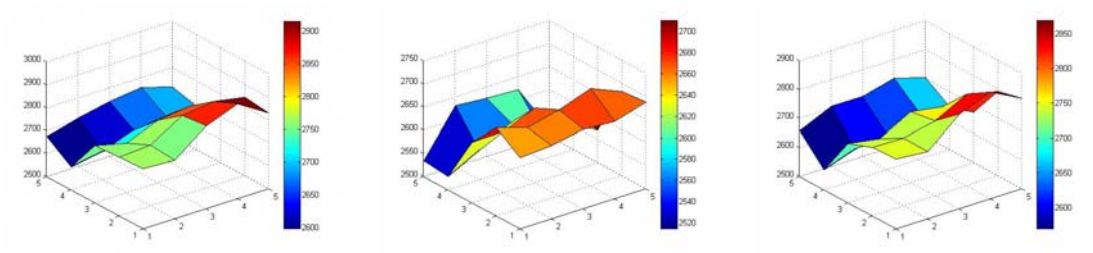

Rho

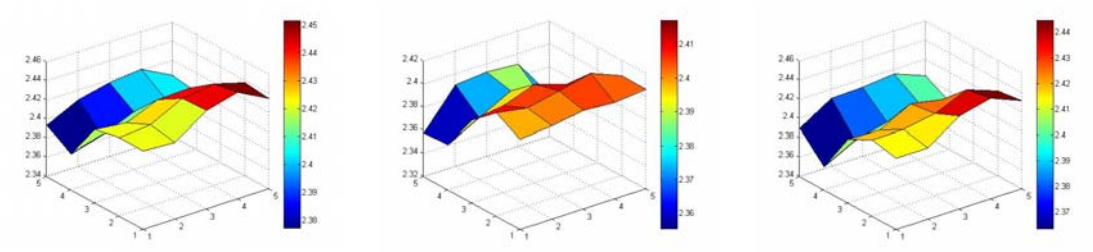

Figure 4.38 Comparison between truth, before PI and after PI in the 2nd test

The PI estimation of porosity is estimated correctly, and there is a little change of the figure of saturation with the truth and input. However, probabilistic inversion cannot give a good pressure estimation related to a random starting distribution.

4.5.3 Test III

In this one, we change the setting options for the starting distributions of saturation and pressure. The settings are shown in the following table (Table 4.29), and all comparisons are in Figure 4.39.

Reservoir property	Starting distribution
SAT (saturation)	Beta (2,2)
PRF (pressure)	Truth distribution
POR (porosity)	Beta (2,4) × 0.5

Table 4.29 Setting options of the starting distributions in the 3rd test

Truth | Before PI | After PI

POR

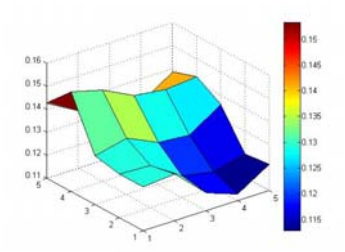
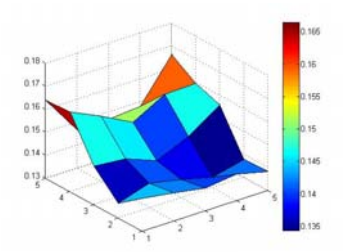
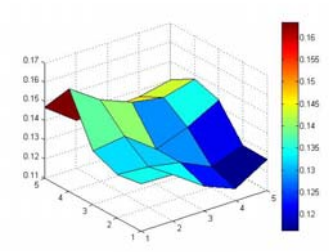

SAT

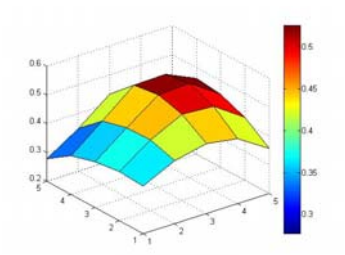
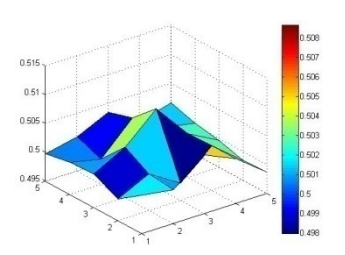
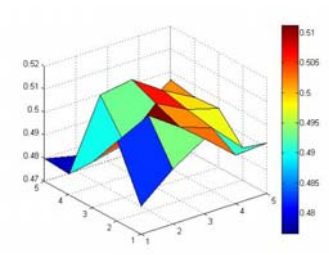

PRF

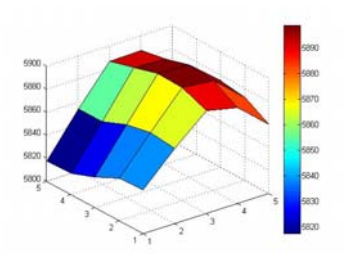
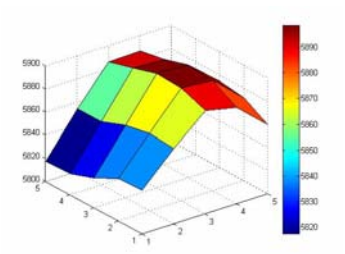
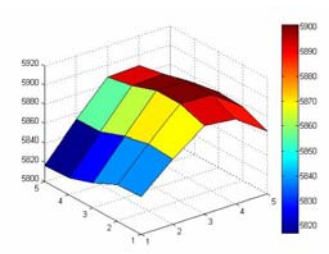

Vp

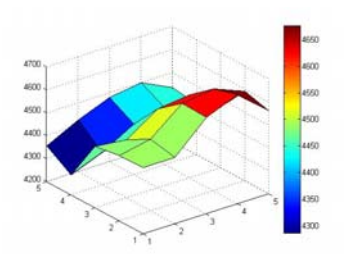
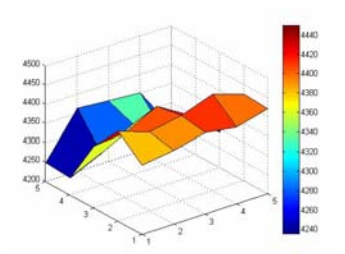
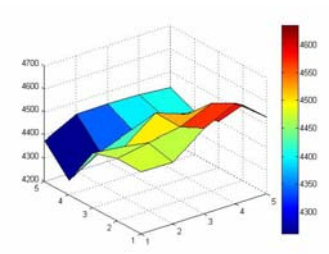

Vs

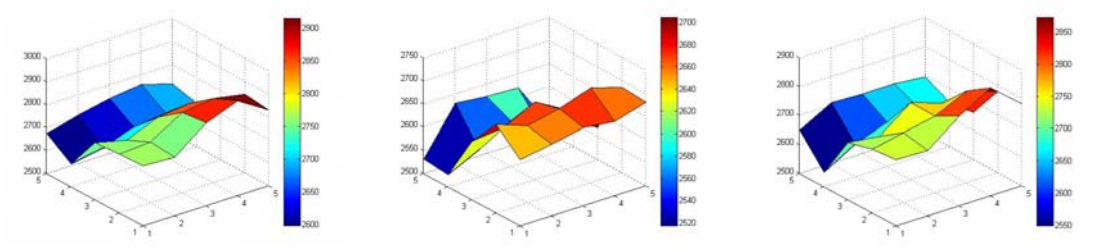

Rho

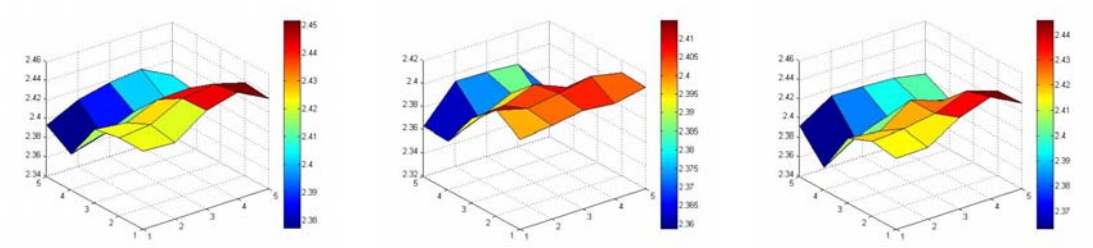

Figure 4.39 Comparison between truth, before PI and after PI in the 3rd test

The results from Figure 4.39 are similar as the previous test, but just change the situations between saturation and pressure, because we adjusted the inputs of those two reservoir properties.

4.5.4 Test for correlation

In order to analyze those results that we obtained above, we decide to perform some sensitivity analysis between different variables. We tend to find out the influence between the reservoir properties and the seismic attributes at a certain grid point or between two neighbor grid points.

We choose the sample from experiment II as a example, and follow this analysis using the program of Unisens at three different grid points such as in the corner, at the edge and in the middle. As for the tests, we choose the 1st, 11th and 17th grid points .

Before solving the problem, some basic measures of dependence and sensitivity analysis between two variables should be given in the following part.

In probability theory and statistics, correlation indicates the strength and direction of a linear relationship between two random variables. There are a number of different correlation coefficients to use for measuring different situation. Simply stated, we

present three correlation coefficients to measure the dependence between seismic attributes and reservoir properties in our project, which are (Pearson) product moment correlation, Spearman's rank correlation and correlation ratio.

1. The Pearson product moment correlation is a common measure of the correlation between two variables. It represents by the Greek letter rho (ρ), while its range is from -1 to 1. A correlation of 1 means that there is a perfect positive linear relationship between two variables, and it means that there is a perfect negative linear relationships. However, variables are independence, when the product moment correlation coefficient equals 0.

2. The Spearman's rank correlation is a non-parametric measure of correlation. It assesses how well an arbitrary monotonic function could describe the relationship between two variables. Spearman's rank correlation coefficient is equivalent to Pearson correlation on ranks, and its range is also from -1 to 1.

3. The correlation ratio is a measure of the relationship between the statistical dispersion within individual categories and the dispersion across the whole population or sample. The correlation ratio takes values between 0 and 1. The value 0 represents the special case of no dispersion among the means of the different categories, while the value 1 means that no dispersion with the respective categories.

In the first part, we check the dependence between the seismic attributes – Vp, Vs, Rho and the reservoir properties – SAT, PRF, POR.

Predicted variable	Base variable	E[Predicted variable]	E[Base variable]	Std[Predicted variable]	Std[Base variable]	Product moment correlation	Rank correlation	Regression coefficient	Correlation ratio
Rho1	POR1	2.3992	0.1434	0.1196	0.0683	-0.9983	-0.9985	-1.7474	0.9965
Vs1	POR1	2648.1226	0.1434	515.5670	0.0683	-0.9874	-0.9999	-7453.0742	0.9998
Vp1	POR1	4384.4502	0.1434	591.7178	0.0683	-0.9806	-0.9908	-8494.7754	0.9848
Vs1	SAT1	2648.1226	0.5004	515.5670	0.2233	-0.0223	-0.0235	-51.4958	0.0006
Vs1	PRF1	2648.1226	5899.4741	515.5670	99.7779	-0.0046	-0.0035	-0.0237	0.0000
Vp1	PRF1	4384.4502	5899.4741	591.7178	99.7779	-0.0036	-0.0025	-0.0211	0.0000
Rho1	PRF1	2.3992	5899.4741	0.1196	99.7779	0.0025	0.0033	0.0000	0.0000
Rho1	SAT1	2.3992	0.5004	0.1196	0.2233	0.0348	0.0325	0.0186	0.0014
Vp1	SAT1	4384.4502	0.5004	591.7178	0.2233	0.0952	0.1000	252.2170	0.0101

Table 4.30 Correlation analysis at the 1st grid point

Predicted variable	Base variable	E[Predicted variable]	E[Base variable]	Std[Predicted variable]	Std[Base variable]	Product moment correlation	Rank correlation	Regression coefficient	Correlation ratio
Rho11	POR11	2.4057	0.1397	0.1146	0.0656	-0.9983	-0.9985	-1.7437	0.9966
Vs11	POR11	2670.8127	0.1397	504.1487	0.0656	-0.9879	-0.9999	-7588.3848	0.9999
Vp11	POR11	4411.7319	0.1397	576.4988	0.0656	-0.9805	-0.9904	-8611.9160	0.9850
Vs11	SAT11	2670.8127	0.5036	504.1487	0.2217	-0.0370	-0.0406	-84.0626	0.0016
Vs11	PRF11	2670.8127	5899.5015	504.1487	100.3196	-0.0101	-0.0092	-0.0506	0.0001
Vp11	PRF11	4411.7319	5899.5015	576.4988	100.3196	-0.0095	-0.0088	-0.0547	0.0001
Rho11	PRF11	2.4057	5899.5015	0.1146	100.3196	-0.0021	-0.0023	0.0000	0.0000
Rho11	SAT11	2.4057	0.5036	0.1146	0.2217	0.0165	0.0162	0.0085	0.0007
Vp11	SAT11	4411.7319	0.5036	576.4988	0.2217	0.0802	0.0853	208.4457	0.0078

Table 4.31 Correlation analysis at the 11th grid point

Predicted variable	Base variable	E[Predicted variable]	E[Base variable]	Std[Predicted variable]	Std[Base variable]	Product moment correlation	Rank correlation	Regression coefficient	Correlation ratio
Rho17	POR17	2.4155	0.1341	0.1077	0.0616	-0.9982	-0.9984	-1.7454	0.9964
Vs17	POR17	2706.6167	0.1341	485.5650	0.0616	-0.9888	-0.9999	-7794.8237	0.9999
Vp17	POR17	4452.2114	0.1341	555.8025	0.0616	-0.9816	-0.9900	-8858.1299	0.9849
Vs17	SAT17	2706.6167	0.5023	485.5650	0.2220	-0.0304	-0.0338	-66.4583	0.0011
Vs17	PRF17	2706.6167	5899.8188	485.5650	99.7836	-0.0056	-0.0062	-0.0275	0.0000
Vp17	PRF17	4452.2114	5899.8188	555.8025	99.7836	-0.0039	-0.0044	-0.0219	0.0000
Rho17	PRF17	2.4155	5899.8188	0.1077	99.7836	0.0023	0.0016	0.0000	0.0000
Rho17	SAT17	2.4155	0.5023	0.1077	0.2220	0.0267	0.0255	0.0130	0.0010
Vp17	SAT17	4452.2114	0.5023	555.8025	0.2220	0.0874	0.0942	218.8926	0.0087

Table 4.32 Correlation analysis at the 17th grid point

From the above three tables, we could conclude that all the seismic attributes are highly dependent on one reservoir property – porosity. However, those are almost independent on other two properties – saturation and pressure. That is why probabilistic inversion technique cannot predict these two properties well but only give a good estimation of porosity.

Now we would like to check whether or not there are some influences between each two neighbor grid points. The results will be shown as follows.

Predicted variable	Base variable	E[Predicted variable]	E[Base variable]	Std[Predicted variable]	Std[Base variable]	Product moment correlation	Rank correlation	Regression coefficient	Correlation ratio
Vp7	SAT6	4405.0415	0.5010	582.9411	0.2235	-0.0004	0.0004	-1.0898	0.0001
Vp7	PRF6	4405.0415	5899.4404	582.9411	99.8685	0.0037	0.0037	0.0215	0.0000
Vp7	POR6	4405.0415	0.1421	582.9411	0.0672	0.0091	0.0094	78.8452	0.0001
Vp7	Vp6	4405.0415	4393.4355	582.9411	586.8085	-0.0096	-0.0092	-0.0096	0.0000
Vp7	Vs6	4405.0415	2655.9060	582.9411	510.7958	-0.0097	-0.0094	-0.0111	0.0000
Vp7	Rho6	4405.0415	2.4014	582.9411	0.1177	-0.0090	-0.0093	-44.7359	0.0001
Vs7	SAT6	2666.2319	0.5010	507.5003	0.2235	0.0000	0.0009	-0.0197	0.0001
Vs7	PRF6	2666.2319	5899.4404	507.5003	99.8685	0.0041	0.0044	0.0207	0.0000
Vs7	POR6	2666.2319	0.1421	507.5003	0.0672	0.0092	0.0094	69.4615	0.0001
Vs7	Vp6	2666.2319	4393.4355	507.5003	586.8085	-0.0097	-0.0091	-0.0084	0.0000
Vs7	Vs6	2666.2319	2655.9060	507.5003	510.7958	-0.0099	-0.0095	-0.0099	0.0000
Vs7	Rho6	2666.2319	2.4014	507.5003	0.1177	-0.0091	-0.0093	-39.2785	0.0001
Rho7	SAT6	2.4042	0.5010	0.1161	0.2235	0.0001	0.0008	0.0001	0.0001
Rho7	PRF6	2.4042	5899.4404	0.1161	99.8685	0.0045	0.0041	0.0000	0.0000
Rho7	POR6	2.4042	0.1421	0.1161	0.0672	0.0095	0.0093	0.0164	0.0001
Rho7	Vp6	2.4042	4393.4355	0.1161	586.8085	-0.0099	-0.0090	0.0000	0.0000
Rho7	Vs6	2.4042	2655.9060	0.1161	510.7958	-0.0101	-0.0094	0.0000	0.0000
Rho7	Rho6	2.4042	2.4014	0.1161	0.1177	-0.0094	-0.0092	-0.0093	0.0001

Table 4.33 Influence between the 6th and 7th grid points

From previous table, we notice that all three correlation coefficients are almost closed to 0, which mean there is no influence between each two neighbor grid points.

After asking the experts, we found out that the reason is the certain reservoir we focus on with a very small porosity, which means the fluid in the reservoir with less activity. Corresponding to the seismic attributes, they could not reflect reservoir properties easily and correctly. Finally, we developed a test with large number of porosity, while we found out that the correlations between seismic attributes and saturation increase. However, the correlations with pressure are still small. (Table 4.34) We can conclude that one of the reservoir properties – SAT has more influence on seismic attributes than another property – PRF, when the porosity of a certain reservoir is not very small. We can try to apply probabilistic inversion to those data in order to predict saturation in the future work.

Predicted variable	Base variable	E[Predicted variable]	E[Base variable]	Std[Predicted variable]	Std[Base variable]	Product moment correlation	Rank correlation	Regression coefficient	Correlation ratio
Rho17	POR17	2.3863	0.1496	0.1415	0.0801	-0.9978	-0.9975	-1.7620	0.9957
Vp17	POR17	3873.9211	0.1496	846.1926	0.0801	-0.9767	-1.0000	-10315.9775	0.9996
Vs17	POR17	2622.2146	0.1496	568.1158	0.0801	-0.9711	-0.9999	-6886.0078	0.9994
Vs17	SAT17	2622.2146	0.4199	568.1158	0.2851	-0.1712	-0.1975	-341.1989	0.0421
Vp17	SAT17	3873.9211	0.4199	846.1926	0.2851	-0.1625	-0.1910	-482.2012	0.0394
Rho17	SAT17	2.3863	0.4199	0.1415	0.2851	-0.0743	-0.1346	-0.0368	0.0138
Vs17	PRF17	2622.2146	5854.7222	568.1158	61.3388	0.0501	0.0518	0.4642	0.0071
Vp17	PRF17	3873.9211	5854.7222	846.1926	61.3388	0.0550	0.0536	0.7591	0.0080
Rho17	PRF17	2.3863	5854.7222	0.1415	61.3388	0.0909	0.0600	0.0002	0.0178

Table 4.34 Correlation at 17th grid point with bigger porosity

Furthermore, another idea is to analyze the relationship between reservoir properties and seismic attributes using time-lapse seismic data which means 4-D seismic data. We notice the changes of seismic attributes at different time to estimate the corresponding changes of reservoir properties. There is no enough time to perform all experiments, and we just develop sensitivity analysis on those changes. The results are shown below. (Table 4.35)

Predicted variable	Base variable	E[Predicted variable]	E[Base variable]	Std[Predicted variable]	Std[Base variable]	Product moment correlation	Rank correlation	Regression coefficient	Correlation ratio
Drho17	Dfi17	0.0406	-0.0174	0.1126	0.0638	-0.9976	-0.9971	-1.7612	0.9955
Dvp17	Dfi17	262.6075	-0.0174	800.4056	0.0638	-0.9839	-0.9929	-12345.7002	0.9705
Dvs17	Dfi17	177.9277	-0.0174	546.7339	0.0638	-0.9803	-0.9915	-8401.8955	0.9640
Dvs17	DS17	177.9277	0.3500	546.7339	0.2521	-0.1726	-0.1625	-374.3614	0.0404
Dvp17	DS17	262.6075	0.3500	800.4056	0.2521	-0.1684	-0.1582	-534.6657	0.0391
Drho17	DS17	0.0406	0.3500	0.1126	0.2521	-0.1174	-0.1111	-0.0525	0.0235
Drho17	DP17	0.0406	103.6803	0.1126	86.5075	-0.0040	0.0229	0.0000	0.0181
Dvp17	DP17	262.6075	103.6803	800.4056	86.5075	0.0226	0.0462	0.2094	0.0180
Dvs17	DP17	177.9277	103.6803	546.7339	86.5075	0.0259	0.0484	0.1636	0.0180

Table 4.35 Correlation at 17th grid point with time-lapse seismic data

From above table, we notice that the correlation between porosity and seismic attributes are still quite high near 1, while these changing attributes have stronger correlation with the changes of saturation. However, the correlations between pressure and seismic attribute are still weak.

In addition, engineers also develop a non-linear transformation using Zoeppritz type

equations, which could change 4-D seismic attributes to other three parameters in order to increase the correlations between changes of reservoir properties and the measurements. The sensitivity analysis is shown in the following table. (Table 4.36)

Predicted variable	Base variable	E[Predicted variable]	E[Base variable]	Std[Predicted variable]	Std[Base variable]	Product moment correlation	Rank correlation	Regression coefficient	Correlation ratio
ds17	dr17	0.2247	0.0186	0.0539	0.0100	0.6243	0.5653	3.3567	0.5043
ds17	dt17	0.2247	-0.0015	0.0539	0.0008	-0.6403	-0.5892	-43.4692	0.4769
ds17	dg17	0.2247	-0.0109	0.0539	0.0174	-0.3531	-0.3186	-1.0950	0.1314
dp17	dt17	-12.0422	-0.0015	15.0307	0.0008	-0.1266	-0.1328	-2396.9238	0.0228
dp17	dr17	-12.0422	0.0186	15.0307	0.0100	0.1191	0.1243	178.6053	0.0203
dp17	dg17	-12.0422	-0.0109	15.0307	0.0174	-0.1086	-0.1074	-93.9234	0.0129

Table 4.36 Correlation between changes of reservoir properties and measurements

In the above table, ds represents the changes of saturation at two different time, while dp is the changes of pressure. (R, G, T) are the outputs of Zoeppritz type equations, where R is a reflect coefficient, G represents how the reflectivity changes, and T is the two-way travel time. dr, dg, dt represent the changes of this parameters at different time. For this part, we just performed a sensitivity analysis, but do not have time to develop experiments. We will mention this part and present some conclusions and recommendations in the final chapter.

5. Conclusions & Recommendations

This is the first time to apply probabilistic inversion technique on seismic data to estimate reservoir properties. We performed hundreds of experiments and tests with different aspects to develop this research. After finished those experiments, we could draw some conclusions concerning this project and recommendations for the future work below.

1. Probabilistic inversion technique is an excellent approach to estimate one of the reservoir properties – POR (porosity) based on some particular information and seismic attributes measurements, even though the starting distribution of porosity is not quite similar as the real one or the truth one that we assumed. For example, we developed a lot of research related to many classes of starting distributions of porosity such as uniform, normal, beta, gamma, lognormal, etc. We can obtain a quite good estimation of porosity each time.

2. After analyzed and compared the results from different experiments, we notice that it is easy for probabilistic inversion to obtain better estimation of porosity, if we could choose a suitable starting distribution for generating samples based on the reservoir information that engineers known. Moreover, using suitable starting distributions is much faster to close the real values than others which may not be similar as the real one. Until now, the Beta and Gamma distribution performed very well and give more reasonable results than other distributions such as uniform and lognormal. In addition, there are some influences on the final estimations with using different distribution parameters. For instance, two parameters α and β should be chosen based on the information of reservoir properties.

3. For probabilistic inversion approach, we find out that there are several ways to improve the method and to obtain good estimations. For example, the input samples are already closed to the truth after using conditional sampling, because those unreasonable samples have been removed. This could help probabilistic inversion to begin with a suitable starting distribution and to solve the problem accurately and easily. When the problem is feasible, we have to apply IPF method to deal with it in order to get fast convergence rate and better results than PARFUM. However, if the problem is infeasible, PARFUM can be used because it converges all the time. Furthermore, taking more quantiles and increasing the number of input samples would help probabilistic inversion to obtain more accurate and correct estimations. As for another factor – the number of iteration steps, there is no dramatic effect on the final results when this number is large enough.

4. After many experiments, we performed sensitivity analysis in order to find out the reason that why probabilistic inversion cannot provide good estimations about saturation and pressure. In the first three tests, we noticed that there is no influence between each two reservoir properties when we applied the rock physics model and probabilistic inversion, while there is no impact for variables between each two neighbor grid points. However, we found that the correlation between porosity and seismic attributes is very large almost equal to 1 and other two correlations are almost 0 at a certain grid point. It means that porosity plays an important role in the rock physics model rather than saturation and pressure. Moreover, in this specific case, the values of porosity are all quite small (<<1) between 0 and 0.3. In physical point of view, saturation and pressure cannot give much impact on seismic attributes under this situation. After changing the situation with bigger porosity, we noticed that saturation has stronger influence on seismic data. As for pressure, it also has a weak correlation with seismic attributes. These are the whole reasons that why probabilistic inversion cannot offer good estimations about saturation and pressure.

5. In the real world, engineers or experts also focus on the relationship between the changes of reservoir properties and the changes of seismic data, which called time-lapse seismic data or 4-D seismic data. In the sensitivity analysis section, we calculated the correlation between these two kinds of changes. The changes of saturation have stronger correlation with the changes of seismic attributes such as Vp, Vs and Rho. By contrast, the changes of pressure cannot provide much information on these.

6. In addition, engineers developed a non-linear transformation called Zoeppritz type equations to analyze the changes of seismic attributes. After we performed the last sensitivity analysis, we noticed that the outputs of Zoeppritz type equations correlated stronger with reservoir properties than the seismic attributes which we used such as Vp, Vs and Rho. Probabilistic inversion can offer better estimation for saturation using combination of the rock physics model and the Zoeppritz type equations in future work.

Several recommendations may be helped for the future work hopefully, while they are presented below.

a. In this project, we performed all of experiments only with 25 grid points which contains 75 variables with 3 or 5 quantiles, and the maximal number of input samples should be less than 70,000. However, along with the development of the computer level and the program that we used, there are several good ways to improve the method for obtaining better results such as taking more quantiles and input samples. Moreover, researcher can apply probabilistic inversion

approach to estimate reservoir properties concerning more variables and grid points.

b. Generating the samples with suitable starting distributions based on some certain geophysical or reservoir background. If one could obtain more information of the reservoir properties, especially saturation and pressure, it may help to improve the method and to make the results close to the truth.

c. Probabilistic inversion technique can provide good estimations when the inputs and outputs of the model do not have quite weak correlation. In the future work, researchers can apply this technique to the time-lapse seismic data for estimating the reservoir properties.

d. In this project, we used MATLAB program for most of calculations. Actually, its performance is excellent for matrix calculations, but it is not a good choice for other operations such as saving some sample files. Using other programs to compute may be much faster than this.